“Development & Experimental Validation of a Novel Computational Model of Retinotopic Mapping”

(Entwicklung und experimentelle Überprüfung eines neuen Computermodells der Entstehung retinotoper Karten)

Zur Erlangung des akademischen Grades eines

DOKTORS DER NATURWISSENSCHAFTEN
(Dr. rer. nat.)

der Fakultät für Chemie und Biowissenschaften der
Universität Karlsruhe (TH)
vorgelegte

DISSERTATION

von

Christoph Gebhardt

aus Altenburg

Dekan: Prof. Dr. S. Bräse
Referent: Prof. Dr. M. Bastmeyer
Korreferent: Prof. Dr. P. Nick
Tag der mündlichen Prüfung: Dezember 2009

Danksagung

Mein herzlicher Dank gilt allen, die zum Gelingen dieser Arbeit beigetragen haben:

Zu allererst Herrn Prof. Dr. Martin Bastmeyer für die Möglichkeit, diese Arbeit nach dem unvorhergesehenen Wechsel aus Jena an seinem Lehrstuhl weiterführen zu dürfen sowie für seine fachliche Unterstützung,

Herrn Prof. Dr. Peter Nick für die Zweitbegutachtung der Arbeit,

Dr. Franco Weth für die hervorragende Betreuung und effektive Diskussionen, die erheblich zum Voranschreiten und Gelingen der Arbeit beigetragen haben,

Herrn Prof. Dr. Friedrich Bonhoeffer für sein kritisches Interesse an dieser Arbeit in unzähligen Treffen der „Retinotektalen“ in Karlsruhe,

Herrn Prof. Dr. Ulrich Schwarz für die freundlicherweise zur Verfügung gestellte Rechenzeit auf dem Institutscluster,

Dr. Anne von Philipsborn für die grundlegende Idee der experimentellen Durchführung der „double stripe assays“.

Ebenso danke ich allen ehemaligen und jetzigen Kollegen der Nachwuchsgruppe Neurogenetik in Jena und der Zell- und Neurobiologie in Karlsruhe.

Vor allem aber möchte ich meiner Familie danken. Ohne Euch wären die Durchführung und der Abschluss des Projekts „Promotion“ nicht möglich gewesen.

On Rigor in Science

…In that Empire, the Art of Cartography attained such Perfection that the map of a single Province occupied the entirety of a City, and the map of the Empire, the entirety of a Province. In time, those Unconscionable Maps no longer satisfied and the Cartographers Guilds struck a Map of the Empire whose size was that of the Empire and which coincided point for point with it. The following Generations, who were not so fond of the Study of Cartography as their Forebears had been, saw that that vast Map was Useless, and not without some Pitilessness was it, that they delivered it up to the Inclemencies of Sun and Winters. In the Deserts of the West, still today, there are Tattered Ruins of that Map, inhabited by Animals and Beggars; in all the Land there is no other Relic of the Disciplines of Geography.

Suárez Miranda: *Viajes de varones prudentes*, Libro Cuarto, cap. XLV, Lérida, 1658.

Jorge Luis Borges

Translation of excerpt taken from: *Historia Universal de la Infamia* (1946)

CONTENTS

I. INTRODUCTION 1

The Retinotectal Projection 1

Mechanisms of Topography Formation 4

Limitations of the Chemoaffinity Theory 6

Quantitative Models of Topographic Guidance 8

Questions & Aims 10

II. Materials & Methods 11

A. Materials & Organisms 11

1. Chemicals 11

2. Solutions, Buffers, Media 12

3. Antibodies 13

4. Recombinant Proteins, Enzymes 13

5. Miscellaneous Materials 13

6. Organisms 14

7. Hard- and Software 14

B. Methods 15

1. Preparation, Fixation and Staining of Retinal Explants 15

2. Stripe Assay with Substrate of Alternating EphA3-Fc and ephrinA2-Fc Stripes 15

3. Protein Modifications 16

4. Enzyme-linked Immunosorbent Assay (ELISA) 17

5. Light-patterning of Substrates 18

6. Model Descriptions & Simulations 19

III. RESULTS 25

A. Computational Modelling to Understand the Functional Properties of Topographic Guidance Cues 25

1. Growth Cone Behaviour on Homogeneous Guidance Cue Substrates 28

2. Growth Cone Behaviour in Diffusion Gradients of Guidance Cues 32

3. Growth Cone Behaviour in Substrate-bound Gradients of Guidance Cues 34

4. Growth Cone Behaviour in Stripe Assays 36

B. A Novel Integrative Model of Topographic Guidance by Antagonistic Pairs of Interacting, Monofunctional Guidance Cues 38

C. Experimental and Computational Evidence for Integrated Forward and Reverse Signalling 42

D. Modelling *in vitro* Evidence for Axonal Receptor - Ligand *cis*-Interactions 45

E. Modelling *in vivo* Evidence for Fibre-fibre-interactions During Topographic Axon Mapping 46

F. First Time Experimental *in vitro* Evidence of Topographically Differential Decision Behaviour of RGC Axons 50

G. Improving *in vitro* Substrates for Studying Retinal Axon Guidance 56
1. Light-controlled Activation of Guidance Proteins 56
2. Fabrication of Alternating Stripes of EphA3 and ephrinA5 with Light-patterning 58
H. Robustness of the Mapping Function against Variations of Absolute Guidance Cue Concentrations and Tectal Size in the Novel Model 60
I. Growth Cone Adaptation in the Retinotectal System during Topographic Axon Guidance 62
1. "Adaptation" on Homogeneous Substrates 62
2. "Adaptation" in Orthogonal Receptor Stripe Assays 64
3. Influence of Adaptation on Topography Formation 66
IV. DISCUSSION 69
Do ephrinAs Have Mono- or Bifunctional Guidance Properties? 69
The Novel Model of Retinotectal Projection Formation Includes All Potentially Existing EphA / ephrinA Interactions 76
The Novel Model Replicates *in vitro* Evidence that Suggested the Existence of *cis*-Interactions between Axonal Receptor and Ligand 78
The Phenotype Seen after EphA3 Knock-in Cannot Satisfyingly Be Explained by Current Chemoaffinity Models Even if Fibre-fibre-interactions Are Included 79
A Topographically Differential Growth Behaviour Is Reconstituted *in vitro* Using "Double Stripe Assays" of EphA and ephrinA 83
The Novel Model Is Robust against Perturbations 86
Conceptual Thoughts on Adaptive Mechanisms during Topographic Guidance 87
Experimental Evidence for Adaptive Mechanisms during Topographic Axon Guidance 90
Topography & Adaptation 94
Suggestions for Future Research 95
APPENDIX 99
References 117
Abstract 125
Zusammenfassung 127

I. INTRODUCTION

The impressive self-organisation of neuronal connections is the most fundamental aspect of embryonic brain development. An almost ubiquitous connection pattern are so called topographic maps, which are characterised by neighbouring neurons in one layer sending their axons to neighbouring neurons in the target layer. The retinotectal projection, i.e. the connection of retinal ganglion cells (RGCs) in the eye and the *Tectum opticum* in the midbrain, is the best studied model system for this type of connectivity in the brain. Graded distributions of molecules of EphA receptors in the retina and ephrinA ligands in the tectum are thought to provide directional and positional cues required for guiding RGC axons to their topographic target. However, recent research suggests that a more complex pattern of molecular interactions might be responsible for this developmental process. Moreover, despite a rich body of experimental evidence, gathered over the years, no coherent and self-consistent developmental model for the formation of topographic maps exists to date.

Therefore, a combinatorial approach of theoretical modelling and *in vitro* experiments was chosen here to facilitate the understanding of the underlying complex signal interplay and to contribute to a comprehensive model of topographic map formation.

The Retinotectal Projection

In the visual system of vertebrates, the retina represents the first processing level of incoming light stimuli. This sensory epithelium develops ontogenetically as an evagination of the diencephalon and is therefore part of the forebrain. The cellular architecture of the retina exhibits a morphological as well as functional layering. The layer containing the actual photoreceptors is located on the light-averted side facing the pigment epithelium. The retinal ganglion cells (RGCs) are situated in the retinal layer facing the vitreous body and integrate the information coming from the previous processing layers. Subsequently, this information is transferred to higher brain areas.

An axon population that connects brain areas of different hierarchical levels is called a projection. The RGC axons form the optic nerve and optic tract and then a projection with their respective target area in the brain.

In mammals, RGC axons project to the *Colliculi superiores* (SC) in the midbrain (=retinocollicular projection) and via axon collaterals to the primary visual nuclei in the thalamus, the *Corpora geniculata lateralia* (=retinogeniculate projection). From this brain area, axonal projections run to the occipital lobe of the cortex where the visual area resides which is the primary instance for processing visual information in the brain of higher vertebrates.

In comparison, the visual system of amphibians, fishes and birds shows a lower level of organisation with respect to structure and function. The projection from the retina runs to the contralateral *Tectum opticum* (OT) in the midbrain (=retinotectal projection). The optic tectum is considered the phylogenetic homologue of the *Colliculus superior* (SC), but serves as main processing area of visual stimuli in these animals.

The retinocollicular projection is mainly studied in mice (McLaughlin *et al.*, 2003a) because of the availability of the complete genome sequence (Waterston *et al.*, 2002) and of elaborated genetic manipulation techniques in this model organism. The extraordinary size of retina and tectum and the accessibility of the embryo in the egg, however, encouraged the use of the chick as a model organism for the investigation of the retinotectal projection [for an overview (Mey and Thanos, 2000; Thanos and Mey, 2001), and references therein].

Although both model organisms share many organising features of the visual apparatus and comparable molecular mechanisms may be operating during development, there are differences considering the growth of the axons into optic tectum and SC. In mice, RGC axons first grow to the posterior extent of the SC (axon overshoot). Subsequently, interstitial branches are formed on the axon preferably at the future target position and the overshooting axon is retracted (Simon and O'Leary, 1990, 1992a, b).

In contrast, in chicks, fishes and amphibians, retinal axons seem to be guided directly to the topographically correct target.

Guidance is achieved by a motile structure at the tip of the outgrowing axon, called the growth cone, a cellular structure sensitive to molecular signals surrounding the axon's path (Dickson, 2002; Huber *et al.*, 2003; Mueller, 1999; Thanos and Bonhoeffer, 1987; Thanos and Dütting, 1987).

Some overshoot seems to occur in chick as well (Nakamura and O'Leary, 1989; Yates *et al.*, 2001). However, this might be attributable to a general imprecision of the initial map rather than a different mechanism of topography formation.

The retinotectal projection is the classic example for a topographic projection. That means, the spatial relationship between the RGC cell bodies in the retina is reflected in the termination points of their axons in the tectal target tissue. Therefore, the representation of an object in the retina is functionally recast in the optic tectum in a scaled but non-perturbed form.

The retinotectal projection is orientated such that RGCs situated in the temporal part of the eye project to the anterior part of the tectum, whereas nasal RGCs terminate in the posterior part of the tectum (Figure I-1). On the other retinal axis, dorsal RGCs project to ventral neurons in the tectum and ventral RGCs terminate at the dorsal tectum.

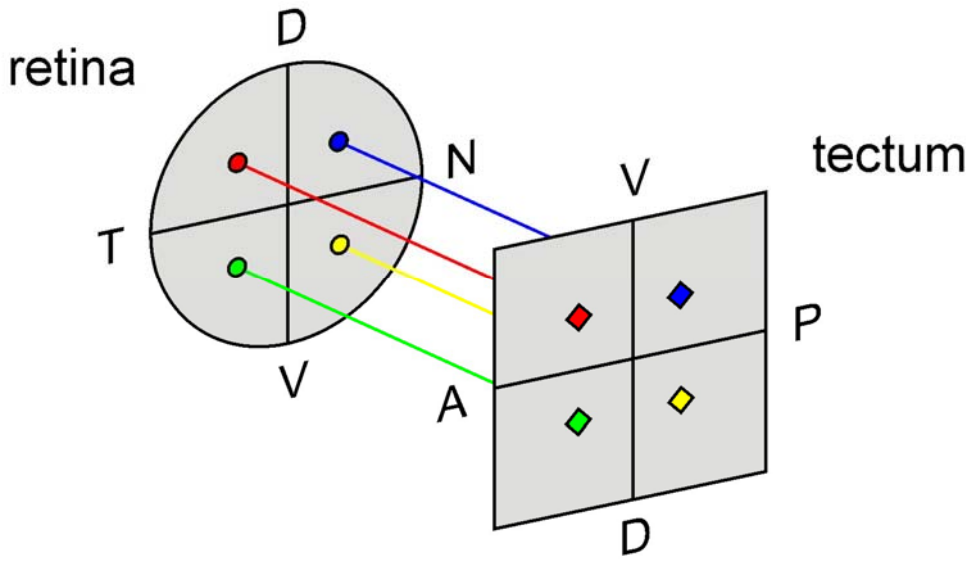

Figure I-1. Schematic Axon Connection Pattern of the Retinotectal Projection.

Depicted are the axonal connections between retinal ganglion cells and tectal nerve cells. The temporal-nasal axis (N/T) of the retina is mapped to the anterior-posterior axis (A/P) of the tectum, whereas dorsal retinal axons are connected with the ventral tectum and ventral retinal axons with the dorsal tectum. Neighbouring RGC send their axons to neighbouring tectal neurons (=topographic map).

Mechanisms of Topography Formation

Roger Sperry demonstrated, that after cutting the optic nerve of fishes or amphibians, retinotectal connectivity was rigidly regenerated even when the eye was rotated, leading to grossly maladaptive animal behaviour (Sperry, 1943, 1963). Furthermore, he found that after ablation of the temporal retina, axons from the remaining nasal half terminated only in the posterior part of the tectum.
Thus, he showed that axons were passing free termination sites in the anterior tectum, choosing to grow to the more distant, but correct target cells instead. These observations led Sperry to formulate his ground-breaking chemoaffinity theory. Due to the observed target selectivity, he postulated chemical markers on retinal and tectal cells which would enable the axons to match the appropriate target positions.
However, he also noted that due to the vast number of nerve cells in the brain, the information stored in the genetic material of an organism might be insufficient to endow every single nerve cell with a unique chemical label. Thus, he proposed that the positional information could instead be conveyed by concentration gradients of only a few molecules.
First evidence about a molecular guidance mechanism was gained by Friedrich Bonhoeffer (Bonhoeffer and Huf, 1980, 1982, 1985). He showed that temporal axons are capable of discriminating between anterior and posterior sections of the tectum *in vitro*. If temporal axons were cultured on tectal monocellular layers, they predominantly avoided the posterior tectal cells and instead preferred to grow on anterior tectal cells. Nasal axons, however, did not show any preference.

Subsequently, to show that the putative guidance cue would have to be membrane-bound, retinal explants were cultured on isolated cell-membrane vesicles made from different parts of tectal tissue instead of tectal monocellular layers were used (Walter *et al.*, 1987b). These membrane substrates were presented as alternating stripes orthogonal to the explant, hence the name “stripe assay”. Temporal axons avoided to grow on membranes prepared from the posterior third of the tectum in such a stripe assay. Nasal axons, again, did not show any preference.

Most surprisingly, the anterior preference of the temporal axons could be abolished by heating or treatment with phosphoinositide-specific phospholipase C (PI-PLC) of the posterior, but not the anterior membranes (Walter *et al.*, 1987a; Walter *et al.*, 1990). This indicated the existence of a GPI-anchored, repulsive protein in the posterior membranes that is responsible for the observed behaviour of temporal retinal axons, which is in fact "posterior avoidance" rather than "anterior preference". Further experiments demonstrated that this repulsive activity could be found in gradual amounts in tectal membranes prepared from different parts along the anterior-posterior axis of the tectum (Bonhoeffer and Huf, 1982). These seminal experiments demonstrated the existence of a repulsive gradient of a chemoaffinity cue on the tectum.

The availability of the stripe assay as functional axon guidance assay facilitated the identification of the molecular underpinnings of this repulsive activity, which were later characterised as members of the GPI-anchored ephrinA protein family (Cheng *et al.*, 1995; Drescher *et al.*, 1995). Using *in situ* hybridisation, ephrinA5 (then called RAGS) and ephrinA2 (formerly ELF-1) were shown to be expressed in anterior < posterior gradients in the chick tectum. Moreover, stripe assays with membranes derived from ephrinA2 over-expressing cells reproduced the decision behaviour of nasal and temporal axons in the original stripe assay with native tectal membranes (Nakamoto *et al.*, 1996).

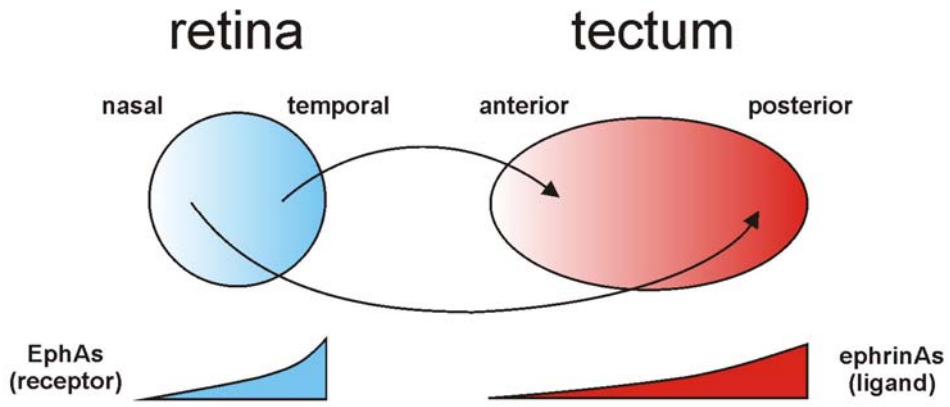

Figure I-2. "Text-book" Model of Topographic Map Formation.

Shown is the current model of a mechanism that topographically maps the retinal n / t axis to the tectal a / p axis. Topographic mapping is achieved by an interaction between graded EphA receptors on the retinal axons that detect graded ephrinA guidance signal in the tectum to identify the correct target position. However, this model does not incorporate additional gradients of ephrinAs found in the retina and EphA gradients in the tectum.

EphrinA2 and ephrinA5 were shown to be ligands for the EphA receptor family, which is expressed in a temporal > nasal gradient in the chick retina (Cheng et al., 1995; Marcus *et al.*, 1996). Furthermore, ephrinA knock-out experiments in mice reinforced the importance of those molecules during the development of the retinotectal projection (Feldheim *et al.*, 2000; Frisén *et al.*, 1998).
Those findings essentially corroborated a “text-book model” of RTP formation (Figure I-2) suggesting that graded sensitivity of retinal growth cones (receptor) leads to a differential stop reaction in the guidance cue gradient (ligand) in the tectum.

Limitations of the Chemoaffinity Theory

The chemoaffinity theory was quite successful in explaining the basic phenomena characteristic for topographic projections. However, several *in vivo* and *in vitro* experiments are not consistent with rigid chemoaffinity (Fraser and Hunt, 1980; Goodhill and Richards, 1999).
In vitro assays have been used extensively to understand the molecular mechanisms of topography formation. However, most *in vitro* assays show an unexpected response of the retinal axons. That means, either all axons react in similar fashion to the guidance cues or, as e.g. in the original stripe assay, a binary response is seen with temporal axons being sensitive to the guidance cues, whereas nasal axons are not responsive at all. These observations are in fact inconsistent with the “text-book model” that predicts either graded or at least topographically differential axon growth behaviour.
Furthermore, clear evidence for the role of interactions between axons during topographic map formation was recently provided by ingenious knock-in experiments (Brown *et al.*, 2000). In this study the authors analysed mice which expressed in nearly half of the RGCs scattered all over the retina, in addition to the native EphA receptors, an EphA3-construct. Thus, RGCs with higher than usual receptor amounts (knock-in, $EphA3^{+}$) are situated next to wild-type RGCs ($EphA3^{-}$). Most notably, a map duplication with one map formed by the knock-in the other one by wild-type RGC axons was reported.

As expected the knock-in map was confined to the anterior part of SC in accordance with their supposed higher sensitivity to the collicular ephrinAs. Surprisingly, the wild-type map, though unaltered in their EphA expression, was compressed, but into the posterior part of the SC. The authors proposed that the wild-type RGC axons might be pushed from the anterior SC by their knock-in counterparts due to the elevated EphA3 receptor in the knock-ins, thus clearly establishing a contribution of fibre-fibre-competition to topographical axon targeting *in vivo*. The actual molecular mechanism for fibre-fibre-interactions is, however, still elusive.

It is a major drawback of all chemoaffinity models that a rigid matching between the gradients on the projecting and the target area is mandatory to achieve a topographic mapping. However, unless these two gradient systems are set-up concomitantly by synchronized mechanisms during development, which is rather unlikely, achieving a precise gradient matching is by far non-trivial. The explanatory power of existing models is thus considerably reduced. Since a correct topographic projection is formed *in vivo* despite expected perturbations, mechanisms must exist that provide robustness and adaptation to the situation provided by the gradients.

It was recently shown that retinal growth cones might be able to adapt to guidance cues (Rosentreter *et al.*, 1998). In these experiments retinal axons growing out from a temporal retinal explant were confronted with an increasing concentration gradient of posterior tectal membranes. All temporal axons entered those gradients and subsequently showed avoidance at exactly reproducible tectal membrane concentration values. However, when the explant was placed on a “concentration pedestal” of tectal posterior membranes in front of and underlying the gradient, axons invaded the gradient and reached higher absolute concentrations than without pedestal.

Further evidence for RGC growth cone adaptation was reported by von Philipsborn and co-workers (von Philipsborn *et al.*, 2006). The authors used micro-contact printing (μCP) to reproducibly fabricate substrate-bound linear ephrinA gradients. When temporal retinal explants were placed in front of those gradients, retinal growth cones showed a distinct stop reaction, which was dependant on the slope of the used ephrinA gradients.

However, precise quantification revealed that the growth cones did not stop at the same absolute ephrinA concentration in gradients of different slopes. It appeared that the steeper the gradient, the higher the ephrinA concentration the retinal growth cones were able to tolerate.
Since these findings are inconsistent with rigid chemoaffinity, both groups suggested that the retinal axons are adapting to the local ephrinA concentration in the ephrinA gradients.

Quantitative Models of Topographic Guidance

Theoretical modelling substantially contributed to a thorough understanding of topography formation and a large number of different models addressing several aspects of topography formation were developed [see e.g. (Fraser, 1980; Gierer, 1981; Goodhill and Richards, 1999; Prestige and Willshaw, 1975; von der Malsburg and Willshaw, 1977; Willshaw and von der Malsburg, 1979)]. However, a comprehensive model, which is capable of explaining the entirety of all biological properties of the system, is still missing.
Instead of a historical review of theoretical approaches to RTP formation, in the following, models are presented, which are of importance for this work.
Among the first, who pioneered a quantitative approach to chemoaffinity, Alfred Gierer pointed out that the observed directional growth of the axon towards its target position could not be explained by a random search mechanism of the growth cone for chemical markers on the tectum (Gierer, 1981). In fact, the axonal targeting is more consistent with steering of the RGC growth cones in a two-dimensional guidance potential within the tectal field towards a minimum or maximum. At this extreme value all directional information is neutralised and the growth cone stops. Furthermore, Gierer suggested that such a potential might be realized by counter-acting effects on axonal growth realised by chemical gradients in each of the dimensions of the retina and tectum.
The position of the minimum or maximum is then specified by a relative influence of those antagonistic effects on retinal axons, which is determined by the amount of chemical markers present on different retinal axons.

A simple one-dimensional potential along one axis, thus, can be generated e.g. by two chemical gradients in the tectum (i.e. the two tectal gradients are monofunctional and functionally opposing each other).

Alternatively, it is also possible that a one-dimensional potential is generated by just one gradient in the tectum. In this case, the tectal gradient must thus be comprised of a bifunctional molecule with two concentration dependant properties: This molecule should first attract and then repel axons depending on its concentration. The switch needs to occur at concentration values representing the axon's topographic target position (Gierer, 1983; Gierer, 1987).

Based on Gierer's potential model, Hisao Honda developed a time-discrete "servo-mechanism" model (Honda, 1998). This model is a simple implementation of the "text-book model" of RTP formation (Figure I-2). That means it only considers an interaction between a graded EphA receptor on retinal axons and a graded ephrinA on the target for topographic axon guidance. Thus, utilizing only one gradient per tectal axis, according to Gierer, the tectal ephrinA needs to be bifunctional to generate topography. The algorithm suggested by Honda calculates the local guidance potential by generating a difference D between a mass-action product, representing the EphA-ephrinA signalling ([EphA]*[ephrinA]) at a certain position on the target, and a reference value S intrinsic to all retinal axons. A retinal axon stops at the position which satisfies D=0. Simulation of the actual axon growth occurs iteratively with the growth cone calculating in each step the guidance parameter D at its current position and at a randomly chosen neighbouring position in the field.

To introduce statistical fluctuations, both D values (present versus prospective position) are fed into a Gaussian error function to determine the probability p to occupy these fields. The probability to stay at a certain position is low when the growth cone is far off from the prospective target position and higher if it is close to its target. Additionally, all axons were assigned a tendency Q_x to choose preferentially a surround field towards the distal end of the simulation field.

Due to its intuitive approach to the problem, Honda's axon growth algorithm was used in this work. However, the algorithm describing the signalling and guidance potential generation for the retinal growth cones was replaced to be more consistent with recent experimental evidence and the *in vivo* situation.

Questions & Aims

Recent research suggests that many guidance molecules and signalling events might contribute to topographic map formation in the brain. Thus, in the past, many theoretical models were published to facilitate accurate predictions of the system's behaviour. Surprisingly, there is nevertheless no model of RTP formation currently available that incorporates all experimentally demonstrated guidance molecules in the system. Therefore, it is the aim of this work to contribute to a comprehensive model of topography formation by incorporating the major guidance cues and potentially arising interactions.
The current "text-book model" of RTP formation suggests a molecular interaction of retinal EphA receptors and tectal ephrinA ligands to explain topographic map formation. However, the existence of additional gradients provides the basis for more molecular interactions that may contribute to topographic guidance, that is reverse signalling, a receptor / ligand interaction in *cis* and fibre-fibre-interactions. A signal-transduction cascade will be proposed that integrates those interactions. Furthermore, simulations of classic *in vitro* experiments are carried out to validate the model's performance. The contribution of fibre-fibre interactions and of axonal receptor / ligand *cis*-interactions to topographic mapping is also examined by simulation of published *in vivo* and *in vitro* experiments. Finally, it is attempted to incorporate adaptation into the presented chemoaffinity model, which was shown to exist *in vitro* and *in vivo*.

In this work, only mapping of the retinal temporal-nasal axis to the anterior-posterior axis of the tectum was investigated. Basic experimental evidences that were used for developing this model came exclusively from studies on the chick retinotectal projection.

II. Materials & Methods

A. Materials & Organisms

1. Chemicals

H_20 stands for deionized water from a TKA MicroLab Pure Water System (TKA, Niederelbert).

If not mentioned explicitly, chemicals were obtained from Sigma-Aldrich (http://www.sigmaaldrich.com/) or Roth (http://www.carl-roth.de/) and were at least of analytical quality.

1,4-Dioxane	Sigma, #42510, http://www.sigmaaldrich.com/
4-Nitrophenyl phosphate	Sigma, #71768
6-Nitroveratryl chloroformate (NVOC-Cl)	Aldrich, #420069
Alexa Fluor 488 phalloidin	Invitrogen, #A12379, http://www.invitrogen.com/
Bovine Serum Albumin (BSA)	Sigma, #A3059
Cy3 // Cy5 Mono-Reactive Dyes	Amersham, PA23001 // PA 25001, http://www.gelifesciences.com/
Diethanolamine	Sigma, #31589
Ethanol	Roth, #9065.3, http://www.carl-roth.de/
HEPES	Roth, #9105.3
Hydroxylamine hydrochloride	Fluka, #55459
L-Glutamine	GIBCO, #25030-081, http://www.invitrogen.com/
Methylcellulose	Roth, #8421.1
MOWIOL	Hoechst
Natural Mouse Laminin	Invitrogen, #23017-015
Penicillin / Streptomycin	Sigma, #P0781
Propyl gallate	Sigma, #P3130
Semicarbazide hydrochloride	Fluka, #84940, http://www.sigmaaldrich.com/
Sulfo-NHS-LC-Biotin	Thermo Scientific Pierce Protein Research, #21327, http://www.piercenet.com/

2. Solutions, Buffers, Media

If not stated otherwise, H_20 was used as solvent. Listed pH values are in reference to room temperature conditions (RT).

ELISA reaction buffer	Diethanolamine	95 ml / l
	1M $MgCl_2$	1 ml / l
	adjust pH to 9.5 with 5M HCl	
ELISA substrate	ELISA reaction buffer	
	4-Nitrophenyl phosphate	2,23 g / l
F12-KM	F12 Nutrient Mixture (Invitrogen, 21700-026), 4x	
	FBS	10% v / v
	CS	2% v / v
	Penicillin/Streptomycin	10 U / ml
	L-Glutamine	146 mg / l
F12-MZ	F12-KM	
	Methylcellulose	0,4% w / v
Fixative	Saccharose	113 g / l
	Paraformaldehyde	4 % v / v
	in PBS at pH=7,4	
Hanks' Solution (w/o Ca^{2+} / Mg^{2+})	NaCl	8 g / l
	KCl	0,4 g / l
	NaH_2PO_4	60 mg / l
	$Na_2HPO_4 \bullet 2H_2O$	60 mg / l
	$NaHCO_3$	0,35 g / l
	Glucose	1,0 g / l
	HEPES	4,8 g / l
	Phenolrot	10 mg / l
	pH=7,4	
PBS	NaCl	8 g / l
	KCl	0,2 g / l
	$Na_2HPO_4 \bullet 2H_2O$	1,15 g / l
	KH_2PO_4	0,2 g / l
	pH=7,4	

Fetal Bovine Serum	PAA, #A15-151, http://www.paa.com/
Chicken Serum	GIBCO, #16110-082, http://www.invitrogen.com/

3. Antibodies

Goat anti human IgG (H+L), Alexa Fluor 488	Invitrogen, #A11013, http://www.invitrogen.com/
Goat anti human IgG (H+L), Alexa Fluor 594	Invitrogen, #A11014

4. Recombinant Proteins, Enzymes

Human ephrin-A5/Fc Chimera	R&D Systems, #374-EA, http://www.rndsystems.com
Human IgG-Fc Fragment	Calbiochem, #401104 (http://www.merckbiosciences.co.uk/html/CBC/home.html)
Mouse EphA3/Fc Chimera	R&D Systems, #640-A3
Mouse ephrinA2/Fc Chimera	R&D Systems, #603-A2
NeutrAvidin Protein, Alkaline Phosphatase Conjugated	Thermo Scientific Pierce Protein Research, #31002, http://www.piercenet.com/

5. Miscellaneous Materials

96-well plates	Nunc, #446442, http://www.nuncbrand.com
Cover slips	Menzel-Gläser, Braunschweig
Filter paper	Whatman, #10311611, http://www.whatman.com/
Mixed cellulose ester filter, 0,45µm	Whatman, #10409770
Petri dishes	Greiner, Nunc
Reaction vials	Greiner, Sarstedt
Sephadex G-25	Pharmacia AB Biotechnology, #17-0033-01, http://www.gelifesciences.com/

6. Organisms

Tissue culture experiments were performed using White Leghorn chicken embryos obtained from Lohmann Tierzucht GmbH (http://www.ltz.de/). Fertile hatching eggs were laid into an egg incubator (37°C, 60% humidity, automatically turning every 6h) and used at embryonic day six or seven (E6-7) for retina preparation.

7. Hard- and Software

Centrifuge 5417R with Rotor F45-30-11	Eppendorf
Confocal LSM Microscope TCS SP5	Leica, Microsystems AG, Wetzlar
Custom Made LED	Klaus Trampert (LTI, TH Karlsruhe)
Egg Incubator	Grumbach Brutgeräte GmbH,
ELISA-Reader TECAN Safire^2	TECAN, Crailsheim
Hamilton Syringe	Sigma, #58382
Hand-held UV Lamp, 365nm, 6W	Benda Laborgeräte, Wiesloch
Mikroskop, Axioplan (ZEISS, Oberkochen) + 3CCD Color Video Camera (Spot, Visitron Systems) with PC and Image-Analysis Software	
Precision Balance R160P	Sartorius, Göttingen
Silicone Matrices	Zhongxiang Jiang (AG Bastmeyer)
SteREO Discovery.V8	ZEISS, Oberkochen
Tissue Chopper McIlwain	Mickel Laboratory Engineering, Guildford UK
Tissue Culture Incubator	Binder GmbH, Tuttlingen
TKA MicroLab Pure Water System	TKA, Niederelbert
Adobe Photoshop CS2	Adobe Systems, San Rose, US (http://www.adobe.com)
MATLAB 7.8.0.347	The MathWorks Inc; Natick, US (http://www.mathworks.com)

B. Methods

1. Preparation, Fixation and Staining of Retinal Explants

Retinae of embryonic day 6-7 chick embryos were dissected in ice-cold Hanks' medium and cut parallel to the temporal-nasal axis in 250µm wide stripes. The retinal explants were placed perpendicular to the stripes on the respective substrates, tethered with metal weights and grown in F12-MZ medium. After 20-24 hours, the retinal explant cultures were fixed for 30 minutes at RT with 4% Paraformaldehyde in PBS containing 0.33M Saccharose. Subsequently the cultures were washed with PBS, permeabilized with 0.1% Triton X-100 in PBS and stained with 0.1µM Alexa-594 phalloidin (diluted 1:50 in 1% BSA from stock solution prepared according to the manufacturer's recommendation). Then the cultures were embedded in MOWIOL and photographed using an Axioplan microscope (Zeiss) and a CCD camera (Spot, Visitron Systems). Images were further processed with Photoshop CS2 software (Adobe).

2. Stripe Assay with Substrate of Alternating EphA3-Fc and ephrinA2-Fc Stripes

For single stripe assays with EphA3-Fc, a modified stripe assay (Hornberger *et al.*, 1999; Vielmetter *et al.*, 1990) was performed. Briefly, a silicon matrix containing parallel channels of 90µm width on its surface was placed upside down onto a petri dish.

Purified EphA3-Fc fusion protein in PBS was used at a concentration of 30µg/ml. Alexa594-labeled anti-human Fc antibody was added to a final concentration of 2µg/ml to allow for discrimination of the stripes. Subsequently, 50µl of the solution was injected into the matrix channels and bound by absorption from solution to the surface of the dish for 3 hours at 37°C. Single stripe experiments with ephrinA2-Fc were performed with 16µg/ml purified ephrinA2-Fc clustered with 48µg/ml Alexa594-labeled anti-human Fc antibody in PBS for 30min at room temperature. For protein-printing, the matrix' channel field was covered with the protein solution for 30min at 37°C, washed with dH_2O and dried with a stream of N_2.

The matrix was then placed with the channel field upside down in a petri dish and removed after 3 hours at 37°C. In this way, the ephrinA2 protein was transferred from the bars of the silicone matrix to the plastic surface.
The remaining binding sites on the plastic surfaces were coated with Laminin (20µg/ml) in Hanks' Solution for 1 hour and the substrate was then covered with F12 culture medium prior to use. Alternating stripes of ephrinA2-Fc and EphA3-Fc were fabricated by first printing ephrinA2-Fc onto the petri dish as described above. Afterwards the EphA3-Fc solution was injected into the channels and allowed to adhere, thereby generating separated alternating stripes of both proteins. EphA3-Fc could not be printed first, because it seemed to loose its activity during the protein printing procedure.

3. Protein Modifications

Biotinylation of EphA3-Fc

To obtain labelled EphA3-Fc, the protein was first diluted in 0.2M carbonate buffer at pH 8.3 to a final concentration of 2mg/ml. Then freshly prepared Sulfo-NHS-LC-Biotin in H_20 was added such that the reaction solution contained 0.5mM Biotin. The biotinylation reaction was allowed to proceed for 30 minutes at room temperature. To stop the labelling reaction and to quench remaining reactive NHS-LC-Biotin molecules in the solution, 1.5M hydroxylamine hydrochloride was added to a final concentration of 140mM and the solution incubated for an additional 30 minutes. Subsequently, the bioEphA3 protein solution was diluted in PBS to a concentration of 15ng/µl and kept at -20°C until use.

Caging of ephrinA5-Fc

Proteins were caged using a chemical compound (6-Nitroveratryl chloroformate, abbreviated NVOC-Cl) which reacts with amino-groups of exposed Lysines. Review of structural data showed two exposed Lysines in the binding surface of ephrinA5 to EphB2. No structural data existed about EphA3.

Therefore, the reaction mixture was prepared by diluting ephrinA5-Fc in 0.1M sodium carbonate buffer (pH 9.9) such that the final concentration was 0.2µM. The caging compound NVOC-Cl in dioxane was added to a final concentration between 20µM and 400µM NVOC-Cl (note: the NVOC-Cl-dioxane mixture was stable and yielded consistent reduction of binding activity of ephrinA5-Fc for a few months when stored at -20°C). The reaction was then allowed to proceed for 30min at room temperature in the dark. Caging was found to be highly pH-sensitive. To stop the reaction and to adjust the protein concentration for further applications, 0.1M acetate buffer pH 5.4 was subsequently added.

Labelling of proteins with fluorescent dyes

Fluorescent probes of ephrinA5-Fc or EphA3-Fc were prepared by dilution of 1mg/ml protein in 0.1M carbonate buffer (pH 9.5). Then 50µg/µl Cy3 or Cy5 Mono NHS ester in DMSO were added to a final concentration of 1µg/µl and allowed to react for 30min at room temperature. Afterwards, unbound dye was separated from the protein solution at 4°C by gel permeation chromatography through a Sephadex G-25 column using PBS as the eluent.
The dye/protein ratio was calculated by measuring the optical density at 280nm and the dyes excitation wave length (552nm for Cy3, 650nm for Cy5) and using the formula provided in the manufacturer's labeling instruction. Dye/protein ratios usually were between 3 and 7 with this protocol.

4. Enzyme-linked Immunosorbent Assay (ELISA)

For determining the binding activity of ephrinA5, caged or uncaged protein was bound to the plastic surface of PolySorp 96-well plates (Nunc) and then detected using biotinylated EphA3-Fc and NeutrAvidin alkaline phosphatase / Nitrophenyl phosphate colour reaction. Caged or uncaged ephrinA5-Fc diluted in 0.1M acetate buffer pH 5.4 was bound overnight at room temperature to the plastic surface of PolySorp 96-well plates. After washing, the wells were filled with acetate buffer pH 5.4 containing 50mM Semicarbazide hydrochloride. Then a custom made LED engine emitting 375nm UV light was placed on top of the wells at a distance of d=5cm.

Irradiation time was generally between 0 and 60 minutes. After irradiation, wells were washed and free binding sites were blocked with 10mg/ml BSA in PBS for 1h at RT. Subsequently, bioEphA3-Fc in 10mg/ml BSA in PBS was added to each well at a concentration of 1.5µg/ml and allowed to bind for 2h at RT. After additional washing with 10mg/ml BSA in PBS, 2µg/ml NeutrAvidin alkaline phosphatase in the same buffer was added to each well and incubated for 30min at RT. Wells were washed again with PBS and afterwards allowed to equilibrate in ELISA reaction buffer for at least 5min at RT. Reaction was started by adding Nitrophenyl phosphate to a final concentration of 6mM and the colour reaction was followed at 405nm with an ELISA reader until the highest OD reached a value of 1 (usually after 40minutes). Standard curves were obtained using 150ng, 100ng, 75ng, 50ng, 37.5ng, 18.75ng and 0ng ephrinA5-Fc per well.

5. Light-patterning of Substrates

An alternative way to fabricate substrates of alternating stripes of ephrinA5-Fc and EphA3-Fc is light-patterning after prior caging of the proteins. The silicone matrices for substrate generation in the modified stripe assays were used here as well. EphA3-Fc and ephrinA5-Fc were mildly caged (protein:NVOC ratio: 1:108) and after dilution with 0.1M Acetate buffer pH 5.4, 30µg/ml caged ephrinA5-Fc was injected into the channels of the matrices. After 3h at 4°C the channels were injected with Laminin in Hanks' Solution (17µg/ml) and incubated for 30min at room temperature.

Then the channels were flushed with PBS, the matrices were removed and the whole substrate covered with caged EphA3-Fc (EphA3 caging proved to facilitate the separation of both receptor and ligand). After an additional incubation of 3h at 4°C, the substrate was washed again and then covered with acetate buffer (pH5.4) containing 50mM Semicarbazide hydrochloride. Irradiation was performed with a 6W hand-held 365nm UV Lamp for 2h (calculated dosage: 9.3Ws/cm^2). Spectra and intensities for the hand-held UV Lamp and the LED engine were obtained beforehand to calculate the required irradiation times for comparable levels of UV dosages.

The whole substrate was subsequently blocked again with Laminin in Hanks' Solution (17µg/ml) for 30min at room temperature and stained, first with Cy3-labelled EphA3-Fc and then Cy5-labelled-ephrinA5 (1:50 from stock solution in 1% BSA).
The protein substrates were embedded in MOWIOL and analysed using a Confocal LSM Microscope (Leica).

6. Model Descriptions & Simulations

Simulations were performed using custom programs written for MATLAB 7.8 (The MathWorks, Inc; Natick, MA). The basic algorithm for simulation of the actual axon growth used in this study was derived from the "servo-mechanism" model proposed by Honda (Honda, 1998). In short, the simulation field, in which growth cones were placed, was represented by a rectangle of 100 x 100 or 200 x 100 increments carrying the guidance cues. Axon outgrowth occurred iteratively. In each step the growth cone calculated the local guidance potential D at its current position and at a randomly chosen neighbouring position. Subsequently, both D values were fed into a simple Gaussian error function with standard deviation σ to account for detection sensitivity of the growth cone:

$$erf = \frac{1}{\sigma\sqrt{2\pi}} e^{\frac{-D^2}{2\sigma^2}}$$

The two probability values (present vs. potential position) were then used to determine if the growth cone will stay within the current field or if it should moved to the chosen position. The different program versions used in this study mainly differed in the way the guidance potential D (see below) was calculated. Minor changes to the above described axon growth algorithm were introduced as well depending on the experimental situation that was simulated and are mentioned where applied.

Simulation of the "Text-book Model" of RTP formation (v0.1)

For simulation of the "text-book model", growth cones were placed in the simulation field and were assigned EphA receptor values R_a according to their position in the retina x_a:

$$R_a(x_a) = e^{0.03\,(x_a - 50)}$$

The ligand substrate L_t in the simulation field had either a homogeneous, striped, concentrically or linearly graded distribution according to the equations given in the respective figure legends in chapter III-A. As suggested by Honda, the local guidance potential was calculated as difference between a global reference value S and the strength of the EphA-ephrinA signalling (R_a*L_t):

$$D(x_t, y_t) = \left| S - R_a \cdot L_t(x_t, y_t) \right|$$

Thus, in a ligand gradient which matches the axonal receptor gradient, a retinal growth cone stops at the tectal position where D=0 (guidance potential minimum).
The original "servo-mechanism" model of Honda (Honda, 1998) introduced a global tendency of the growth cones to extend to the distal end of the simulation field. In contrast, for the simulations of the "text-book" model each growth cone was assigned a tendency Q_x to preferentially choose a surround field in the direction of previous growth. That means, the growth cone calculates a mean direction over a pre-determined number of past steps and chooses in the next step with high probability a surround field which lies in the same direction.

Novel Counter-Gradient Model of Topography Formation (v0.2 & v0.25)

In simulations of the presented counter-gradient model, growth cones were endowed with reciprocal exponential levels of EphA receptor R_a and ephrinA ligand L_a according to their position x_a in the retina:

$$R_a(x_a) = e^{-b(x_a - 50)}$$
$$L_a(x_a) = e^{b(x_a - 50)}$$

The steepness b of the exponential gradients in the retina was 0.01 or 0.03 and is indicated where applied. The substrates consisted either of reciprocal exponential tectal ligand and receptor gradients or of parallel ligand and/or receptor stripes each of constant value (for the equations used for substrate simulation please refer to the respective figure legends in chapter III-B to I).
Due to the proposed signalling integration, the local guidance potential $D(x_t,y_t)$ for a particular retinal growth cone was given by:

$$D(x_t,y_t) = \frac{L_a \cdot [R_t(x_t,y_t) + R_a + R_{\hat{a}}(x_t,y_t)]}{R_a \cdot [L_t(x_t,y_t) + L_a + L_{\hat{a}}(x_t,y_t)]}$$

R_a, $R_{\hat{a}}$, $R_t(x_t,y_t)$ represent axonal and tectal EphA receptor concentrations at tectal position (x_t,y_t) whereas L_a, $L_{\hat{a}}$ and $L_t(x_t,y_t)$ stand for axonal and tectal ephrinA ligand concentrations at the same position. L_a*R_a and R_a*L_a symbolise EphA receptor / ephrinA ligand interactions occurring on one axon (*cis*-interactions), whereas L_a*$R_{\hat{a}}$ and R_a*$L_{\hat{a}}$ describe EphA receptor / ephrinA ligand interactions with neighbouring axons (fibre-fibre-interactions).

A growth cone reaches its target point when forward and reverse signalling are exactly balancing each other, i.e. when D acquires the numerical value of 1. Thus, for mathematical reasons, a logarithmic function was introduced to adapt the guidance potential to the error function.

$$p(x_t, y_t) = erf\left[\left|\ln D(x_t, y_t)\right|\right]$$

As in the original “servo-mechanism” model all axons were assigned a global tendency Q_x to grow to the distal end of the simulation field.
In case the growth cone successfully changed its position, the programme deposits at the previous position in the simulation field the respective ligand and receptor values of the growth cone. In this way, the trajectory of the axon is traced in the simulation field and other growth cones can interact with the axonal receptor and ligand. Implementation wise, it is easier to use the axon trajectory instead of the axon itself, but due to that, minor changes to the algorithm were introduced. The unaltered algorithm results in axonal ligand and receptor being placed at the previous position of a growth cone. However, since the previous position is in the next step also a potential target position this may lead to erroneous axon behaviour. In other words, the growth cone might be pushed forward by its own axon. Thus, a correction routine was introduced, that clears the surround field of a growth cone (Figure III-7) from its own receptor and ligand values and does not allow an interaction of one growth cone with its own axon for the next 10 iteration steps

For simulations of the EphA3 knock-in experiments (v0.25), the guidance potential D was not only incorporating the guidance cue concentration value seen at the current and potential future growth cone position, but the mean concentration value in the respective surround field (3x3 cells), thus increasing the potential influence of interactions between growth cones. Furthermore, Q_x was dynamically adjusted and coupled to the topographical signal D such that Q_x showed became zero at the respective collicular target point of the growth cone and positive or negative before or after the target point.

Adaptation Model (v0.3)

The modelling of adaptation during topographic guidance was based on the presented counter-gradient model (v0.2). However, in each step, the axonal receptor and/or ligand concentrations changed depending on previous encounters of ligand or receptor substrate. In particular, a growth cone calculated the reciprocal mean of the tectal ligand L(t') or receptor values seen in the past. Then this mean was weighted with an exponential decline function to account for a long-term or short-term memory of the growth cones ($\tau \to \infty$: long-term memory; $\tau \to 0$: short-term memory). Thus, the adapted axonal receptor at each time step was:

$$R_{adapt}(t) = \frac{1}{\frac{e^{-t/\tau}}{\tau} \sum_{t'=0}^{t} L(t') \cdot e^{t'/\tau}}$$

The adapted axonal ligand was calculated using the underlying inverse relationship with the axonal receptor. The local guidance potential D and growing probabilities were determined as before according to the novel counter-gradient model (v0.2).

III. RESULTS

Topographic maps are a salient organizational feature of almost all centralized nervous systems throughout the animal kingdom. They are used to spatially encode environmental information in the brain. Topographic maps are characterised by neighbouring neurons in the projecting area being connected with neighbouring neurons in the target. Thus, the spatial order within the stimulus is recast in higher brain areas. The best-studied model system for topographic projections is the retinotectal projection (RTP) of lower vertebrates, the axonal connection between the retina in the eye and the tectum in the midbrain. The formation of the retinotectal projection is commonly explained by an interaction of complementary graded chemical markers in retina and tectum. These markers label positions in retina and tectum such that retinal axons can find their correct target position in the tectum according to their position in the retina.

A. Computational Modelling to Understand the Functional Properties of Topographic Guidance Cues

Axons from different positions in the retina enter the sheet-like tectal surface and grow directly to the topographically correct target zone in the tectum (Fujisawa, 1981; Fujisawa *et al.*, 1981a, b). This suggests that an axon's guidance towards a topographic target may be mathematically described as growth in a two-dimensional potential field towards a minimum or maximum. Alfred Gierer pointed out that such a potential can be realised by antagonistic chemical gradients along each of the dimensions of the tectum (Gierer, 1981). The position of the respective minimum or maximum would then be specified by the relative influence of those antagonistic tectal gradients on retinal axons, which is determined by the axons' topographical identity encoded by their own chemical markers.

Along one target axis, such a guidance potential can for instance be generated by two functionally antagonistic gradients on the tectum (each monofunctional, i.e. either repulsive or attractive).

Alternatively, this potential can also be generated by just one graded molecular species in the tectum, provided that is has two opposing effects on axonal guidance (bifunctional, i.e. attractive and repulsive). The functional switch must then occur at the axon's topographic target position.

With respect to the tectal anterior / posterior-axis, the current "text-book model" of RTP formation suggests that a singular ephrinA protein gradient in the tectum is detected by EphA proteins on the retinal axons. According to Gierer, this model generates topography only when the ephrinA is bifunctional. However, it was also shown that in addition to the tectal ephrinA gradient a counter-gradient of EphAs, which shows axon guidance functions, exists (Gebhardt, 2005; Rashid *et al.*, 2005). Furthermore, in addition to the retinal EphAs, a counter-gradient of ephrinAs was reported to exist (Hornberger et al., 1999). Thus, the tectal ephrinA might indeed be monofunctional and constitutes the guidance signal only in combination with the tectal EphA gradient. Theoretical modelling of a biological problem can help to formulate, investigate or reject hypotheses. Therefore, as a first step a computational model was used to examine the guidance properties of ephrinAs and eventually trying to discriminate between monofunctional and bifunctional guidance through ephrinAs. To this end, published *in vitro* assays of ephrinA function were revisited and simulated with either mono- or bifunctional guidance cues. Subsequently, the simulations were compared to the reported *in vitro* results.

The developed computational model used for these simulations was based on an algorithm suggested by Honda ["servo-mechanism" model, (Honda, 1998)] which is a simple implementation of the "text-book model" of RTP formation. It only considers one retinal EphA gradient and a graded bifunctional ephrinA on the target as axon guidance signal.

In order to achieve topographic mapping, the algorithm suggested by this model iteratively evaluates the guidance potential by calculating a difference D between a constant reference value S intrinsic to all retinal axons and a mass-action term, representing the strength of the EphA-ephrinA signalling ([EphA]*[ephrinA]) at that position on the target. A retinal growth cone should stop at the tectal position where D=0 (guidance potential minimum). This position is topographically differential depending on the amount of EphA that a retinal growth cone exhibits.

Simulation of the actual axon growth in Honda's "servo-mechanism" model occurs iteratively with the sensitive axon tip structure, the growth cone, calculating in each step the guidance parameter D at its current position and at a randomly chosen neighbouring position in the simulation field.

Both D values (present versus potential position) are fed into a Gaussian error function to determine the probability p to occupy these positions. The probability at a certain position is low when the growth cone is far away from the prospective target position (i.e. where the absolute value of D is large) and maximal when it reaches the target (i.e. where D is zero). Therefore, the growth cone tends to move towards its target position at which the reference value S and the EphA-ephrinA signalling are balancing each other.

The original "servo-mechanism" model assigned to all retinal axons a global tendency Q_x to choose with a slight preference a surround field towards the distal end of the simulation field. *In vivo*, this could easily be interpreted in terms of an attractive source for retinal axons at one end of the tectum, but such a source is clearly not existent *in vitro*. Therefore, for this study, an axon-intrinsic and non-global tendency to choose a surround field in the mean direction of the last growing steps, modelling axon rigidity, was introduced.

A bifunctional or monofunctional effect of the guidance cue in the "servo-mechanism" model hinges on the value assigned to S. If S is equal to zero, D is always different from zero wherever the guidance cue is seen. Therefore, the tectal guidance cue acts in a monofunctional fashion. For a bifunctional effect, S has to be adjusted such that it is equal to [EphA]*[ephrinA] at the target position. Thus, the model can be switched between a mono- and a bifunctional mode just by changing S between zero and the respective finite value according to the gradient equations used.

Due to its intuitive approach to the problem the "servo-mechanism" model seems to be well-suited for differentiating between a mono- and bifunctional axon guidance through ephrinAs.

1. Growth Cone Behaviour on Homogeneous Guidance Cue Substrates

According to theoretical considerations, the “text-book model” of RTP formation requires the tectal ephrinA to be bifunctional in order to generate a topographic mapping of retinal axons. The supposedly strongest evidence to date for this type of model was published by Hansen and co-workers (Hansen *et al.*, 2004).

In this study, the authors report experiments in which they cultured retinal explants from contiguous positions along the nasal-temporal axis for a fixed period of time on homogeneous cell membrane substrates containing different amounts of transfected ephrinA2. They observed, depending on retinal position of the explant, a differential and biphasic axon outgrowth response.

In particular, maximum axon outgrowth at a fixed ephrinA2 concentration was shown by explants originating from the middle of the nasal retina and decreased in both nasal and temporal directions. By comparing any particular outgrowth with the corresponding outgrowth when the substrate contained no ephrinA2 (“neutral conditions”) the authors found that the differential outgrowth was caused by an outgrowth promoting effect of pre-target ephrinA2 concentrations and an inhibitory effect of post-target ephrinA2 concentrations.

Although it is hard to understand why an outgrowth on neutral substrate might be the appropriate behaviour at the target, this biphasic response might indicate a bifunctional action of the guidance cue. If this conclusion were true, only a model with a bifunctional ephrinA should be able to reproduce the observed experimental outcome.

Therefore, this experiment was simulated with the original “servo-mechanism” model and the ephrinA was assigned either monofunctional or bifunctional guidance properties.

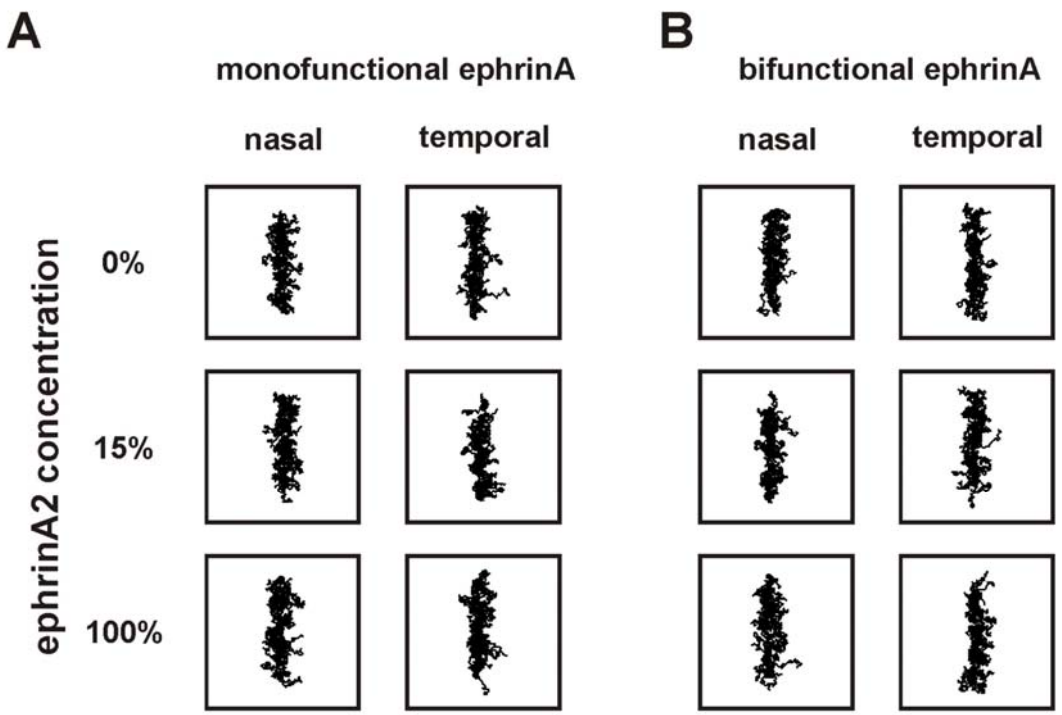

Figure III-1. Simulation of RGC Axon Growth on Homogeneous Mono- or Bifunctional Guidance Cue Substrates.

Retinal explants of temporal (R_a=4.5) or nasal origin (R_a=0.22) growing on homogeneous distributions of different ephrinA concentrations (0%: L_t=0; 15%: L_t=0.675; 100%: L_t=4.5) were simulated (basic gradient equations: $R_a(x_a)=\exp(0.03(x_a-50))$, $L_t(x_t)=\exp(0.03(x_t-50))$). No differential outgrowth was observed on various ephrinA substrates or with explants of different retinal origin. Furthermore, no outgrowth differences were seen between substrates consisting of either monofunctional ephrinA (A) or bifunctional ephrinA (B). (v0.1, 50 growth cones, 100 iterations, sigma=0.1, Q_x=0.1)

In contrast to the experimental observation, no differential axon growth was seen at any ephrinA concentration value or retinal position in those simulations. Even more important, simulations with mono- or bifunctional ephrinA could not be distinguished from each other regarding the axon outgrowth (Figure III-1A and B). Therefore, in contrast to Hansen and co-workers conclusion, an interpretation of their experimental results cannot be derived from the “text-book model” of RTP formation.

The formal concept of topographic axon guidance in a potential field means in particular that a retinal growth cone is guided by concentration differences of guidance cues found at adjacent positions rather than the absolute value at one position.

Vice versa, the experimentally observed axon outgrowth at one particular concentration of a guidance cue concentration is not necessarily an indicator for the guidance cue's directional guidance properties.
Axon outgrowth behaviour on homogeneous substrates according to the "text-book model" is in fact independent of mono- or bifunctional guidance signal properties. In fact, differential axon outgrowth on homogeneous ephrinA substrates is consistent with either mono- or bifunctional guidance cues.

An alternative explanation for the results reported by Hansen et al. would be that the observed differential outgrowth is rather indicative of differential axon growth velocities, which are adjusted according to the axon's position in the potential field. Although not necessarily correlated, it is possible that the cellular mechanisms determining the direction of growth might be coupled to a mechanism controlling the speed of growth.
To explore this hypothesis, the outgrowth normalized to the highest value observed for any retinal position was taken from the original data of Hansen et al. and plotted against retinal position and ephrinA concentration.
EphrinA concentration was expressed here as corresponding tectal position (0% ephrinA: anterior, 100% ephrinA: posterior) calculated with the ephrinA gradient equations used in these simulations (Figure III-2). A maximal outgrowth at tectal position 36 (i.e. 15% ephrinA2 according to the notation used by Hansen et al.) was evident for almost all retinal positions (Figure III-2A**)**.
If growth velocity is indeed coupled to the guiding potential, a correlation of the velocity function and the potential minimum should be apparent.
In a model with bifunctional ephrinA the guidance potential minima for all retinal axons would lie on a diagonal line in a diagram in which tectal position is plotted against retinal position. On contrary, for monofunctional ephrinA, which cannot topographically guide axons without a counter-force, being undoubtedly absent in this experiment, these potential minima would be found at tectal position zero for all retinal positions.

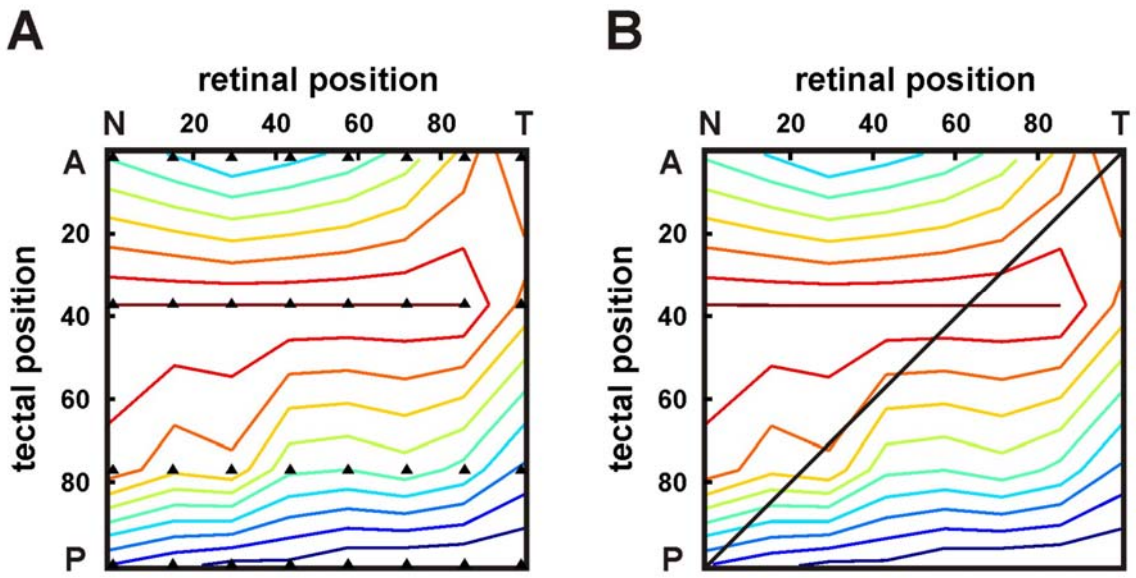

Figure III-2. Analysis of the Differential Retinal Axon Outgrowth on Homogeneous ephrinA2 Substrates Reported by Hansen et al.

Observed retinal outgrowth was taken and normalized to the highest outgrowth value at each retinal position (see Hansen et al., 2004 for detail). These values were then plotted against retinal position and tectal position which were calculated according to the gradient equations ($R_a(x_a)=\exp(0.03(x_a-50))$, $L_t(x_t)=\exp(0.03(x_t-50))$) used for the simulations (A, red contour lines represent highest outgrowth values, blue lines the lowest, black triangles indicate original sampling positions). The axon outgrowth seems to be consistent with a monofunctional guidance cue, since the maximum of the outgrowth velocity function is a parallel line to the potential minima function for monofunctional cues, (expected at tectal position zero for every retinal position). No correlation was apparent with the potential minima suggested by a bifunctional cue (the minima are expected to lie on the depicted diagonal curve representing a topographic map). (B)

The characteristics of the outgrowth velocity function immediately suggests monofunctional properties of ephrinA since the maximum of the outgrowth function is a line parallel to the monofunctional minima curve (at tectal position zero for all retinal positions) rather than a diagonal line as required for bifunctional ephrinA (Figure III-2B).

In summary, computational simulation of the experiment by Hansen and colleagues revealed that the reported differential biphasic behaviour is hardly indicative of bifunctional properties of ephrinAs relevant for topographic guidance. On contrary, even after accounting for secondary effects of ephrinAs on growth velocity, the observed axon outgrowth might rather suggest monofunctional guidance of retinal axons by ephrinAs.

2. Growth Cone Behaviour in Diffusion Gradients of Guidance Cues

Turning assays are regularly used to investigate the properties of diffusible guidance cues. To this end, a growth cone is exposed to a diffusible guidance cue gradient released from a micro-pipette and any trajectory change of the axon, towards or away from the micro-pipette, is recorded. Weinl and colleagues used diffusible ephrinA5 released from a micro-pipette and measured the turning response of retinal growth cones (Weinl *et al.*, 2003). They saw that temporal RGC axons turned towards the micro-pipette, when they were cultured on Laminin suggesting an attractive ephrinA5 effect on axon growth.

This result was surprising given that the stripe assays, performed with substrate-bound ephrinAs against Laminin, clearly pointed to a repulsive effect of ephrinAs rather than an attractive one. However, the authors stated as well that this turning occurred at a high background level of general growth cone collapse, which is usually interpreted as an axon's response to a strong repulsive cue.

In order to see if the “servo-mechanism” model may help to understand these confusing results, axon behaviour in a stable concentric gradient, like the one supposed to be generated through pulsed release from the tip of a micro-pipette, was simulated.

Absolute ephrinA values of the gradient in this simulation were in the range the growth cones usually encounter when topographically growing into a simulated tectum. Again, ephrinA was set to be either mono- or bifunctional. In simulations in which ephrinA was monofunctional, nasal as well as temporal axons always turned away in a curve from the centre of the gradient (Figure III-3A and A').

However, when ephrinA had bifunctional properties, an additional attractive response was observed under certain conditions: If the gradient was quite shallow, nasal and temporal axons grew both towards the gradient centre. If it was very steep they grew both away from the gradient centre. At intermediate steepness, a differential turning was observed with temporal axons being repelled and nasal axons being attracted to the gradient centre until they reached their respective concentration contour line. For simulation of the results of Weinl et al., which showed that temporal RGC axons were attracted by the ephrinA5 gradient, a shallow gradient steepness was assumed to have been present in these experiments (Figure III-3B and B').

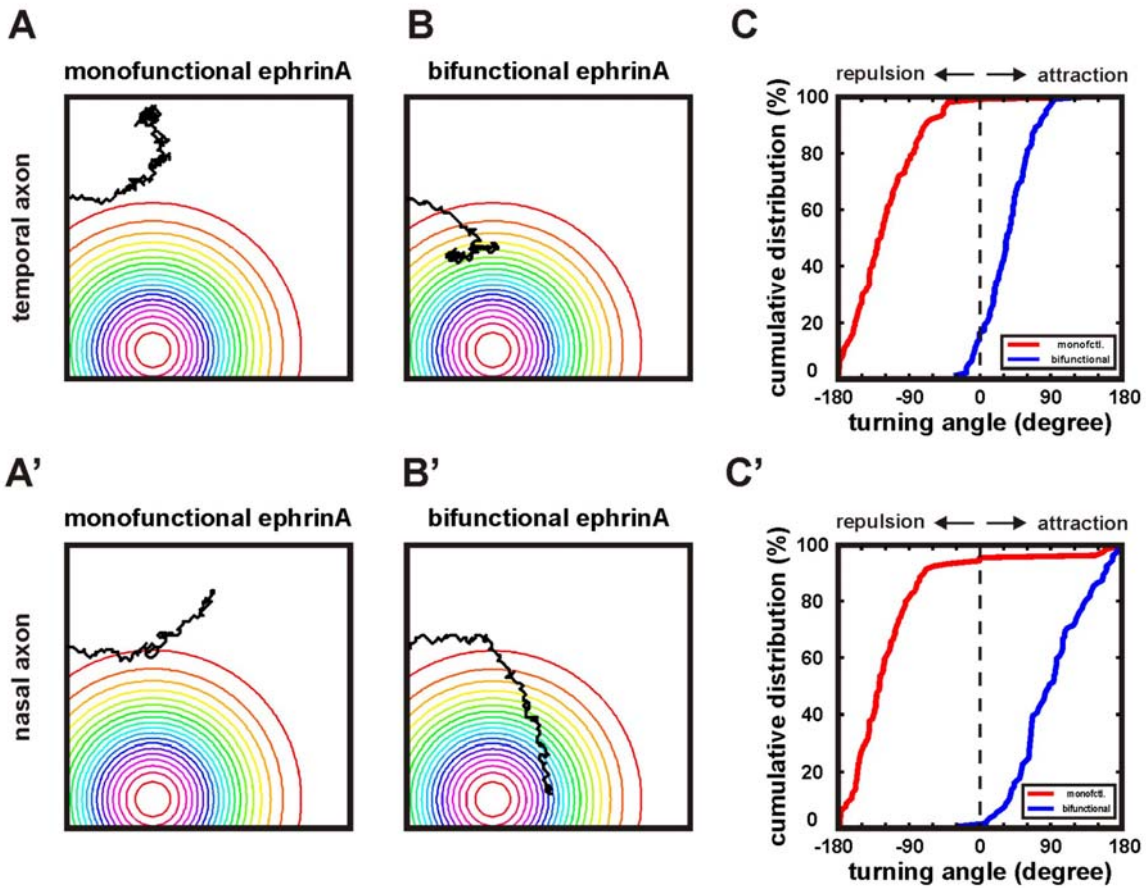

Figure III-3. Simulation of the RGC Axon Response to Concentric ephrinA Gradients.
Concentric ephrinA gradients (similar to diffusion gradients) were simulated and the response of nasal (R_a=0.22) and temporal RGC axons (R_a=4.5) was recorded. When ephrinA was assigned monofunctional properties, temporal (A) and nasal axons (A') turned away from the centre of the gradient (indicating the position of a simulated micro-pipette generating the gradient). However, in the case of bifunctional ephrinA, all axons grew towards the gradient centre (B, B'). Cumulative plots of the turning angle distributions (N = 100 axons) showed for the monofunctional ephrinA a shift to negative angle values (away from the gradient centre). For the bifunctional ephrinA a shift to positive angles towards the gradient centre was found (cumulative plots were kindly provided by Adrian Friebel, v0.1, one growth cone, 300 iterations, sigma=0.1).

A cumulative plot of the turning angles of 100 axons for each condition also confirmed attraction of temporal axons to bifunctional ephrinA. The monofunctional ephrinA triggered a strong repulsion (Figure III-3C and C').

Thus, it seems intriguing to explain the above mentioned unexpected experimental evidence of an attractive axon response to diffusible ephrinAs with bifunctional properties of the guidance cues. However, this interpretation is seriously hampered by the high background of general growth cone collapse in those experiments:

This collapse is usually interpreted as a strong repulsive effect pointing to a monofunctional effect of ephrinAs on axon guidance. Furthermore, recently a turning assay with temporal RGC axons was reported, using ephrinA2 instead of ephrinA5 as in Weinl's experiments, that did not indicate any attraction of the growth cones towards the micro-pipette (Kolpak *et al.*, 2009).

3. Growth Cone Behaviour in Substrate-bound Gradients of Guidance Cues

EphrinAs are membrane-bound proteins and it has been shown that membrane attachment or artificial clustering is required for strong axonal EphA activation (Davis *et al.*, 1994; Egea *et al.*, 2005).

To account for that *in vitro*, basically two experimental approaches have been published to generate linear gradients of substrate-bound ephrinA (Rosentreter et al., 1998; von Philipsborn et al., 2006). In both studies a more or less slope-independent non-differential stop or avoidance reaction of temporal retinal growth cones was observed, when they were growing into such linear gradients. Nasal growth cones, however, were unaffected by the gradients.

To see if these experiments contain any indication of whether ephrinAs are mono- or bifunctional, these assays were simulated with a single axon that is growing into a linear gradient of ephrinA. The axons grew in more or less straight lines into gradients of bifunctional ephrinA until they reached their target concentration (Figure III-4A).

In contrast, axons turned away from the gradient in a curved fashion when ephrinA was monofunctional (Figure III-4B).

Corresponding *in vitro* experiments always showed a straight growth and a uniform stopping reaction rather than a curved growth of axons. In fact, this absence of curved axon outgrowth in ephrinA gradients raised serious doubts in the past about ephrinA being the actual guidance cue for the retinal axons (Drescher, 2004). Therefore, these simulations seemed to provide an intriguing answer to this long-standing question of the missing curved axon outgrowth. That is to say, the ephrinAs would be bifunctional.

However, the model also suggested, if ephrinA were indeed bifunctional, a differential stopping of the axons should be expected in a linear gradient (Figure III-4C), which was actually never observed *in vitro*.

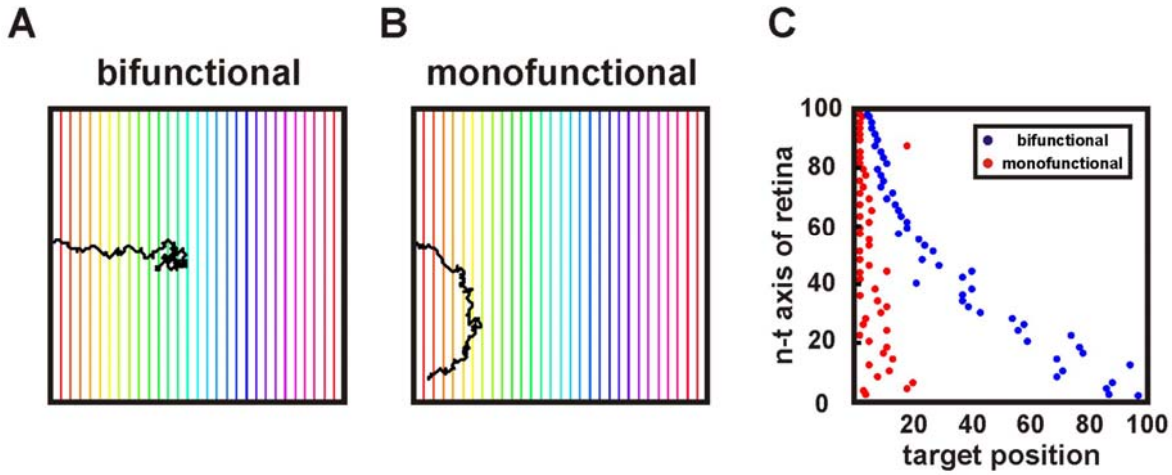

Figure III-4. Simulation of RGC Axon Response to Linear ephrinA Gradients.

Linear gradients of the tectal ephrinA were simulated and the response of RGC axons analysed. When the ephrinA was bifunctional, the axons grew rather straight to their respective target position (A, v0.1, one growth cone with R_a=1, 300 iterations, sigma=0.1, substrate: $L_t(x) = 0.02*x_t$). On a monofunctional ephrinA substrate axons tended to grow in curves away from the gradient (B, same parameters as in A). When whole explants were simulated on a linear gradient made of bifunctional ephrinA a clear differential stop reaction was observed, whereas when ephrinA was set monofunctional a rather uniform distribution was seen (C, v0.1, 50 growth cones, 10000 iterations, sigma=0.1, substrate: $L_t(x_t) = 0.04*x_t$). The stop reaction for the simulations with bifunctional ephrinA, though being topographic, was not evenly spaced. The reason is that it was assumed that the exponential EphA distribution in the retinal explant would not change *in vitro*. Therefore the mapping function changed from being linear to hyperbolic.

Taken together, without any additional assumption, a definite distinction regarding the guidance properties of ephrinAs on the basis of these linear gradient experiments seems difficult.

4. Growth Cone Behaviour in Stripe Assays

Stripe assays have been a major *in vitro* tool to characterize putative guidance cues. In those experiments, the response of axons emanating from a retinal explant to purified ephrinA proteins vs. a neutral substrate (e.g. Laminin) is analysed.

When *in vitro* stripe assays were performed using high concentrations of purified ephrinA5 or ephrinA2, both temporal and nasal axons showed a striped outgrowth pattern and a decision against ephrinAs. Reducing the ephrinA concentration successively led to a loss of nasal axon decision and subsequently of temporal axons as well [(Hornberger et al., 1999; Monschau *et al.*, 1997) and data not shown].

Assuming that the ephrinA is bifunctional, the simulation of the above experiment resulted in temporal axons avoiding the ephrinA stripes whereas nasal axons grew on the ephrinA stripes (Figure III-5A).

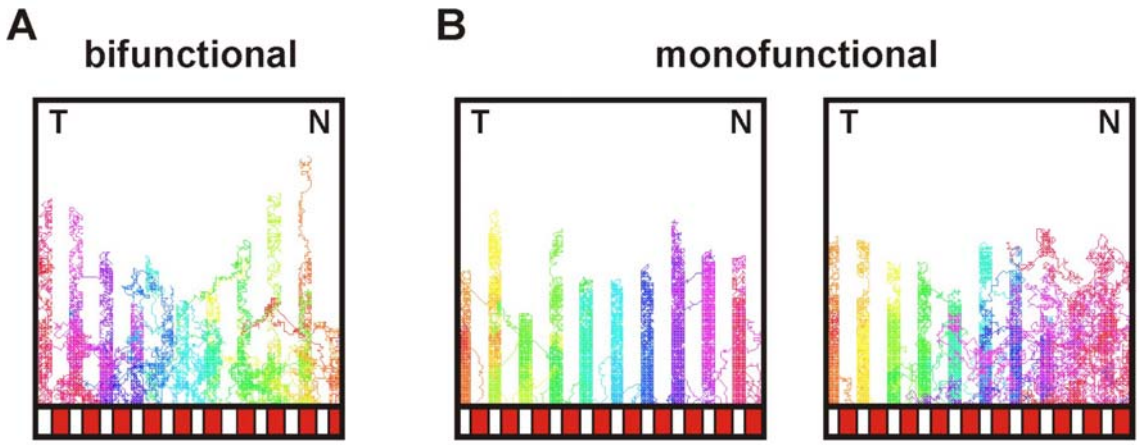

Figure III-5. Simulation of RGC Axon Response to Stripes of ephrinA vs. a Neutral Substrate. Substrates of alternating ephrinA and neutral stripes were simulated (stripe assay). When ephrinA was bifunctional a topographically differential behaviour of a retinal explant was seen, i.e. nasal axons (N) grew on ephrinA stripes whereas temporal axons (T) avoided them (A, L_1=2 vs. L_2=0). However, all axons decided against monofunctional ephrinA stripes on high concentrations (B, left, L_1=2 vs. L_2=0) whereas when lowering the ephrinA concentrations nasal axons started to grow criss-cross over ephrinA and neutral stripes (B, right, L_1=0.5 vs. L_2=0). (v0.1, parameters: 60 growth cones, 1500 iterations, sigma=0.1).

Adjusting the ephrinA concentrations shifts the switching point along the nasal-temporal axis, but does not lead to a loss of responsiveness on the nasal side of the retina.

However, when ephrinA was set to be monofunctional, a clear decision of all retinal axons against the ephrinA stripes was seen at high concentrations, which could be gradually abolished, starting with nasal axons, by lowering the ephrinA concentration (Figure III-5B). Therefore, the outcome of the ephrinA stripe assays is consistent with a guidance of retinal axons through a monofunctional tectal ephrinA and clearly inconsistent with a bifunctional guidance cue.

Using computational simulations, it was shown that *in vitro* experiments with substrate-bound and diffusion gradients can hardly be used to discriminate between mono- and bifunctional models of guidance cue function (Table III-1). Axon growth in the stripe assay simulations and the growth cone behaviour on homogeneous substrates, however, clearly suggest a monofunctional guidance of RGC axons by ephrinAs.

Table III-1: Comparison of Simulation Results with Implemented Mono- or Bifunctional Guidance Cue Properties and the Respective Experimental Data.

Bifunctional Guidance Cue		Monofunctional Guidance Cue
-	homogeneous guidance cue substrates	✓
inconclusive	diffusion gradients of guidance cues	inconclusive
inconclusive	substrate-bound gradients of guidance cues	inconclusive
-	stripe assays	✓

If that is true, a counteracting force to the tectal ephrinA must exist in order to generate topographic mapping. The reported expression of a tectal EphA counter-gradient in addition to the well-studied ephrinA gradient (Connor *et al.*, 1998; Rashid et al., 2005) might be an indication of such a guidance mechanism.

However, it is still unclear in which way the tectal EphA and ephrinA gradients are integrated to yield topographic guidance. Therefore, a novel computational model was developed to explore topographic guidance of retinal axons by two monofunctional counter-graded molecules in the tectum. Subsequently, predictions made by this model were tested *in vitro*.

B. A Novel Integrative Model of Topographic Guidance by Antagonistic Pairs of Interacting, Monofunctional Guidance Cues

The “text-book model” of topography formation considers only one retinal gradient (EphA) and one gradient on the tectum (ephrinA). According to that, ephrinA has to be bifunctional, for which unequivocal evidence is still lacking (see chapter III-A). However, the “text-book model” is also not fully consistent with further important *in vitro* and *in vivo* evidence: In addition to the EphA gradient a counter-gradient of ephrinA exists in the retina (Hornberger et al., 1999) that was shown to contribute to topographic guidance. Moreover, it was demonstrated that a tectal EphA counter-gradient to the ephrinA might be involved as well (Rashid et al., 2005). Therefore, a computational model was developed in which those additional gradients and all potentially occurring molecular interactions among the components of this guidance apparatus were implemented (Figure III-6, Table III-2).

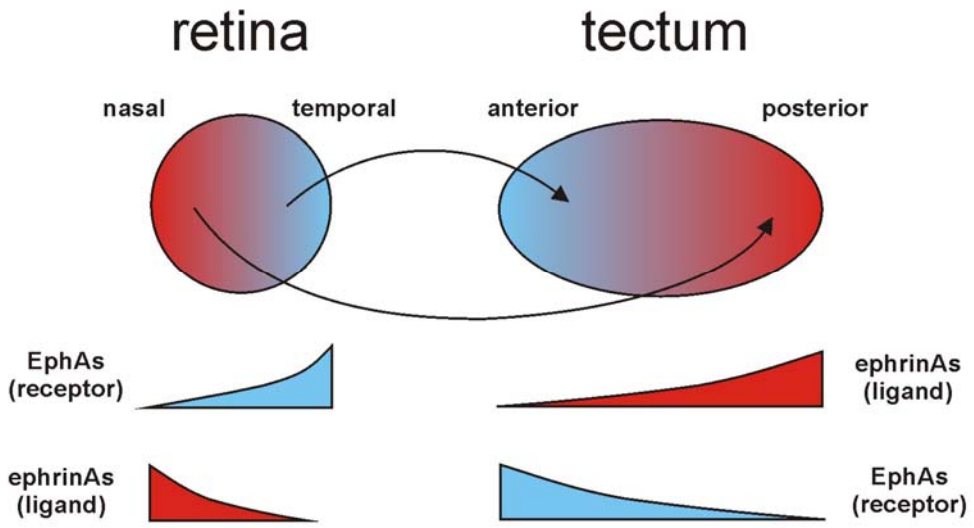

Figure III-6. Projection of RGC Axons and Scheme of the Expression Patterns of EphAs and ephrinA.

Nasal axons terminate in the posterior tectum and temporal ones in the anterior tectum. Counter-gradients of EphAs and ephrinAs are expressed in the retina as well as the tectum. Several ephrinAs and EphAs are expressed in both tissues. To simplify matters and in accordance with the ephrinAs promiscuous binding to EphAs, all gradients were merged into single exponential gradients in the simulation as expected *in vivo*.

There is convincing evidence for bidirectional signalling in the ephrinA/EphA system. Since retinal axons and tectal cells are endowed with EphAs as well as ephrinAs, forward signalling can be realised by the well-established tectal-ephrinA-axonal-EphA interaction whereas reverse signalling might occur through an interaction between axonal ephrinA and tectal EphA. Indeed, retinal axons can react to the presence of their tectal EphA counterpart in an ephrinA-dependant way (Davy *et al.*, 1999; Gebhardt, 2005; Huai and Drescher, 2001; Marquardt *et al.*, 2005; Rashid et al., 2005).

EphAs and ephrinAs were originally identified as receptors and ligands for each other, but due to the existence of bidirectional signalling this distinction seems rather artificial now. However, for historical reasons “EphAs” and “receptors” as well as “ephrinAs” and “ligands” are used interchangeably in this work.

Table III-2: Comparison of the Molecular Interactions Implemented in the “Text-book Model” and the Novel Model of RTP Formation

	“Text-book Model”	Novel RTP Model
forward signalling	✓	✓
reverse signalling	-	✓
cis - interaction	-	✓
fibre-fibre-interactions	-	✓

Implementing retinal ephrinA gradients into the model allowed for simulation of interactions between EphAs and ephrinAs on the same retinal axon (*cis*-interactions), for which there is ample evidence (Hornberger et al., 1999). Furthermore, the axonal termination site on the target was shown to be influenced by the EphA concentrations of neighbouring axons, indicating fibre-fibre-interactions (axonal *trans* - interactions) to play a major role in topographic guidance (Brown et al., 2000). Since retinal axons carry both EphAs and ephrinAs, such fibre-fibre-interactions might be realized by means of forward and reverse signalling. These additional signals have to be taken into account or else it has to be explained why they should not play a role in topographic guidance.

It is still unknown, however, in which way forward and reverse signalling, *cis*- and fibre-fibre interactions might be integrated.

As already demonstrated two monofunctional counter-acting forces are required for topographic guidance of RGC axons (see chapter III-A). To explore this, a signal transduction cascade was proposed in which a hypothetical intracellular integrator is activated by reverse signalling and inhibited by forward signalling (Figure III-7A). The activity of this integrator would translate to the local guidance potential $D(x_t,y_t)$ for a certain retinal axon. In analogy to enzyme kinetics, this integrator activity can be mathematically described by a ratio with every activating component in the numerator (reverse signalling) and any inhibiting component in the denominator (forward signalling). The local guidance potential $D(x_t,y_t)$ for a particular retinal growth cone is therefore:

$$D(x_t,y_t) = \frac{L_a \cdot [R_t(x_t,y_t) + R_a + R_{\hat{a}}(x_t,y_t)]}{R_a \cdot [L_t(x_t,y_t) + L_a + L_{\hat{a}}(x_t,y_t)]}$$

R_a, $R_{\hat{a}}$, $R_t(x_t,y_t)$ represent axonal and tectal EphA receptor concentrations at tectal position (x_t,y_t) whereas L_a, $L_{\hat{a}}$ and $L_t(x_t,y_t)$ stand for axonal and tectal ephrinA ligand concentrations at the same position. L_a*R_a and R_a*L_a symbolise EphA receptor / ephrinA ligand interactions occurring on one axon (*cis*-interactions) whereas $L_a*R_{\hat{a}}$ and $R_a*L_{\hat{a}}$ describe EphA receptor / ephrinA ligand interactions with neighbouring axons (fibre-fibre-interactions).

Simulation of the actual growth of an axon was based on the “servo-mechanism” algorithm (Honda, 1998): In short, the growth cone calculates in each step the local guidance potential D at its current position and at a randomly chosen neighbouring position in the field. Both D values (present versus potential position) are fed into a simple Gaussian error function to determine the probability p to stay within the respective field. The probability at a certain position is low when the growth cone is far away from the prospective target position and at a maximum when it reaches the target position (Figure III-7B).

However, in contrast to the original “servo-mechanism” model in which an axon stopped when the arbitrary reference value S was balanced by the forward signal, in the presented model the growth cone stops due to the balancing of forward and reverse signalling.

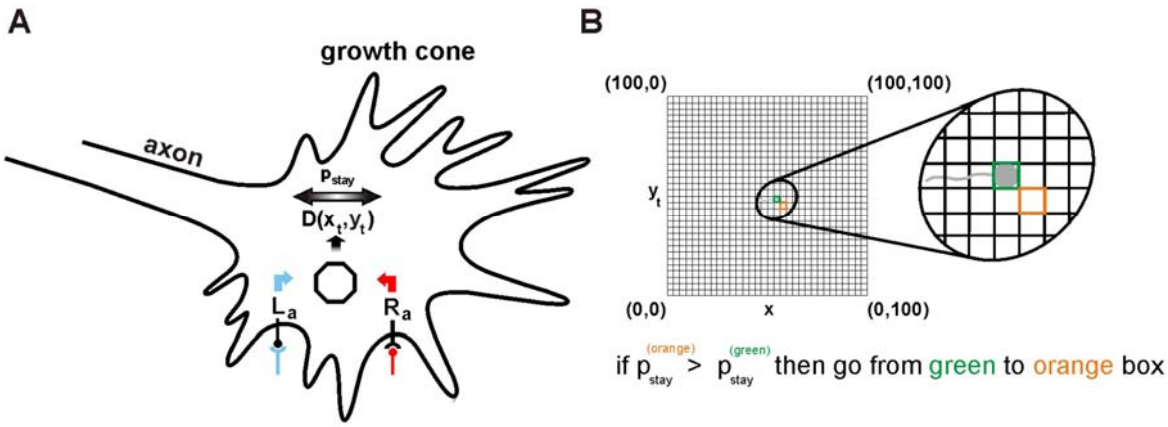

Figure III-7. A Novel Model of RTP Formation.

A growth cone detects the tectal receptor and ligand at its current position and a neighbouring field of choice with its own receptor R_a and ligand L_a (A). The resulting reverse signalling activates whereas the forward signalling inhibits the activity of an intracellular integrator. This activity translates to the guidance parameter D, which is subsequently fed into an error function p_{stay} to determine if the growth cone is more likely to stay at its current field (B, green) or change to the new field (B, orange). The growth cone reaches its target position when reverse and forward signalling are balancing each other.

First, it was analysed if the new model is able to generate a topographic projection. Therefore, simulations were performed with this computational model in which 60 RGC growth cones from different nasal-temporal origins in the retina were placed on the y-axis of a (100x100) simulation field. The field, representing the tectum in this case, contained two inversely related exponential counter-gradients of receptor (anterior high, posterior low) and ligand (anterior low, posterior high) according to the distribution of the respective molecules *in vivo* (Figure III-6). The simulation was allowed to proceed for 900 steps and the stopping point of each axon in the simulation field was plotted in a diagram of retinal position against target position in the tectum.

The target points of nasal as well as temporal axons did not drift once they reached their projected target positions indicating convergence at the potential minimum and lay roughly on a single line (Figure III-8).

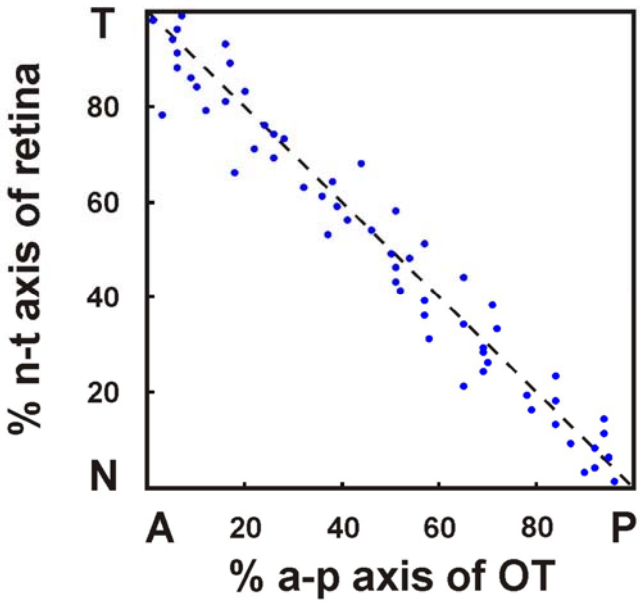

Figure III-8. The Novel Integrative Model of RTP Formation Is Topographic.
Topographic mapping of the retinal temporal-nasal to the tectal anterior-posterior axis is generated by a model that includes forward and reverse signalling, *cis*-interactions and fibre-fibre-interactions (v0.2, parameters: 60 growth cones, 900 iterations, sigma=0.05, Q_x=0, substrate: $L_t(x_t)=\exp(0.01(x_t-50))$, $R_t(x_t)=\exp(-0.01(x_t-50))$).

In summary, the implementation of the full set of potential molecular interactions into the model is fully consistent with a topographic order of RGC growth cones.

C. Experimental and Computational Evidence for Integrated Forward and Reverse Signalling

Stripe assays have been widely used to characterize the forward signalling, triggered by the tectal ephrinA (Cheng et al., 1995; Drescher et al., 1995), and the reverse signalling, activated by the tectal EphA (Rashid et al., 2005). In particular, when retinal nasal-temporal explants were given the choice between lanes of high ephrinA and a neutral substrate (Laminin) all axons, independent of retinal origin, always grew on the neutral substrate. When the same experiment was performed with EphA and neutral Laminin, the result was indistinguishable from the ephrinA stripe assay. That is to say, all retinal axons grew on the neutral substrate.

This observation is remarkably consistent with monofunctional guidance cues as laid out earlier (see chapter III-A). However, the implementation of forward and reverse signalling as antagonistic forces initially raised questions, if antagonistic axon responses in ephrinA and EphA stripe assays were to be expected as well.
To answer that, simulations were performed in which the starting points of 60 RGCs were placed in the simulation field and assigned receptor / ligand values such that they represented a retinal explant from nasal to temporal. The simulation field was filled with 20 parallel stripes, each 5 cells wide, containing ligand and a neutral substrate alternately. All axons showed a striped outgrowth avoiding the ligand-containing stripes in the simulations (Figure III-9A).

For validation of the model, corresponding *in vitro* experiments were performed. And indeed, *in vitro* ephrinA2 stripe assays (Figure III-9B) were found to agree with the model's prediction of the same experiment. Consistent with the presented model and ephrinA's function as monofunctional guidance cue, the outcome of the experimental ephrinA2 stripe assay was depending on the protein concentrations used (see also Figure III-5B on the right):
An avoidance of the ephrinA2 stripes by all axons was seen at high concentrations and could be gradually abolished starting on the nasal side of the retinal explant by lowering the ephrinA2 concentration (data not shown).
Next, reverse signalling was analysed as well, first in a simulated stripe assay with EphA. Stripe assay simulations were set up as before, but this time with alternating receptor against the neutral substrate. RGC axons grew in stripes avoiding the receptor, reminiscent of their behaviour in the ligand stripe assay.
The corresponding *in vitro* stripe assays using purified EphA3-Fc again confirmed the result predicted by the simulations (Figure III-9C and D).
Although counter-intuitive, the implementation of forward and reverse signalling as antagonistic forces into the novel model does not lead to antagonistic axon responses in the simulations and is thus remarkably consistent with the outcome of the ephrinA and EphA stripe assays.

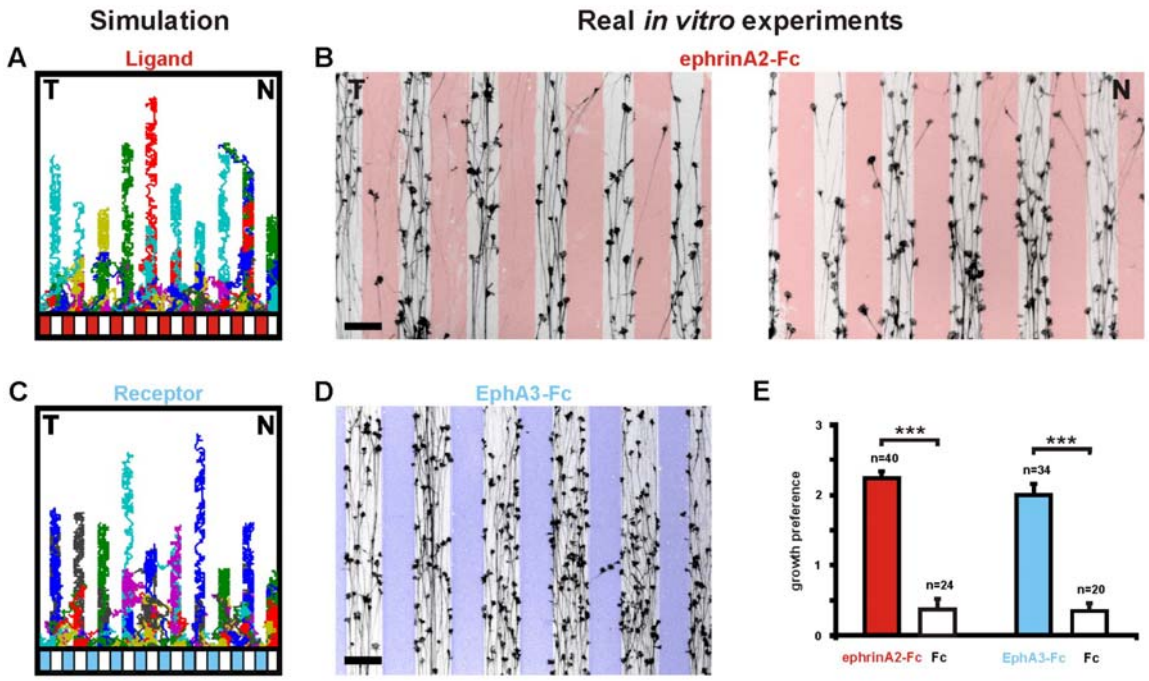

Figure III-9. RGC Axon Behaviour in Response to ephrinA2 and EphA3.

(A) Simulation of a modified stripe assay with alternating stripes of ligand (red, L_1=5 // R_1=0) vs. a neutral substrate (white, L_2=0 // R_2=0) in the simulation field. RGC axons are assigned random colours to facilitate discrimination. All axons, temporal (T) as well as nasal (N) ones, avoid growing on the stripes containing the ligand, which is consistent with the inhibiting effect of the underlying forward signalling implemented in the model. (B) Real *in vitro* stripe assay showing RGC axon responses to 16µg/ml ephrinA2-Fc (red). Nasal and temporal axons prefer to grow on 20µg/ml Laminin containing stripes thus avoiding ephrinA2. The black bar corresponds to a length of 90µm. (C) Simulation of a modified stripe assay with alternating stripes of receptor (blue, L_1=0 // R_1=5) against a neutral substrate (white, L_2=0 // R_2=0). Again, temporal and nasal RGC axons avoid growing on the stripes containing the receptor. (D) Real *in vitro* stripe assay with EphA3-Fc (blue, pseudo-colour). Nasal and temporal axons avoid growing on 30µg/ml EphA3-Fc containing stripes which is in accordance with the models prediction. The black bar corresponds to a length of 90µm. (E) Quantification of RGC axon growth preference. All stripe assays were evaluated according to the scoring system of Walter et al. (1987) with 0 indicating no response and 3 referring to very strong axonal response. Both axon responses to ephrinA2-Fc and EphA3-Fc are statistical highly significant when compared to responses on control substrate containing Fc-Protein only ($p<0.001$, students t-test). Error bars represent SEM (v0.2, parameters: 60 growth cones, 900 iterations, sigma=0.05, Q_x=0.1).

It must be mentioned, however, that existent *in vitro* stripe assays fail to reproduce a topographically differential behaviour. All retinal axons independent of their nasal-temporal origin show the same avoidance behaviour, which is undoubtedly inconsistent with the current “text-book model” of RTP formation.

D. Modelling *in vitro* Evidence for Axonal Receptor - Ligand *cis*-Interactions

Hornberger and colleagues showed that ephrinAs are expressed on chick RGC axons in a nasal>temporal counter-gradient to the retinal EphA gradient. Furthermore, they presented evidence for an interaction of ephrinAs and EphAs localised on the same axon (*cis*-interaction), which was shown to be relevant for the topographic guidance of retinal axons (Hornberger et al., 1999).

The function of the axonal ligand during topographic guidance was characterised in this study using ephrinA stripe assays. In a stripe assay with low ephrinA2 concentrations, only temporal axons show a decision against the ligand stripes while nasal axons show no preference (see also Figure III-5B). However, when ephrinA5 was retro-virally over-expressed in the retina, temporal axons did not show any response at all to the ephrinA2 stripes. Conversely, after removal of the GPI-anchored axonal ephrinAs with PI-PLC (phosphoinositide-specific phospholipase C), nasal axons suddenly became sensitive to the ephrinA2 substrate and avoided the ephrinA2 stripes like the temporal RGC axons.

Led by these observations, Hornberger et al. proposed that a *cis*-interaction of axonal ligand and receptor might lead to a masking of the axonal receptor. Receptor molecules which are bound in *cis* would be unavailable for ligand substrate recognition in *trans*. Thus, after artificially over-expressing ephrinA in the retina, all axonal receptor molecules may be occupied, hence no axons would show any avoidance of ephrinA2 in a stripe assay. According to the authors, nasal axons are endowed with an excess of axonal ligand compared to the receptor. Therefore, they are non-responsive to the ephrinA2 substrate. However, when the axonal ligand was removed, nasal axons became sensitive and avoided the ephrinA2 stripes.

Since the presented model contained *cis*-interactions based on receptor-ligand signalling, it was used to simulate the above mentioned experiments. However, in contrast to the interpretation of Hornberger and co-workers, the *cis*-interaction was not implemented as masking mechanism but as constitutively active and antagonistic reverse and forward interactions.

Most notably, despite this difference, the presented model was able to reproduce the experimental observation (Figure III-10) suggesting that these results might be explained on the basis of reduced or enhanced reverse signalling as well.

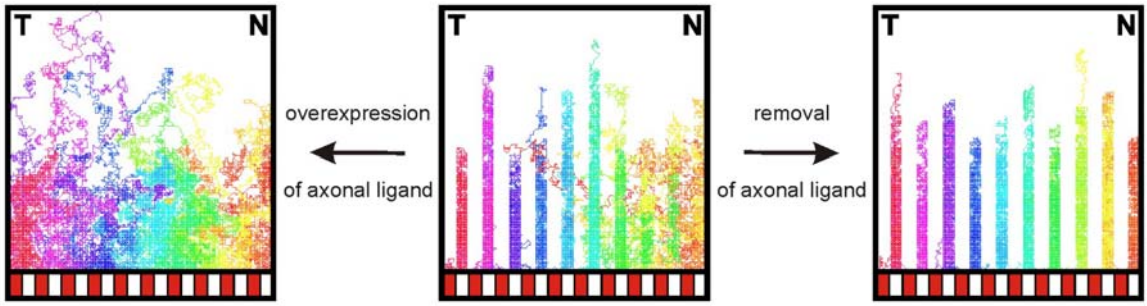

Figure III-10. Simulation of the Effect of Axonal Receptor / Ligand cis-Interactions on Axonal Decision Behaviour in an ephrinA2 Stripe Assay.

A modified stripe assay with alternating lanes of ligand (red, L_1=0.5 // R_1=0) vs. a neutral substrate (white, L_2=0 // R_2=0) was simulated with the presented counter-gradient model. At relatively low ligand concentrations (L_1=0.5) temporal axons (T) decided against ligand containing stripes (red) whereas nasal axons (N) did not show any response. When a constant high amount of retinal ligand was introduced (L_a=5, "overexpression") all axons showed no preference for either stripe. On contrary, after removal of the axonal ligand (L_a=0.01) nasal axons did show a decision against the ligand stripes as well. The presented model is therefore consistent with the axon decision behaviour seen *in vitro* (v0.2, parameters: 60 growth cones, 900 iterations, sigma=0.1, Q_x=0.1).

E. Modelling *in vivo* Evidence for Fibre-fibre-interactions During Topographic Axon Mapping

A study showing that, in addition to the tectal guidance cues, fibre-fibre-interactions might influence the position of the axonal termination site was published by Brown and colleagues (Brown et al., 2000).

They used an ingenious knock-in technique in mice and expressed in nearly half of the RGCs, in addition to the native EphA receptors, an EphA3-construct. Thus, RGCs with higher than usual receptor amounts (knock-in, EphA3$^+$) were situated next to wild-type RGCs (EphA3$^-$).

Most notably, the authors observed a map duplication, with one map formed by the knock-in, the other one by wild-type RGCs. As expected the knock-in map was confined to the anterior part of the superior colliculus (SC) in accordance with their increased sensitivity to the collicular ephrinAs.

Somehow unexpected, the wild-type map, though consisting of axons which are unaltered in their EphA expression, was compressed as well, but into the posterior part of the SC (Figure III-11A). This effect was less severe in heterozygous knock-in animals suggesting a dependence on EphA concentration.

The authors proposed that the wild-type RGCs might be pushed from the anterior SC by their knock-in counterparts with elevated EphA receptor expression, establishing a contribution of fibre-fibre-competition to topographical axon targeting *in vivo*.

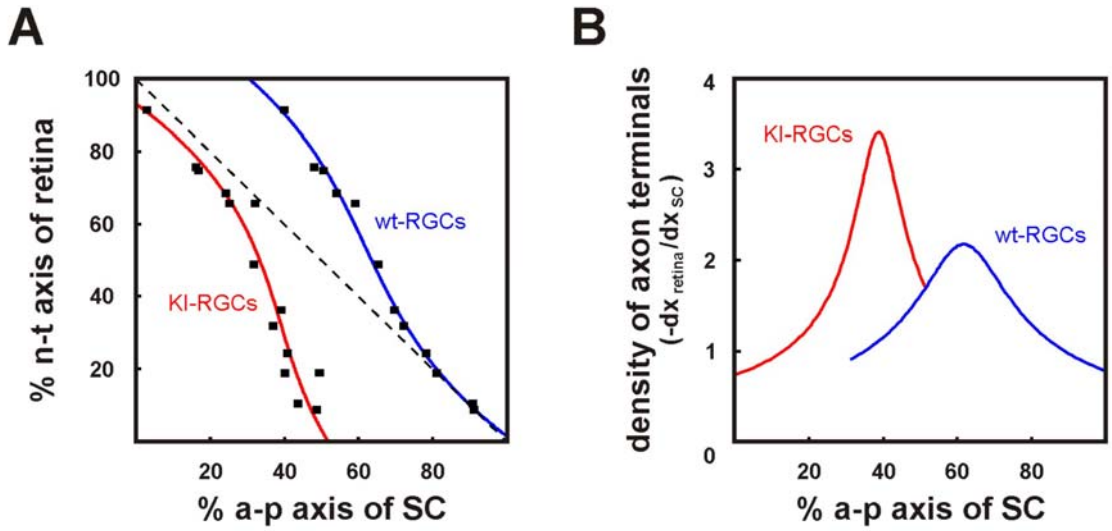

Figure III-11. Analysis of the Mapping Functions in EphA3 knock-in Mice.

The original data was taken from the paper by Brown et al., 2000 showing the map duplication and a posterior displacement of the wild-type map by the knock-in RGC axons (A). For the analysis of RGC terminals density, collicular position was plotted against the first derivation of the respective fitted mapping functions (red and blue curves from A). Both wild-type as well as knock-in terminal distribution showed a distinct but slightly overlapping map and were not equally distributed but rather showed a maximum each near the overlapping region (B). Please note that most knock-in RGC axons, carrying unusually high receptor concentrations, grew quite far into the superior colliculus.

In order to understand the experiment, the RGC map duplication was first analysed using the data set from the original study. Plotting the derivatives of the original mapping curves at any position in the SC (as an indication of axon terminal densities) showed the two distinct but slightly overlapping maps (Figure III-11B). Both RGC terminal populations are not equally distributed within their collicular target region, but each curve shows a characteristic maximum near the overlapping regions of the maps.

Since the publication of this work, several studies have been published that tried to formally explain the system's behaviour. Although they surely catch the salient features of the map duplication, all seem to have their limitations (see chapter IV for a detailed discussion of these models). Thus, it was analysed in detail whether fibre-fibre-interactions in a chemoaffinity setting could indeed be responsible for the observed map duplication.

Since the model presented here contained fibre-fibre-interactions based on receptor-ligand signalling, it was used to simulate this experimental situation. It became clear, however, that growth cone interaction events were quite sparse, compared to the number of growth cones and the size of the simulation field. Therefore, the new model was further refined (v0.25). In particular, randomized starting positions of the growth cones along one axis were introduced to facilitate interaction events between growth cones of different retinal origins approximating the *in vivo* situation. To increase the influence of growth cone interactions even more the calculation of the guiding parameter D was extended. D was now determined such that it was not only incorporating the guidance cue concentration value seen at the point of current and potential future growth cone position, but the concentration values in the respective surround field (3x3 cells) as well.

Furthermore, the magnitude of the inherent drive of the growth cones, Q_x, was coupled to the topographical signal D such that Q_x became zero at the respective collicular target point. That is to say, a growth cone had the highest tendency to move when it was far away from its respective target and no tendency when it reached this position. Normal topographic mapping was unaltered by those modifications with equal spacing and equal distribution of growth cone terminals across the target field (Figure III-12A).

Slightly increasing the amount of receptor in one half of the growth cone population induced the formation of a second map with the knock-in growth cones terminating in the anterior SC and the wild-type growth cones remaining in place.

At higher knock-in values a shifting of the temporal wild-type RGC axons to more posterior target points corresponding to a segregation of the two maps was seen. This effect was, however, not as pronounced as the one in the actual experiment. The reason might be that the knock-ins did not grow far enough into the target field (compare Figure III-11A & Figure III-12D, red curves).

The axon terminal distributions showed that at higher knock-in values wild-type displacement was more stringent as indicated by amplitude of the wild-type curve, but at the same time the maximum of knock-in terminal density retracted towards the anterior edge (Figure III-12B'-D', blue curves).

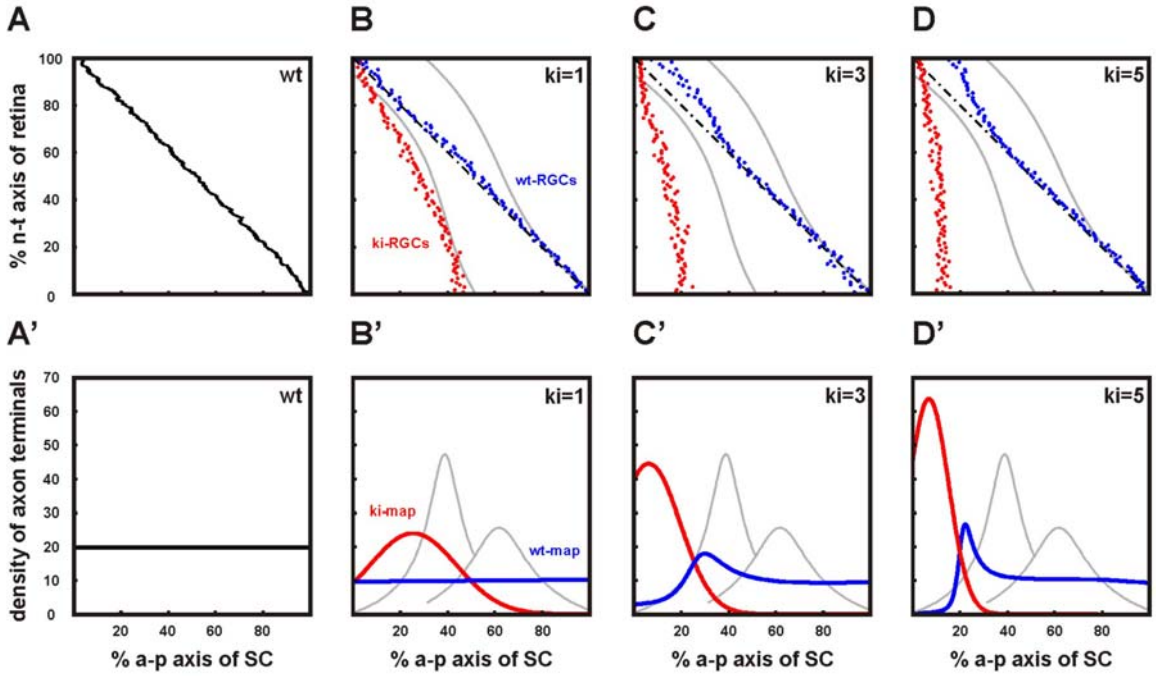

Figure III-12 Simulation of the EphA3 knock-in Effect on RGC Mapping.

2000 growth cones from different retinal origins were randomly distributed along one axis of a 100x100 tectal field and allowed to grow for 40000 steps until equilibrium was reached. For knock-in simulations (B-D) every second growth cone was assigned an additional constant amount of receptor (ki). Then a / p position of each axon terminal was plotted against its retinal position to obtain the mapping function. Map duplication was observed at any knock-in value, but a displacement of the wild-type map was seen only at higher knock-in values (C and D). The number of growth cones at a certain a / p position was plotted to analyze the axon terminal distribution in the target field (B'-D'). Wild-type map displacement was most prominent at high receptor knock-in concentrations but knock-in RGCs failed to grow very far in to the target field. The grey curves indicate the mapping function (B-D) or termination densities (B'-D') as obtained from the original data set. (v0.25, parameters: 2000 growth cones, 40000 iterations, sigma=0.1, substrate: $R_t(x_t)=\exp(-0.03(x_t-50))$, $L_t(x_t)=\exp(0.03(x_t-50))$).

Taken together, all qualitative features of this elegant experiment are replicated by the presented model suggesting that fibre-fibre-interactions might contribute to the observed mapping abnormalities. However, it is obvious that additional mechanisms, like e.g. adaptation of the knock-in RGC axons to the tectal cues or activity dependent refinement, must play a role as well to explain the quantitative details of the *in vivo* results.

In summary, the presented model not only explains topography formation, but also reproduces major evidences accumulated in recent years for the particular roles of forward / reverse signalling, *cis*- and fibre-fibre-interactions in the mapping process.

F. First Time Experimental *in vitro* Evidence of Topographically Differential Decision Behaviour of RGC Axons

Established stripe assays surprisingly fail to reproduce a topographically differential behaviour of RGC axon growth, which in fact remains a major discrepancy between these experiments and the prevailing chemoaffinity theory. Using the novel computational model, an as yet unrealised type of stripe assay with a substrate consisting of alternating stripes of receptor and ligand ("double stripes") was simulated. The simulation in this case surprisingly predicted a topographically differential decision of the axons such that nasal axons grow on the ligand-containing stripes whereas temporal axons grow on receptor-containing stripes (Figure III-13).

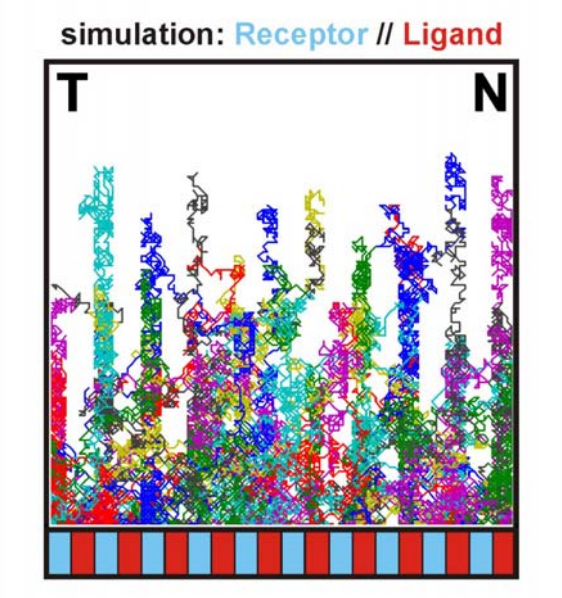

Figure III-13. Simulation of a Stripe Assay with Alternating Stripes of Receptor and Ligand as Substrate for Retinal Axons.

60 growth cones emanating from a temporal-nasal explant were simulated to grow into a substrate consisting of alternating receptor (blue) and ligand (red) lanes. The computational model predicted topographically differential axon growth behaviour i.e. temporal (T) axons grow on receptor stripes and nasal axons (N) grow on ligand stripes (v0.2, parameters: 60 growth cones, 900 iterations, sigma=0.05, Q_x=0.1, substrate: blue lanes: R_1=5, L_1=0, red lanes: L_2=5, R_2=0).

This result is intriguingly reminiscent of the axons' respective target choice *in vivo* [temporal → (anterior = high receptor), nasal → (posterior = high ligand)]. This suggests that the absence of a topographically differential growth in ephrinA or EphA stripe assays might be due to insufficient *in vitro* conditions. Either the receptor or the ligand respectively might be missing in the respective stripe assay substrates.

Thus, a stripe assay substrate containing both receptor and ligand stripes as suggested by the computational model had to be fabricated to test this hypothesis. The method routinely applied for stripe generation uses a silicone matrix, consisting of a field of 90µm wide channels separated by bars. The matrix is placed onto a glass or petri dish surface (Hornberger et al., 1999; Vielmetter et al., 1990) and the channels are subsequently filled with protein solution.

After incubation to adhere the protein to the plastic surface and removal of the matrix, a striped protein substrate is generated. By covering the whole stripe field with a second protein solution, which binds only to the remaining free sites on the surface, the second stripe type can be fabricated. This strategy, however, seemed to be inappropriate here due to the very high affinity of EphA and ephrinA for each other, which prevents a clear separation in distinct stripes. The second applied protein species will not only bind to the unoccupied sites at the surface, but also to its binding partner in the other stripe.

Therefore, a modified protein printing technique was used to separately attach the proteins to a plastic surface (see Materials & Methods).

In short, the silicon matrix bars were coated with ephrinA2-Fc and the protein printed onto the petri dish surface. Then the EphA3-Fc stripes were generated by suction of the EphA3-Fc solution through the channels.

Applying this method produced clearly separated stripes of EphA3-Fc and ephrinA2-Fc protein. However, inhomogeneities in the printed ephrinA2-Fc stripes could not be avoided due to the surface of the matrices being rather uneven (Figure III-14).

Figure III-14. *In vitro* Substrate of Alternating Stripes of Receptor and Ligand as Substrate for Retinal Axons. In order to fabricate alternating stripes of EphA3 and ephrinA2, a combination of protein printing and the routine method of sucking the protein solutions through silicone matrix channels was used (see Materials & Methods for a detailed description). For proof of principle, equal amounts (8µg/ml) of EphA3-Fc (blue) and ephrinA2-Fc (red) were applied. EphrinA2 was always printed first. EphA3 subsequently adhered to the petri dish surface out of solution in the matrix channels. This sequence had to be obeyed, because EphA3 gets inactivated during printing. Both proteins were labelled prior to use with different clustering antibodies. A clear separation of the proteins was achieved with this method with no apparent overlap of labelling throughout the whole substrate. However, inhomogeneities of the printed ephrinA2-Fc could not be avoided.

According to the model, topographically differential growth of the axons should be highly sensitive to the receptor and ligand ratio used for generating the stripes. In particular, it predicts that if both proteins are not applied in equal amounts all axons would grow either on the receptor stripes or on the ligand stripes depending on whose activity would be in excess (Figure III-15A, C).

Therefore, a wide range of possible ligand and receptor ratios was tested starting with the usual concentrations used in the stripe assays with only EphA3 (30µg/ml) or ephrinA2 (16µg/ml). Consistent with the model's predictions, relatively low EphA3 (20µg/ml) compared to high ephrinA2 ligand concentrations (20µg/ml) resulted in all axons growing preferentially on the EphA3 receptor (Figure III-15A, B).

However, in some cases nasal axons did not show any growth preference at all suggesting that ephrinA2 activity was too low in those experiments.

Conversely, at high EphA3 (50µg/ml) and low ephrinA2 concentrations (8µg/ml) all retinal axons always decided against EphA3 (Figure III-15C, D).

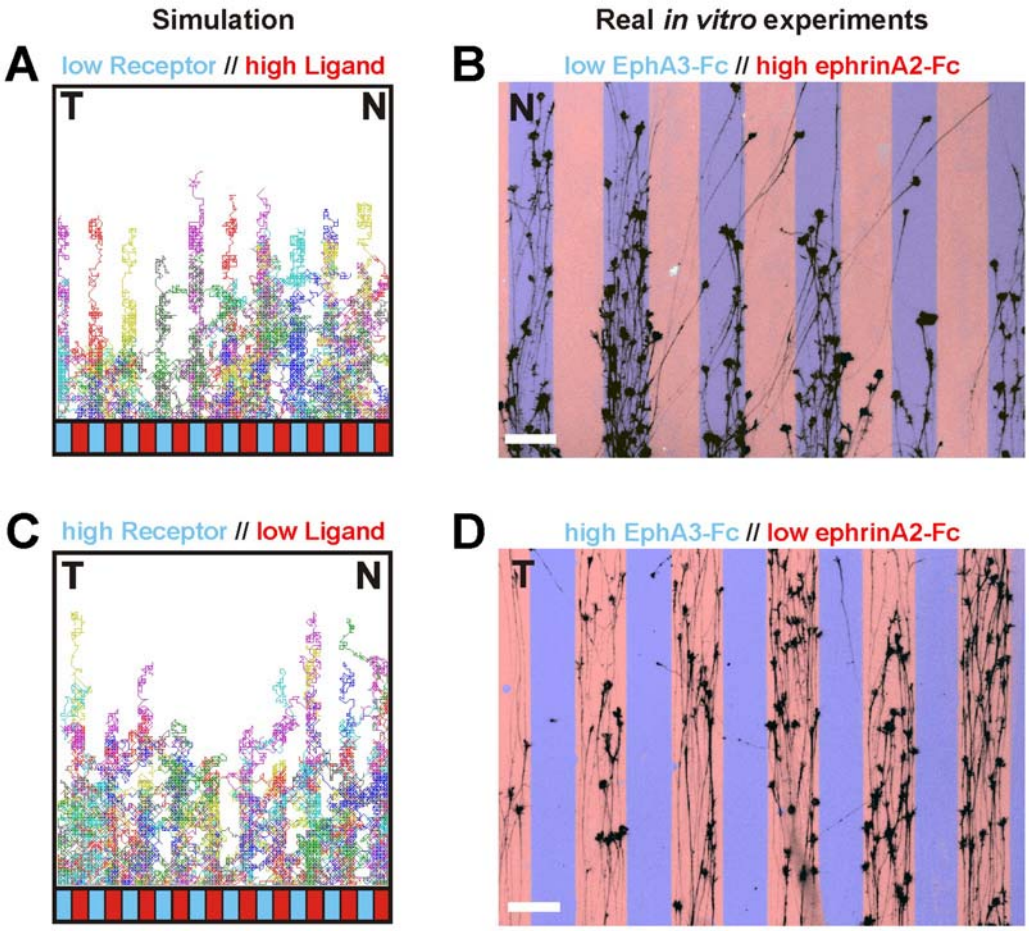

Figure III-15. Sensitivity of RGC Axon Response to the Concentration Ratios of Ligand and Receptor in a "Double Stripe" Assay. If ligand and receptor values were not in balance the model predicted all axons to grow on either receptor or ligand, depending on which had a higher activity (A and C, v0.2, 60 growth cones, 900 iterations, sigma=0.05, Q_x=0.1, substrate: R_1=3, L_1=0 // R_2=0, L_2=7 in A or R_1=7, L_1=0 // R_2=0, L_2=3 in C). In accordance with these predictions, when retinal axons were confronted with a relatively low receptor concentration (20µg/ml) vs. a high ligand concentration (20µg/ml), all axons grew on the receptor stripes (B, only the nasal axons are depicted due to their increased sensitivity to low receptor concentrations caused by their endowment with high ligand concentrations). However, when substrates with relatively high receptor concentration (50µg/ml) vs. a low ligand concentration (8µg/ml) were used, all axons grew on the ligand stripes (C, only the temporal axons are depicted because they are endowed with high receptor concentrations and should be highly sensitive to low ligand concentrations).

Most notably, at intermediate concentrations of both proteins (30µg/ml EphA3 vs. 16µg/ml ephrinA2) a topographically differential behaviour of RGC axons was seen for the first time in *in vitro* assays with purified guidance cues. In fact, the absence of topographic differentiality *in vitro* had been a major point of concern to date.

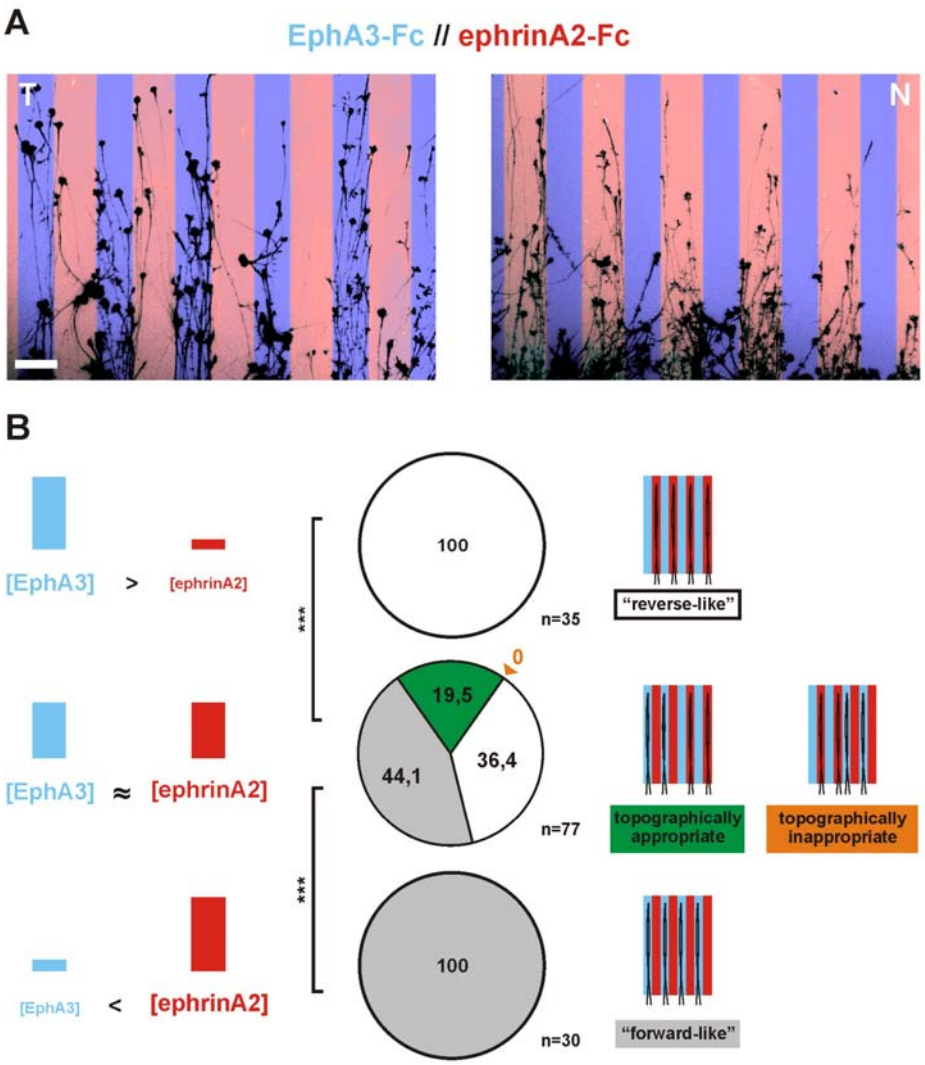

Figure III-16. Topographically Differential Growth Behaviour of Retinal Axons on Substrates with Alternating Stripes of Receptor and Ligand.

On the "double stripe" substrates, retinal axons showed for the first time under defined conditions a topographically differential growth behaviour (A), i.e. temporal axons grew on receptor stripes (resembling receptor distribution at their *in vivo* target in the anterior tectum) and nasal axons grew on ligand stripes (in accordance with the distributions found at their target in the posterior tectum). Different concentration ratios of EphA3 and ephrinA2 were tested. Retinal axons on high concentrations of EphA3 vs. low concentrations of ephrinA2 (B, first row, 50µg/ml EphA3 // 8µg/ml ephrinA2) always avoided the EphA3 stripes ("reverse-like" behaviour). When retinal axons were cultured on low concentrations of EphA3 vs. high concentrations of ephrinA2 (B, third row, 20µg/ml EphA3 // 20µg/ml ephrinA2) temporal and nasal axons mostly avoided to grow on ephrinA2 stripes. Occasionally nasal axons did not show any decision suggesting that ephrinA2 concentrations were too low ("forward-like" behaviour). Only at intermediate concentrations (B, second row, 30µg/ml EphA3 // 16µg/ml ephrinA2) topographically differential axon growth was seen. Topographically inappropriate decision behaviour (nasal axons on EphA3, temporal axons on ephrinA2) was never observed. The significance was tested with a k*2-Chi-Quadrat -Test after Brandt-Snedecor ($p<0.005$).

In particular, in the double stripe assays, nasal axons grew on ephrinA2-Fc containing stripes and temporal axons on EphA3-Fc stripes (Figure III-16A, B), which is surprisingly consistent with the *in vivo* behaviour of retinal axons. Axons emanating from the centre of the retinal explant did not show any decision indicating a continuous position-dependent transition of the axon growth behaviour (data not shown).

At intermediate concentrations, the axons' response was to some extent prone to fluctuations (Figure III-16B). That means despite using the intermediate amounts of EphA3 and ephrinA2, all retinal axons occasionally decided against either ephrinA2 or EphA3 (“forward- or reverse-like” behaviour). However, there is evidence that those fluctuations may have been caused by the intrinsic limitations of the protein printing method: As already shown, the ephrinA2 stripes, which were fabricated with the protein printing method, were rather inhomogeneous. The production process of the silicon matrices unfortunately does not prevent the matrix surface to be uneven. Thus, it is highly likely that this surface roughness might be the cause for the substrate inhomogeneities observed in the printed lanes.

Therefore, it might be possible that despite using the same protein concentration for every experiment replication, the actual active amount of ephrinA2-Fc on the surface differed locally quite strongly. This might also be indicated by nasal axons showing no decision occasionally, when high ephrinA2 amounts were used, compared to EphA3 absorbed out of solution where no such fluctuations were observed. Hence, it is conceivable that the required ratio of ephrinA2 and EphA3 was not obtained everywhere in the substrate and the axons responded according to which protein's activity was higher. This is in fact consistent with the model's prediction.

However, most notably despite those intricacies, no single case was observed in which nasal retinal axons grew on EphA3-Fc and temporal axons on the ephrinA2-Fc stripes from one explant. Thus, the non-topographic cases (“forward- or reverse-like”) at intermediate concentrations correspond to failures of displaying full topographical differentiality rather than “anti-topographic” behaviour arguing that the presented results reflect a true topographically differential decision of retinal axons *in vitro*.

Consistent with the presented computational model, this outcome corroborates the previous suggestion (see chapter III-A) that retinal axons might be topographically guided by two monofunctional counter-graded molecules on the target cells.

G. Improving *in vitro* Substrates for Studying Retinal Axon Guidance

As shown in the previous paragraph a topographically differential axon decision in the “double stripe” assay was highly dependant on an exact balancing of ephrinA and EphA amounts. Although showing in principle the predicted outcome, the *in vitro* experiments were prone to fluctuations regarding the axon decision. There is evidence that intrinsic limitations of the protein printing method are the major cause for that. In particular, the unevenness of the silicon matrices used for printing might have resulted in concentration inhomogeneities of the protein substrates.
To solve those problems and because it might eventually be of use to generate improved axon guidance substrates for a variety of applications another method using light-patterning of protein substrates was developed.

1. Light-controlled Activation of Guidance Proteins

As a first step towards generating substrates with precisely adjusted protein concentrations, a technique for defined patterning of protein substrates using chemical inactivation (“caging”) and subsequent reactivation with UV light was established. In short, proteins were first inactivated using a photo-labile chemical compound (6-Nitroveratryl chloroformate, abbreviated NVOC-Cl), which reacts with amino-groups of exposed Lysines, and afterwards bound to a plastic surface.
Subsequently, the proteins were reactivated in a spatially patterned manner by irradiation with UV light of 375nm (Cambridge *et al.*, 1997; Kossel *et al.*, 2001; Marriott, 1994).
Initially, the optimal conditions for caging of ephrinA5 were determined. The goal was to reduce its binding to EphA3 considerably. This was done in an ELISA format in which the modified caged ephrinA5 proteins were bound to the plastic surface of a 96-well plate and subsequently detected using biotinylated EphA3.

Indeed, the binding activity of biotinylated EphA3 to caged ephrinA5 could be successively reduced using constant amounts of ephrinA5 and increasing concentrations of NVOC-Cl. At final concentrations of 200µM NVOC-Cl and 0.2µM ephrinA5 (i.e. a molecular protein:NVOC-Cl ratio of approximately 1:1000) a reduction of the binding activity to around 10% was seen.
This residual binding activity could not be reduced any further by higher NVOC-Cl concentrations and thus may be owed to unspecific binding of the biotinylated EphA3 or the inability of NVOC-Cl to block all potential EphA3 binding sites in ephrinA5 (Figure III-17A).

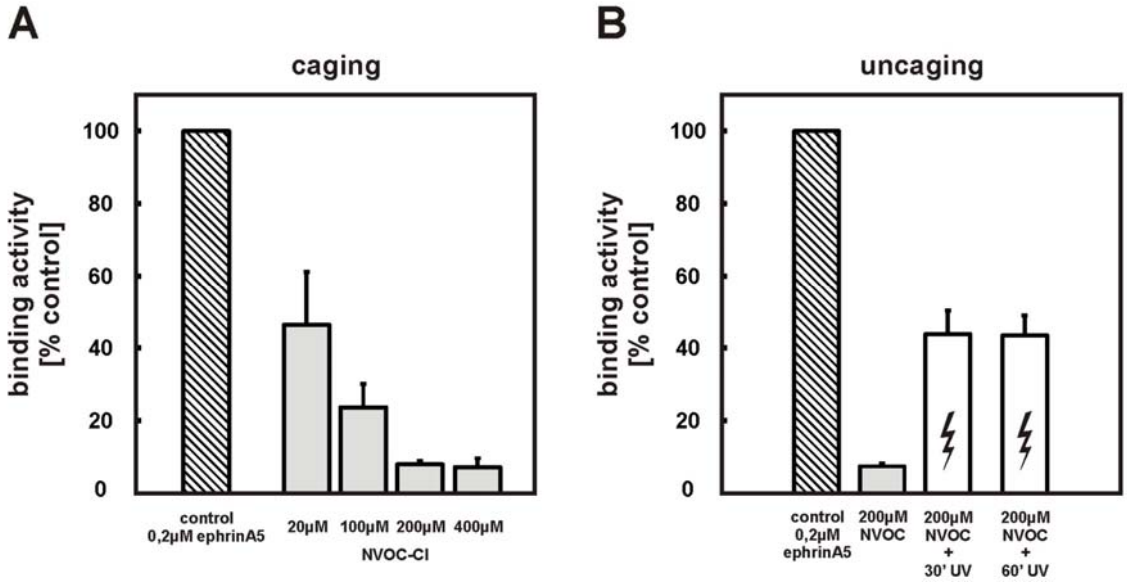

Figure III-17. Reversible Inactivation of ephrinA5-Fc.

Shown is the successful blocking of (biotinylated) EphA3 binding activity to ephrinA5, when ephrinA5 was treated with the caging compound NVOC-Cl. At 200µM NVOC-Cl blocking reached saturation (~10% binding activity) as it could not be decreased any further by higher NVOC-Cl concentrations (A). EphrinA5-Fc, caged with 200µM NVOC-Cl, was illuminated with UV light of 375nm wavelength for 30 or 60 minutes (B, measured dosage: 11 and 21.9 Ws/cm² respectively). After 30 minutes, binding activity reached its maximum at approximately 45%. Binding activity was normalized to untreated ephrinA5 (control). Error bars represent SEM.

A wide range of NVOC-Cl concentrations was tested, but the uncaging was eventually performed with 200µM NVOC-Cl, because the most favourable caging:recovery ratio was gained here.

After 30 minutes of irradiation with a custom made LED engine emitting UV light of 375nm, partial recovery to around 45% binding activity was observed. 60 minutes of irradiation did not increase binding activity any further suggesting saturation of the uncaging process (Figure III-17B) after 30 minutes. A loss of EphA3 binding was neither observed after mere UV irradiation of uncaged ephrinA5 nor caused by the accompanying chemicals without NVOC-Cl itself (data not shown).
Using this method, improved substrates can be generated, which might be valuable for overcoming the restrictions of contemporary *in vitro* substrates and may thus be of help for studying retinal axon guidance in more detail.

2. Fabrication of Alternating Stripes of EphA3 and ephrinA5 with Light-patterning

The routine approach for protein stripe generation uses a silicone matrix, consisting of a field of parallel 90µm wide channels separated by bars. It is placed onto a glass or petri dish surface (Hornberger et al., 1999; Vielmetter et al., 1990) and the channels are subsequently filled with protein solution. After incubation for protein adsorption and removal of the matrix, a striped protein substrate is left on the surface.
By covering the whole stripe field with a second protein solution, which usually binds only to the remaining free sites on the surface, the second stripe type can be fabricated. When this strategy is applied to fabricate ephrin/Eph double stripes, the second-applied protein does not remain confined to the second stripe. This is due to the high-affinity binding of the ephrinAs to the EphA receptors. In fact, the protein applied first, becomes an affinity matrix for the second protein (Figure III-18).
Previously, the desired substrate pattern was generated with a protein printing method, but concentration inhomogeneities were inevitable with this approach. However, the respective pattern can also be easily fabricated with caging and subsequent photo-reactivation. First, EphA3-Fc was bound to the surface of a petri dish using a silicon matrix as before. Subsequently the matrix was removed and the whole substrate was covered with caged ephrinA5-Fc, which cannot bind to the EphA3 stripes but to the plastic surface.

Then the whole substrate was irradiated with a 6-W hand-held 365nm UV lamp (2h, measured dosage: 9.3Ws/cm²).

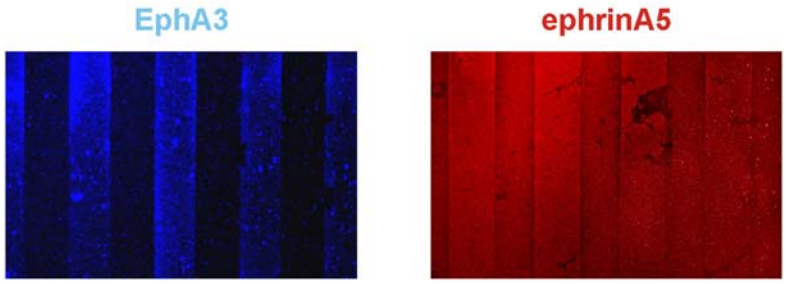

Figure III-18. Trial to Fabricate Alternating Stripes of EphA3-Fc and ephrinA5-Fc Using the Conventional Modified Stripe Assay Technique. The EphA3 stripe was prepared by injecting EphA3-Fc into the silicon matrix channels. After matrix removal ephrinA5 was allowed to cover the whole substrate. The stripes were then stained with fluorescent affinity probes. Presumably due to high binding affinity of ephrinA5 and EphA3, ephrinA5 staining (right image, red) was also found in the stripes shown to be occupied by EphA3 (left, blue).

Staining of the prepared substrates showed a clear separation of ephrinA5-Fc and EphA3-Fc in distinct stripes (Figure III-19) with no inhomogeneities suggesting that protein was equally distributed within each stripe. It has to be mentioned, however, that for best separation a mild caging of EphA3 had to be done as well suggesting that by caging ephrinA5-Fc alone not all mutual binding sites were blocked (see also Figure III-17A). In the above mentioned ELISA experiments biotinylation of EphA3 may have fulfilled the same role.

Figure III-19. Alternating Stripes of ephrinA5 and EphA3. Stripes were prepared as previously described using the modified stripe assay technique but this time ephrinA5 and EphA3 were caged prior to stripe preparation. After binding to the surface, substrates were subsequently irradiated with 375nm UV light (2h, measured dosage: 9.3Ws/cm^2) and stained with fluorescent affinity probes. A clear separation of EphA3 (blue) and ephrinA5 (red) in stripes was observed.

In summary, the application of this novel method was successful in fabricating alternating and clearly separated lanes of EphA3 and ephrinA5 protein. Although being quite laborious this technique might be used in future applications for defined substrate patterning.

H. Robustness of the Mapping Function against Variations of Absolute Guidance Cue Concentrations and Tectal Size in the Novel Model

As long as the gradients in projecting and target area are independently patterned during development, achieving the precise matching of guidance cue concentrations required by chemoaffinity is by far non-trivial. Furthermore, fluctuations of the position guidance cue concentrations might interfere with the formation of smooth topographical maps. The explanatory power of existing chemoaffinity models is thus considerably reduced, because a multitude of variations are definitely to be expected in noisy biological systems. Nature's remarkable ability to cope with such perturbations, while at the same time keeping the system's output stable, is subsumed under the term “robustness”.

Surprisingly, by introducing forward and reverse signalling as counter-forces during topography formation, robustness of the mapping function is achieved quite easily for a number of pivotal cases:

For example, if the concentrations of tectal receptor and ligand are both increased by 1.5fold the model still reproduces an almost perfect evenly spaced map (compare Figures III-20A and C). Furthermore, the size of an animal, hence the extent of tectum, may also vary across individuals. Under conditions where the tectal a/p extent is doubled the model predicts a robust topographic mapping of growth cones onto the larger target area (compare Figures III-20A and B). Basically, the same holds true for a combination of both, changing concentrations as well as tectal extent (compare Figures III-20A and D).

For this kind of robustness to occur, receptor and ligand concentrations in retina and tectum may be determined independently. However, the respective counter-gradients must still obey a fixed relationship which can be realized by receptor and ligand being inversely related by mutual repression or alternatively due to antagonistic regulation by a common organiser.

Any change of this organiser's activity will then lead to comparable concentration changes in both tectal gradients. Indeed, there is recent evidence that both gradients on the target may be induced by diffusible FGFs released from the isthmic organiser at the mid brain hindbrain boundary (Chen *et al.*, 2009).

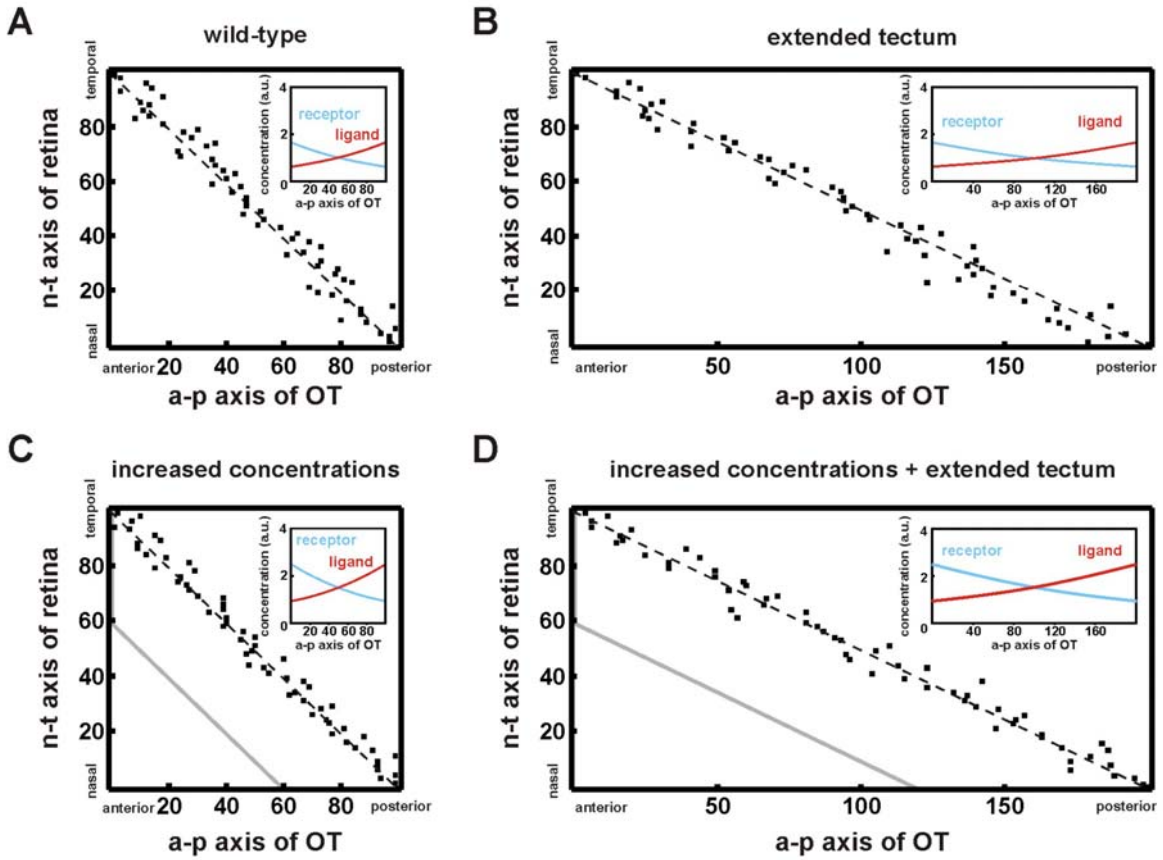

Figure III-20. Enhanced Robustness of the Mapping Function.

Due to the implementation of counter-gradients of tectal receptor and ligand in the proposed model, robust mapping onto a simulated tectum (OT) with varying gradients (shown: 1.5x increase, compare e.g. Figures A and C or B and D) as well as different extents of the tectum (compare e.g. Figures A and B or C and D) was achieved. Perfect topographic mapping (nasal>posterior and temporal>anterior) is indicated by dashed lines in the diagrams. The grey lines in C and D indicate the simulation result when the “servo-mechanism” model, which incorporates only the tectal ligand gradient, was used. Exponential gradient distribution along the a-p axis is depicted as inset (v0.2, parameters: 60 growth cones, 3000 iterations, sigma=0.05, $L_t(x_t)=a*\exp(b*(x_t-l/2))$, $R_t(x_t)=a*\exp(-b*(x_t-l/2))$, in A: a=1, b=0.01, l=100 in B: a=1, b=0.005, l=200, in C: a=1.5, b=0.01, l=100, in D: a=1.5, b=0.005, l=200).

In summary, due to the implementation of counter-acting forward and reverse signalling, the presented model achieves robust topographic mapping when varying the size of the tectum or the gradients of guidance cues, which is a feature rigid chemoaffinity models fail to achieve.

I. Growth Cone Adaptation in the Retinotectal System during Topographic Axon Guidance

Retinotopic guidance described by growth in a field potential towards a minimum or maximum relies on matching distributions of the underlying retinal and tectal gradients [gradient matching, (Gierer, 1981; Löschinger *et al.*, 2000)]. However, there is currently no experimental evidence which suggests that retinal and tectal gradients mirror each other. In fact, it is doubtful that nature would have evolved such an error prone mechanism in order to form highly precise topographic connections.

As already shown, relative mapping is able to considerably improve robustness of topographic mapping, but it fails as soon as the relation between tectal receptor and ligand is subject to change. Adaptation, i.e. the re-adjustment of the transduction of an external signal based on prior experience of the very same signal might help to overcome those restrictions. Indeed, there is convincing experimental evidence of adaptive responses of retinal growth cones to the guidance cues (Brown et al., 2000; Rosentreter et al., 1998; von Philipsborn et al., 2006).

When trying to understand adaptation in the retinotectal system, it is imperative to make a clear distinction between growth cone behaviour which is unequivocally adaptive and behaviour that can be explained by other mechanisms.

Moreover, while potentially providing a means of increasing map robustness and precision, an unrestricted adaptation is incompatible with topography. RGC growth cones that adapt indiscriminately will loose the ability to find their correct target.

1. “Adaptation” on Homogeneous Substrates

Retinal axons are able to grow on high concentrations of homogeneously distributed ephrinA with ease. Because ephrinA was described to be repulsive, it has been suggested that growth cones must adapt or desensitize in order to be able to grow on such a substrate. However, when simulating this experiment with the model presented here, which does NOT include any adaptation or desensitization mechanism, retinal axons grew equally well on all ephrinA concentrations (Figure III-21).

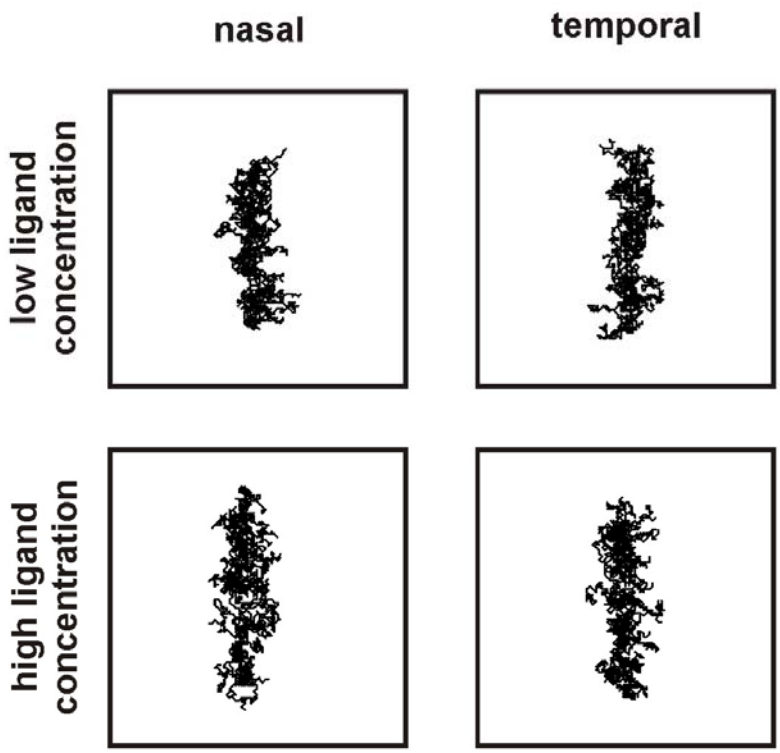

Figure III-21. Simulation of Nasal or Temporal Retinal Explants Growing on Different Amounts of Ligand. Explants of 50 growth cones originating from nasal (R_a=0.22, L_a=4.5) or temporal retina (R_a=4.5, L_a=0.22) were simulated on either low (L_t=0.22) or high homogeneous concentrations of ligand (L_t=4.5). Axons were able to grow out on every substrate with no apparent differences between high or low concentrations of ligand. Usually the axons' ability to grow on high concentrations of repulsive ligand is assumed to be a sign of axonal adaptation to the guidance signal. However, axon guidance in a potential field towards a minimum with no additional adaptation mechanism is sufficient to explain this behaviour perfectly (v0.2, parameters: 50 growth cones, 200 iterations, Q_x=0.1, sigma=0.05).

The determining factor for topographic axon guidance by a potential field is the detection of concentration differences rather than the absolute concentration at a certain position.

Thus, axon growth on homogeneous ephrinA substrate is not necessarily caused by a desensitization process, but is already inherent to the currently accepted model of topographic guidance.

2. “Adaptation” in Orthogonal Receptor Stripe Assays

An experimental situation that might be indicative of RGC axon adaptation to a guidance signal was done by Bernd Schlupeck (Schlupeck, 2008). He performed stripe assays with EphA3 receptor substrates, but placed the retinal explants in parallel to the stripes.

Because axons are avoiding the EphA3 stripes in usual stripe assays (Figure III-9D), one would have expected a stopping of all axons in front of the first stripe in this experiment. Surprisingly, under these conditions axons seem to be able to cross at least a certain number of EphA3 stripes with ease. After crossing the first EphA3 stripe, the majority of axons turned into the following Laminin lane, whereas the remainder again crossed the next EphA3 stripe and so on until all axons grow more or less in the Laminin lanes (Figure III-22C).

Growth cone desensitisation (adaptation) to the receptor stripes might be the reason for this unexpected behaviour. However, when this experiment was simulated with the new RTP model, which does not contain any adaptation mechanism, it was surprisingly revealed that axons grew over the receptor stripes and occupied the neutral substrate in-between.

This might be due to the implementation of fibre-fibre-interactions into the model: Advancing growth cones might be pushed over the first stripe by trailing axons, which in turn can cross the first stripe because their forerunners are paving the way for them. This hypothesis was investigated with the presented computational model. Fibre-fibre interactions can easily be turned off by assigning $R_{\hat{a}}$ and $L_{\hat{a}}$ in the guidance parameter equation the value of zero throughout the simulation:

$$D(x_t,y_t) = \frac{L_a \cdot [R_t(x_t,y_t) + R_a + R_{\hat{a}}(x_t,y_t)]}{R_a \cdot [L_t(x_t,y_t) + L_a + L_{\hat{a}}(x_t,y_t)]}$$

$$\Downarrow$$

$$D(x_t,y_t) = \frac{L_a \cdot [R_t(x_t,y_t) + R_a]}{R_a \cdot [L_t(x_t,y_t) + L_a]}$$

R_a, $R_t(x_t,y_t)$ represent axonal and tectal EphA receptor concentrations at tectal position (x_t,y_t) whereas L_a and $L_t(x_t,y_t)$ stand for axonal and tectal ephrinA ligand concentrations at the same position.

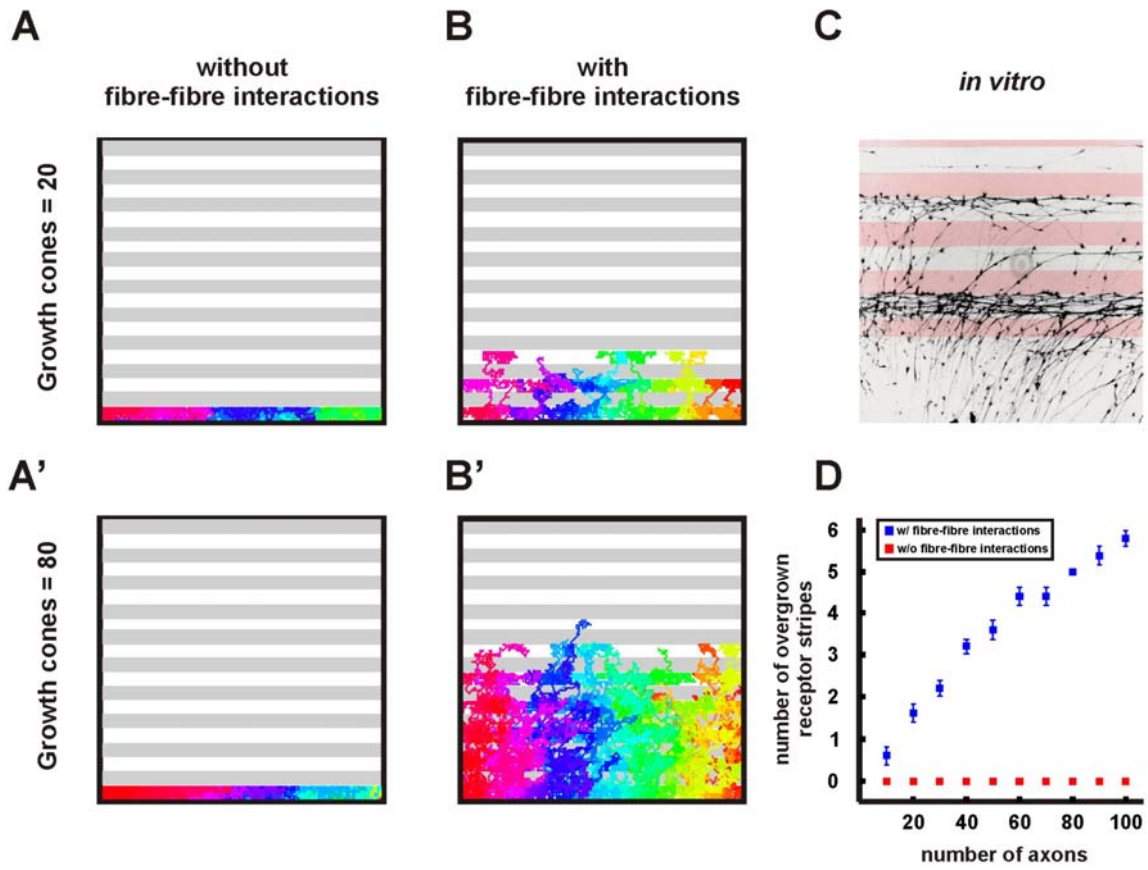

Figure III-22. Simulation of Receptor Stripe Assays with Explants Placed Parallel to the Stripes.

Axons growing from retinal explants positioned in parallel to receptor stripes were able to overgrow these stripes (C, picture was kindly provided by Bernd Schlupeck), a behaviour not usually seen when the explant was oriented perpendicular to the stripes. A reason might be adaptation of the reverse signalling. Using the model, a nasal-temporal explant was placed in front of the substrate and axons could not cross even the first receptor stripes when fibre-fibre interactions were turned off (A, A'). However, when fibre-fibre interactions were turned on, axons were enabled to overgrow the stripes (B, B'). This behaviour was strongly correlated with axon number suggesting that increased fibre-fibre interactions provide the basis for this adaptation-like axon growth behaviour (D, N=5 for each condition; v0.2, parameters: 900 iterations, Q_x=0.2, sigma=0.05, substrate: R_1=0, L_1=0 // R_2=5, L_2=0). Error bars represent SEM.

As assumed, when retinal explants were simulated with fibre-fibre interactions switched off, clearly no axon was able to cross the first stripe, consistent with the outcome of the usual receptor stripe assay (Figure III-22A, A').

The ability of the axons to cross the stripes was also dependent on the number of axons used (Figure III-22B', D) indicating the direct contribution of fibre-fibre-interactions in the model to this phenomenon.

Simulation of a stripe assay experiment with a perpendicular placement of the retinal explant was not affected by switching fibre-fibre-interactions on or off (data not shown).
In summary, what might look like an adaptation phenomenon can in principle be explained as well by fibre-fibre interactions and is thus in accordance with a rigid chemoaffinity mechanism without adaptation.

3. Influence of Adaptation on Topography Formation

As a first step towards an understanding of real adaptive processes in the retinotectal system, an unrestricted adaptation mechanism against the topographic signal (Block *et al.*, 1983; Delbrück and Reichardt, 1956) was introduced into the presented counter-gradient model. This algorithm was originally used to describe bacterial chemotaxis in a diffusion gradient of attractants or repellents, which is in fact the best studied biological model system for unrestricted or perfect adaptation to an external signal.
In short, for axonal receptor adaptation the growth cone calculates the reciprocal mean of the tectal ligand values L(t') seen in the past weighted with an exponential decline to account for a long-term or short-term memory of the growth cones ($\tau \to \infty$: long-term memory, $\tau \to 0$: short-term memory):

$$R_{adapt}(t) = \frac{1}{\frac{e^{-t/\tau}}{\tau} \sum_{t'=0}^{t} L(t') \cdot e^{t'/\tau}}$$

The adaptation of the axonal ligand was determined using the underlying inverse relationship with the axonal receptor. The guidance signal $D(x_t,y_t)$ was subsequently calculated according to the equation used in the presented counter-gradient model (see chapter III-B).
When no adaptation was used, an evenly spaced topographic map was observed (Figure III-23A). As expected, when both axonal receptor and ligand were allowed to adapt to their respective tectal counterparts, topographical mapping was lost (Figure III-23B).

But most surprisingly, when only the axonal receptor was undergoing adaptation to the tectal ligand, while the axonal ligand was kept differential, an almost perfect map was retained (Figure III-23C).

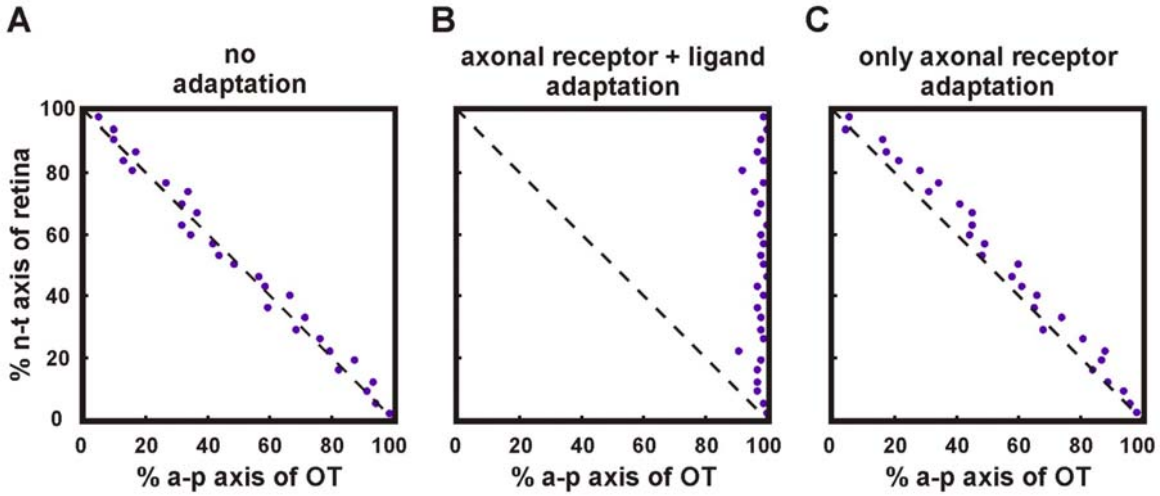

Figure III-23. Topography and Unrestricted Adaptation to the Tectal Guidance Signals.
30 growth cones were simulated in a tectal field containing exponential counter-gradients of ligand and receptor (v0.3, 30 growth cones, steps=10000, sigma=0.1, tau=4, substrate: $L_t(x_t)=\exp(0.01(x_t-50))$, $R_t(x_t)=\exp(-0.01(x_t-50))$). When no adaptation was allowed the growth cones form a perfect topographic map (A). When both axonal receptor and ligand were indiscriminately adapting to their tectal counterparts, topography is lost and all growth cones grow to the posterior end of the tectum (B). Most surprisingly, however, when only the axonal receptor was allowed to adapt, while the axonal ligand did not change, a normal topography was still observed (C).

This finding is encouraging because it suggests that it is in principle possible to introduce adaptive mechanisms in a model of topographic mapping without the axons' loosing their differential identity. In which way adaptation to the topographic signal might be realized *in vivo*, however, has to be subject to future research.

IV. DISCUSSION

The chemoaffinity theory suggests that retinal axons are guided to their topographic target in the tectum by graded chemical markers. The discovery of a repulsive ephrinA gradient on tectal cells and correspondingly graded axon guidance receptors of the EphA family on RGC axons essentially corroborated this theory. Since then, a particularly simple chemoaffinity model incorporating only a retinal receptor and tectal ligand has been widely accepted to explain topographic map formation. However, despite its intuitive character, in its current form it fails to explain important *in vitro* and *in vivo* evidence.

Additional counter-gradients of ephrinAs in the retina and of EphAs in the tectum are involved in topographic axon guidance, but their integration is not well understood. In addition to ligand-receptor interactions between axon and target tissue, it was recently shown that receptor and ligand molecules on one axon might interact as well (*cis*-interactions). Furthermore, the axonal termination site in the tectum strongly hinges on the receptor concentrations of neighbouring axons, possibly indicating fibre-fibre-interactions to play a major role. There is also intriguing *in vitro* and *in vivo* evidence that adaptation of retinal axons to the tectal guidance cues contribute to topographic guidance.

In an attempt to resolve these intricacies and to contribute to a comprehensive understanding of topographic map formation, a novel model of RTP formation is proposed in this work and major predictions are validated using adequate *in vitro* experiments.

Do ephrinAs Have Mono- or Bifunctional Guidance Properties?

Axons originating from different positions in the retina can enter the tectal surface and approach the topographically correct target zone in the tectum on a direct, non-meandering trajectory (Fujisawa et al., 1981a, b). This suggests that axonal targeting may be mathematically described as guidance in a two-dimensional potential field towards a minimum or maximum. In accordance with chemoaffinity, Alfred Gierer demonstrated that such a potential might be realized by counter-acting effects of two chemical gradients in each of the dimensions of the tectum (Gierer, 1981).

The position of the minimum or maximum is then specified by the relative influence of these antagonistic effects on retinal axons, which is determined by the topographical identity of different retinal axons. A simple potential along one axis, thus, can be generated by two chemical gradients on the tectum (i.e. the two tectal gradients are monofunctional and functionally opposing each other). Furthermore, he suggested that it is also possible that this guidance potential is generated by just one gradient in the tectum. In this case, the tectal gradient must thus be comprised of a bifunctional molecule: It has to attract or to repel growing axons depending on concentration and the switch needs to occur at the axon's topographic target position.

The current "text-book model" considers only an ephrinA ligand gradient in the tectum and an EphA receptor gradient in the retina. According to Gierer's argumentation, this model therefore only generates topography if the tectal ephrinA ligand is at least implicitly assumed to be bifunctional. However, the finding of an additional EphA receptor gradient in the tectum (Rashid et al., 2005) and an ephrinA gradient in the retina (Hornberger et al., 1999) suggests rather a monofunctional interpretation of the tectal gradients.

Thus, a computational model was used to examine the guidance properties of ephrinAs and eventually trying to discriminate between a monofunctional and a bifunctional model of topographic guidance through ephrinAs. To this end, published *in vitro* assays of ephrinA function were revisited and simulated with the guidance cue in the simulations being either mono- or bifunctional.

The used algorithm was based on the "servo-mechanism" model proposed by Honda (Honda, 1998). It is a particularly simple implementation of the explicitly bifunctional "text-book model" of topography formation, i.e. it only includes the retinal receptor and tectal ligand. However, the algorithm allows to easily switch the tectal ligand from mono- to bifunctional. Thus, this model seemed well-suited for differentiating between the two conceptually different modes of topographic axon guidance.

The “text-book model” of RTP formation requires the tectal ephrinA ligand to be bifunctional to achieve topographic targeting of retinal axons. Recent work seems to suggest that ephrinA ligands might indeed be bifunctional (Hansen et al., 2004). In this study the authors reported a differential and biphasic outgrowth of retinal explants on homogeneous ephrinA2 depending on retinal origin of the explant and ephrinA2 concentration. It might be concluded that this result is evidence for a bifunctional topographical guidance of retinal axons by ephrinAs.
According to this interpretation, only a model with a bifunctional ephrinA should be able to reproduce the observed experimental results. Therefore, this experiment was simulated with the “servo-mechanism” model and the ephrinA was assigned either monofunctional or bifunctional guidance properties.
However, contrary to the experimental observation, no differential outgrowth was seen when simulating this experiment with the “servo-mechanism” model (Honda, 1998). Moreover, on the basis of those simulations, no discrimination could be made between bifunctional and monofunctional ephrinA. Therefore, the conclusion that the differential biphasic response of RGC growth cones to homogeneous substrates might be indicative of the bifunctionality of the guidance cues is invalid.
This is in fact not surprising, because generally in a chemoaffinity model assuming guidance in a potential field, concentration differences rather than absolute concentrations are instructive for guiding axons. Even from a theoretical point of view, it is highly questionable whether topographic guidance might be realized by staggered outgrowth of the axons. A basic requirement for this type of guidance mechanism would be that axons are strictly growing into the tectum from one side without any turning possible, which is clearly not necessary.
In conclusion, a differential axon outgrowth on homogeneous ephrinA substrates is so far consistent with either mono- or bifunctional guidance cues.

Instead of contributing to topography formation, the reported differential outgrowth may be rather indicative of differential axon growth velocities that are adjusted according to the axon's position in the potential field. In order to achieve that, the cellular mechanisms controlling the speed of growth might secondarily be coupled to the mechanisms determining the direction of growth.

According to the experimental data, outgrowth velocity would be high on pre-target ephrinA2 concentrations, at an optimum at the target and low on post-target ephrinA2 concentrations. This is somewhat counter-intuitive, since one would expect that axons are slowing down at their target position rather than showing optimal growth speed.

Nevertheless, based on the experimental data of Hansen and colleagues, analysis of the relationship between axon outgrowth and the guiding potential suggests that retinal growth cones might be guided by a monofunctional rather than a bifunctional tectal guidance cue.

An alternative mechanistic interpretation of the biphasic growth velocity curves would be that the differential axon outgrowth was completely unrelated to topography formation and was instead caused by different levels of growth cone adhesion. In fact, a simple mechanical model of cell migration suggests that little adhesion does not provide sufficient traction for migration, whereas too much adhesion impedes cell migration as well (DiMilla *et al.*, 1991).

EphA receptors and ephrinA ligands bind to each other with high affinities (Monschau et al., 1997). Thus, biphasic response behaviour of the growth cones with fast growth occurring at low receptor occupancy and slow growth occurring at either zero or high receptor occupancy might be sufficient to explain the reported differential outgrowth behaviour.

Turning assays are frequently used to analyse the properties of diffusible guidance cues. To this end, a growth cone is exposed to a diffusible guidance cue gradient released from a micro-pipette. Subsequently, any trajectory change of the axon, towards or away from the micro-pipette, is recorded.

Two major observations were made in simulations using concentric exponential ligand gradients that are supposed to resemble the diffusion gradients made with a micro-pipette: In a gradient of monofunctional ligand, axons always grew away from the centre of the gradient, independent of the concentration at the point of first exposure and gradient distribution. Second, when the ligand was assigned bifunctional properties, attraction as well as repulsion was observed depending on the guidance cue concentrations when first encountering the gradient.

In particular, if a growth cone, at its entry point in the gradient, encounters concentrations higher than the concentration at its supposed target site, it turned away; otherwise it turned towards the centre of the gradient.

Most *in vitro* assays of ephrinA function established their role as repellents for RGC axons. However, Weinl and colleagues published a study in which they showed that temporal chick RGC axons were indeed attracted towards the tip of a micro-pipette containing soluble ephrinA5-Fc (Weinl et al., 2003). At a distance between growth cone and micro-pipette of 100µm, no turning was visible, instead a concentration dependant collapse could be observed. When reducing the distance to 60µm, i.e. increasing the local ephrinA concentration at the growth cone, suddenly an attractive turning response was seen, but again at a high background level of growth cone collapse as the authors report. Comparing these experimental results with the results of the simulations, one is tempted to take an attractive response to otherwise repulsive guidance cues as an indication of bifunctional properties. However, several lines of evidence argue against such an interpretation:

For one, the high level of growth cone collapse in the turning assays raises serious concerns about a bifunctional model of ephrinA function. Usually, growth cone collapse is accompanying strong axonal repulsion and not attraction (Fan and Raper, 1995; Kapfhammer and Raper, 1987; Walter et al., 1990). The fact that collapse rate and attraction increase concomitantly in Weinl's experiments casts serious doubt on the turning towards the micro-pipette representing a genuinely attractive response.

Furthermore, a very recent report of turning assays with temporal RGC axons, using ephrinA2 instead of ephrinA5 as in Weinl’s experiments, did not indicate any attraction of the growth cones towards the micro-pipette (Kolpak et al., 2009).

In summary, although an intriguing experiment, it seems unlikely that bifunctional properties of ephrinAs can be inferred from this study. Moreover, the high level of ephrinA5 induced growth collapse is rather consistent with a monofunctional repellent effect of ephrinAs on retinal axon guidance.

EphrinAs are membrane-bound proteins and it has been shown that membrane attachment or artificial clustering is required for strong axonal EphA activation (Davis et al., 1994; Egea et al., 2005). Therefore, *in vitro* assays were developed that measured the response of retinal axons to substrate-bound gradients of ephrinAs (Rosentreter et al., 1998; von Philipsborn et al., 2006). In these experiments, a slope-independent stop or avoidance reaction of temporal retinal axons was observed.

When such linear gradients were simulated, axons showed a qualitatively different behaviour on a bifunctional as compared to a monofunctional guidance cue: In particular, in gradients made of bifunctional cues axons tended to grow along straight trajectories up to their target concentration. In contrast, axons were pushed into a monofunctional gradient by their inherent forward drive Q_x and subsequently grew in curves turning away from the gradient.

In vitro, temporal retinal axons, when growing into a gradient of tectal membranes or purified proteins, showed a straight growth and uniform stop reaction, which seems to be consistent with the ephrinAs being bifunctional. However, real ephrinA bifunctionality would at the same time require the axons' response to be topographically differential in a gradient, which has never been observed so far, whereas a monofunctional ephrinA is more consistent with the observed uniform stop zone.

In conclusion, without any additional assumptions, it is quite hard to differentiate between mono- and bifunctional ephrinA properties from this experiment as the data can be interpreted either way.

Stripe assays are a major *in vitro* tool to characterize putative guidance cues. In these experiments, the response of axons emanating from a retinal explant to purified ephrinA proteins vs. a neutral substrate (e.g. Laminin) is analysed.

Therefore, stripe assays were examined for any indication of bifunctional or monofunctional properties of ephrinAs. According to the simulations of ligand stripe assays, axons should show a topographical differential decision if the ligand was indeed bifunctional. That means, temporal axons would avoid the ligand stripes, whereas nasal axons would decide for the stripes containing the ligand.

In fact, such behaviour was never seen when using pure ephrinA2 or ephrinA5 in a stripe assay. However, in a monofunctional model, the axons avoided the ligand stripes irrespective of their nasal-temporal origin.

This is a very clear indication for retinal axon guidance by monofunctional ligands, because this simulation is fully consistent with the observed *in vitro* growth of retinal axons on ephrinA stripe substrates.

On a side note, bifunctional guidance molecules require the existence of a molecular mechanism that explains how a guidance cue can adopt qualitatively different properties at different concentrations.

Two axonal receptors with different affinities for the tectal signal would be sufficient, but their signalling has to be precisely adjusted such that the switch occurs at topographically differential concentrations depending on the origin of the retinal axons. Alternatively one receptor existing in two distinct states (clustered vs. monodisperse) might be able to accomplish this task. Although these possibilities exist, no experimental evidence currently supports this line of thought.

In summary, by using computational simulations, it was shown that the existing *in vitro* data is either inconclusive with regard to mono- or bifunctionality of the guidance cues (substrate-bound and diffusion gradients) or rather suggests a monofunctional effect of ephrinA on retinal axons (homogeneous substrates and stripe assay).

If the latter is true, a counter-force to the tectal ephrinA must exist that acts in concert with the ephrinA to generate topographic mapping.

Indeed, a tectal EphA counter-gradient to the ephrinA gradient was shown to exist. However, its specific contribution to topographic guidance is not very well-understood. Therefore a novel computational model was developed to explore topographic guidance of retinal axons by two monofunctional counter-graded molecules in the tectum. Subsequently, predictions made by this model were tested by adequate *in vitro* experiments.

The Novel Model of Retinotectal Projection Formation Includes All Potentially Existing EphA / ephrinA Interactions

In this study, a model of RTP formation was developed which incorporates the actually existent counter-gradients of the ephrinA/EphA guidance cues in retina and tectum. Due to the experimentally demonstrated binding promiscuity, all existing gradients of one type (receptor or ligand respectively) were merged into one functional gradient, each with an exponential distribution.

In addition to the well-studied forward signalling (ephrinA → EphA), the model also included reverse signalling (EphA → ephrinA). Despite ephrinAs being GPI-anchored, there is solid evidence of axonal co-receptors that might transduce the reverse signal into the ephrinA bearing RGC axon (Davy et al., 1999; Huai and Drescher, 2001; Lim *et al.*, 2008; Marler *et al.*, 2008; Marquardt et al., 2005; Rashid et al., 2005).

Furthermore, consistent with experimental findings, the model included *cis*-interactions (Hornberger et al., 1999) and fibre-fibre-interactions (Brown et al., 2000) realised by axonal receptor and ligand interplay.

Based on *in vitro* stripe assays and computational modelling, it was previously suggested that tectal EphAs and ephrinAs would be both repulsive with regard to growth of axonal side branches (Rashid et al., 2005; Yates *et al.*, 2004). This is, however, inconsistent with guidance in potential field because two indistinguishable counter-graded repellents would add up to a homogeneous repulsive surface instead of a guidance potential. Moreover, the authors assume, in contrast to the presented study, that ephrinAs and EphA receptors have no influence on the primary axon, but only on interstitial branches along the axon. However, as shown by collapse and stripe assay experiments (Drescher et al., 1995; Rashid et al., 2005), the primary axon is indeed sensitive to ephrinAs and EphAs.

Therefore, it is still not very well understood in which way forward and reverse signalling would be integrated. In accordance with the requirement of counteracting forces for topographic guidance, a signal transduction cascade was proposed in which a hypothetical intracellular integrator is activated by reverse signalling and inhibited by forward signalling.

This basic hypothesis of the model is supported by recent findings that signalling through the EphA receptor inhibits, whereas signalling through the ephrinA ligand might activate cellular responses (Huai and Drescher, 2001; Konstantinova *et al.*, 2007; Marquardt et al., 2005). However, more direct experimental evidence for the suggested integration is still scarce. Thus, it was first investigated if counter-acting forward and reverse signalling is still consistent with topographic mapping by implementing this signal integration in a computational model of topography formation.
The model was found to yield topographic order of axons in a simulated tectum.

A previous version of a comparable model containing only the retinal EphA and tectal ephrinA gradients (Honda, 1998) implemented the required guidance potential instead of two counter-acting signals by referencing one signal (forward signalling) to an universal “reference value” S, for which no biological evidence exists.
Due to counteracting forward and reverse signalling the presented novel model generates en passant a guidance potential with a minimum at the topographically correct target.

One way to evaluate a theoretical model describing a biological system is to determine its ability to reproduce and explain crucial experimental evidence that has been gained on the system so far.
The presented model was first used to replicate stripe assays with purified EphA3 (receptor) or ephrinA2 (ligand) respectively. In both experiments, retinal axons avoid growing on these guidance cues. That means, the axon response to either guidance cue cannot be distinguished. Somewhat counter-intuitively, due to the antagonistic implementation of forward and reverse signalling, these important *in vitro* experiments were nevertheless reproduced by the novel computational model.
In fact, the unexpected axon response in the “reverse signalling stripe assay” (with EphA containing stripes) can best be figured out by considering the behaviour of nasal axons in this simulation (which should be most sensitive to the EphA due to their high ligand endowment). Nasal axons terminate in the posterior tectum, which is characterised by high ligand but low receptor concentrations.

In an EphA stripe assay, however, positional information of being in the anterior tectum is conveyed to the axons by the receptor stripes. Consequently, nasal axons avoid growing on the receptor stripes.
Taken together, the novel integrative model presented in this work is consistent with topographic map formation and important *in vitro* data.

The Novel Model Replicates *in vitro* Evidence that Suggested the Existence of *cis*-Interactions between Axonal Receptor and Ligand

Recent evidence indicated that axonal ligands and receptors on the same axon might interact (*cis*-interactions). Manipulations of this interaction, via retinal over-expression or enzymatic shedding of the axonal ligand, established the involvement of *cis*-signalling in topographic guidance (Carvalho *et al.*, 2006; Hornberger et al., 1999). Based on these experiments, it was suggested that the *trans* ligand binding ability of axonal receptors may be abolished by ligand molecules in *cis* (“receptor masking”).
The presented model has the *cis*-interaction implemented as constitutively active reverse and forward signalling rather than a ligand-induced masking of the axonal receptor because a masking might render the nasal axon population (low receptor, high ligand) unable to find their correct target according to the “text-book model”. Nevertheless, the presented counter-gradient model was able to fully reproduce the experimental evidence suggesting that these *in vitro* results are in fact consistent with changed reverse signalling due to shedding or over-expression of the axonal ligand.
In particular, after removal of the axonal ligand, the overall guidance signal for nasal axons is mainly determined by the signal through the axonal receptor (forward signalling). Thus, without any balancing reverse signalling, nasal axons show a strong avoidance reaction to the ligand stripes under these conditions. In contrast, when the axonal ligand is increased, temporal axons become non-responsive to the ephrinA2 stripes due to the relatively high signalling through the axonal ligand (reverse signalling) that out-balances the forward signalling conveyed by the substrate.

The Phenotype Seen after EphA3 Knock-in Cannot Satisfyingly Be Explained by Current Chemoaffinity Models Even if Fibre-fibre-interactions Are Included

EphA3 knock-in in a scattered population of nearly half of the RGCs resulted in a map-duplication in the superior colliculus corresponding to distinct knock-in and wild-type maps (Brown et al., 2000).
Most surprisingly neither map was normal: Knock-in growth cones terminated in the anterior SC, but wild-type terminals were shifted to the posterior part of the superior colliculus. The common explanation for this phenotype is that the knock-in growth cones pushed the temporal wild-type growth cones out of their usual target zone in the anterior superior colliculus (through fibre-fibre-interactions).
If that were true, a chemoaffinity model incorporating fibre-fibre interactions via the topographic guidance apparatus should in principle be able to reproduce the observed map features. Using the novel model, all basic experimental observations of this study (map duplication, wild-type map displacement) could be reproduced suggesting that fibre-fibre-interactions indeed may contribute to topographic mapping.
However, although considerable displacement of temporal wild-type terminals was observed in these simulations, it was not as pronounced as reported in the original study. Further analysis immediately revealed that knock-in axons did not grow very far into the superior colliculus due to their unusually high receptor values. Lowering the added receptor values in turn reduced the knock-in growth cones' ability to displace the wild-type growth cones through fibre-fibre-interactions efficiently.
Led by those findings, other chemoaffinity models were reviewed to see, if they were able to explain the EphA3 knock-in phenotype.

Koulakov and co-workers (Koulakov and Tsigankov, 2004) suggested a Markov chain model that is not based on axon guidance in a potential field. It incorporates only the retinal receptor and collicular ligand gradient to explain the map duplication and the wild-type displacement. Their model was able to reproduce the features of this experiment quite nicely.

However, the proposed mechanism generates a topographic map on any tectum/SC irrespective of the shape of the retinal and tectal gradients by simply sorting axons according to their receptor values. Albeit probably intentional to create a certain level of map robustness, the consequences are quite fundamental and not consistent with the current understanding of RTP formation: When for instance the temporal retina is ablated, nasal axons would, according to Koulakov et al., topographically map at once to the whole SC/tectum. That means, nasal axons rely on temporal axons to find their correct target, which is in fact in stark contrast to the findings of Roger Sperry that led him to formulate his chemoaffinity theory in the first place: Even in the absence of temporal axons nasal axons exclusively terminate in the posterior tectum (Sperry, 1963).

Another model, not based on axon guidance in a pre-existing potential field, to explain the map duplication does in fact consider counter-gradients in retina and SC (Willshaw, 2006).
According to that study, the target tissue is initially set to be void of any graded guidance cues, which are subsequently induced by single RGC growth cones. However, recent work on a zebrafish mutant lacking all RGCs incidentally showed that ephrinA5 expression is unchanged without RGC innervation of the optic tectum (Gosse *et al.*, 2008). Furthermore, topographic mapping is not affected when single RGCs are explanted into those mutants. Thus, although suggesting a quite intriguing mechanism for topographic mapping, current evidence argues in fact against a model of marker induction during retinocollicular and retinotectal projection formation.

Honda used a one-dimensional version of his original “servo-mechanism” model to simulate the EphA3 knock-in phenotype (Honda, 2003). His model does not include counter-gradients in retina and SC and therefore relies on introduction of a somewhat artificial mechanism of competition for collicular space with reference to a critical population density to simulate fibre-fibre-interactions. In an attempt to increase this competition, the author had to elevate the number of RGC terminals in the knock-in phenotype, while keeping the collicular space the same, thus forcing knock-in terminals farther into the SC.

Although fitting the wild-type distribution with this method, the knock-in map still did not show the distribution curve suggested by the original data. Due to the chemical markers on the tectum the knock-in axons with unusually high receptor values do not grow very far into the SC.

A recent paper published by O'Leary's Lab (Yates et al., 2004), also incorporating counter-gradients in retina and tectum, suggested forward and reverse signalling to be both repulsive to the growth of axonal side branches. According to them, in principle ephrinAs and EphA receptors have no influence on the primary axon but only on interstitial branches along the axon shaft. This might be the case in the mouse in which axon overshoot and subsequent axon retraction is seen in the colliculus and the actual target zone is formed along the axonal shaft.
However, in lower vertebrates the primary axon is indeed sensitive to ephrinAs, as shown by all collapse and stripe assay experiments (Drescher et al., 1995). When the authors used that model to simulate the receptor knock-in phenotype, almost no displacement of temporal wild-type terminals was seen.

The model probably receiving the most attention so far suggested a pure interaction among growth cones as driving force that governs topography in RTP formation, rather than axon guidance in a potential field (Reber *et al.*, 2004). Growth cone interaction in this model was constituted by sorting of neighbouring RGC growth cones based on a comparison of ratios of EphA receptor signalling. Apart from orienting the map, the model does not rely on any directional guidance cue in the tectum for topographic mapping. Nevertheless, previous ephrinA knock-out and *in vitro* studies provide convincing evidence that ephrinAs indeed serve as topographic guidance cues.
The authors' main focus was the observed map collapse point seen in heterozygous EphA3 knock-in mice. In these animals the wild-type map is not exclusively confined to the posterior SC (as in homozygous knock-in mice) but extends over the whole SC and converges with the knock-in map in the anterior SC into a single coherent map. The position of the collapse point in the SC was nicely explained by this model. However, no complete mapping function of the map duplications was provided.

The authors suggested that the axon with the highest receptor value R_T (i.e. the most temporal knock-in or wild-type axon respectively) would be used as reference to all other axons in this sorting process [$R_T/R(x_a)$]. The axon with the lowest receptor value R_N would automatically occupy the most posterior position in the colliculus. It can be easily shown that under these conditions any axon with receptor value $R(x_a)$ occupies the relative position x_t/x_{t0} along the anterior-posterior axis in the target field (with x_{t0} representing total target length) according to:

$$\frac{x_t}{x_{t0}} = -\frac{R_N}{R_T - R_N} + \frac{R_N}{R_T - R_N} \cdot \frac{R_T}{R(x_a)}$$

After generating the mapping function with this basic rule of the model, it becomes evident that this model also falls short of accurately reproducing the observed *in vivo* distribution of knock-in and wild-type axons (Figure IV-1).

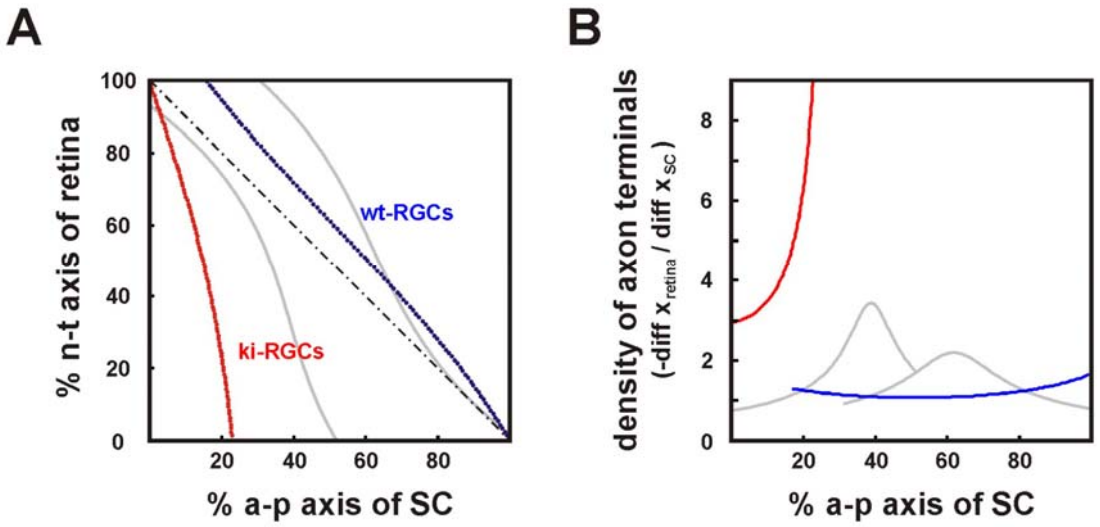

Figure IV-1. Simulation of the Map Duplication in Homozygous EphA3 knock-in Mice according to the Mechanism Proposed by Reber et al. 2004.

For 50 knock-in and 50 wild-type growth cones, receptor ratios were calculated using the gradient equations published by Reber et al. Then they were sorted such that the growth cone with the highest receptor amount was assigned the most anterior position and the growth cone with the lowest receptor amount to the most posterior position as the authors suggest. Map duplication was observed, but a displacement of the wild-type map was rather modest compared to the original report (A). Furthermore, the axon terminal distribution in the SC did not fit with the observed distribution *in vivo* (B). The grey lines indicate the mapping function (A) or termination densities (B) as obtained from the original data set.

The most serious issue this model faces, however, is that it basically fails to reproduce correct mapping of major parts of the temporal retina in wild-type animals. The reason for that is the empirically found lower ratio limit of 1.36 for discriminating different EphA concentrations, which the authors needed to explain the position of the map collapse point. However, in major parts of the temporal retina axons simply do not exceed this ratio and thus cannot find the correct target.

In summary, it appears established from experimental and theoretical data that fibre-fibre-interactions are at least in part contributing to the observed map duplication and the displacement of the wild-type map. However, neither of the current models based on chemoaffinity is able to reproduce satisfyingly the observed phenotype. Especially the intriguing behaviour of the temporal knock-in axons, that is, their ability to enter the superior colliculus despite their unnaturally high receptor endowment, remains unexplained.

It seems obvious that a conceptually different, but not necessarily exclusive mechanism, other than a strict guidance by chemical markers might be involved if the EphA3 knock-in phenotype were to be reconciled with the current model of topographic axon guidance. Adaptation of the growth cones in response to the guidance cues might be a candidate mechanism for that.

A Topographically Differential Growth Behaviour Is Reconstituted *in vitro* Using “Double Stripe Assays” of EphA and ephrinA

In vitro assays have been successfully applied in axon guidance research to characterize and identify the molecules involved in topographical guidance of axons. However, these experiments surprisingly fail to reproduce a fundamental prediction of chemoaffinity, namely a substrate choice of retinal axons that is topographically differential according to their target *in vivo*. Usually, either a uniform reaction of nasal and temporal axons to the guidance cues or only a decision of temporal axons while nasal axons are unresponsive can be observed. The reason for that is still elusive.

The presented model with implemented counter-balancing of reverse and forward signalling predicted for a stripe assay with alternating stripes of receptor and ligand that nasal retinal axons would grow on the ligand containing stripes, whereas temporal ones would prefer the stripes with receptor. In other words, this model suggested a topographically differential axon decision consistent with the chemical marker choice of the RGC axons *in vivo* as long as both cues are present.

Alternating stripes of receptor and ligand cannot be produced with the standard technique of stripe fabrication due to the high affinity of both molecular species that prevents a separation in distinct adjacent stripes. Therefore, a special protein-printing technique was applied. Clearly separated stripes of EphA3 and ephrinA2 could be generated with this new method.

When performing this special stripe assay experiment, nasal and temporal axons indeed showed topographically differential growth consistent with the simulation and the *in vivo* behaviour. Axons from the centre of the retinal explant did not show any decision which might indicate evidence for continuous topographical differentiality rather than just a nasal-temporal difference of axon decision.

Due to limitations in generating stripe substrates with precise protein concentrations on the surface, the reported differential growth behaviour was not observed in all “double stripe” experiments in the used concentration range. Nevertheless, the validity of the presented results is supported by two inherent controls: On “double stripe” substrates both axon populations change their behaviour.

Nasal axons switch onto the ligand stripe compared to the ligand “single stripe” assay, whereas temporal axons on the very same substrate stay off the ligand stripe indicating its functionality. At the same time, temporal axons switch onto the receptor stripe compared to the receptor “single stripe” assay, whereas nasal axons avoid the receptor on the same substrate, indicating the functionality of the receptor stripe respectively.

And despite the seen fluctuations, no single explant was found where nasal axons grew on EphA3-Fc stripes and temporal axons on the ephrinA2-Fc stripes at the same time which would amount to “anti-topographic” behaviour.

Also in another context, it is worth noting that both axon populations, the nasal axons as well as the temporal ones, switch their preference in the “double stripe” experiments. It has been shown that an axon’s response to a guidance cue is strongly modulated by the axon’s internal state [cGMP, Ca^{2+} concentration, (Nishiyama *et al.*, 2003; Song *et al.*, 1997)] which e.g. determined by axon exposure to different extra-cellular matrix molecules (Hopker *et al.*, 1999; Nguyen-Ba-Charvet *et al.*, 2001).

However, the observed “switching” of the RGC axon behaviour in a double stripe assay suggests that the effect of an individual guidance cue can even be changed by other guidance cues that are present, depending on the axonal receptor-ligand ratio. Given the fact that guidance molecules are often expressed in a highly combinatorial manner in the brain, this data strongly points out the importance of a systemic approach to deciphering guidance cue function.

There is a single previous report of a differential axonal growing behaviour *in vitro.* For their stripe assay, the authors used tectal membranes gained by a special fractionation technique, which were of course undefined substrates (von Boxberg *et al.*, 1993). Hence, this effect could not be explained with the activity of specific guidance cues or even underlying molecular interactions.

In summary, the experimental observation of a topographically differential substrate choice by retinal axons, shown for the first time under defined conditions, suggests that previous choice assays failed to reproduce such behaviour because of the absence of either reverse or forward signalling *in vitro*.

Taken together, experimental work and theoretical modelling demonstrated that retinal axons might be topographically guided by two monofunctional counter-graded molecules on the target cells rather than only one gradient as the “text-book” model of RTP formation would suggest.

The Novel Model Is Robust against Perturbations

Despite its explanatory power, strict chemoaffinity is in fact also a quite error-prone mechanism for the topographic sorting of axons. As chemoaffinity suggests, position would be encoded by different concentrations of chemical markers. Therefore, any variation of this relationship of position and chemical marker concentrations is considerably reducing the mechanism's precision. However, such variations are to be expected in biological system, be it that the size of the tectum varies or that the marker inducing processes are susceptible to fluctuations. Nevertheless, a precise topographic map is almost always formed *in vivo,* which raises questions about how this amazing robustness is realized.

Several control mechanism have been suggested for that task such as activity dependent refinement (Cang *et al.*, 2008; McLaughlin *et al.*, 2003b; Ruthazer and Cline, 2004; Torborg and Feller, 2005) or competition for target-derived neurotrophic factors (Fraser and Perkel, 1990; Goodhill and Xu, 2005). However, such mechanisms might play a less prominent role in lower vertebrates, where the axon targeting is quite precise from the beginning.

As was shown in this study, a substantial degree of robustness of topographic mapping can already be achieved by implementing forward and reverse signalling as opposing guidance forces. The proposed model mechanism is able to counter-balance variations of gradient concentrations and tectal length. In both cases topographic mapping is perfectly retained. In terms of the model, this is achieved by simultaneous increase or stretching of the two tectal gradients. The resulting overall signal stays the same. For this type of robustness the tectal gradients need to be initially set up simultaneously by one organizing structure at one side of the target region via e.g. a diffusible substance or mutual regulation after induction of only one gradient.

The organiser's activity then determines the eventual distribution of the gradients. It was recently shown that diffusible FGFs, released from the isthmic organiser at the midbrain-hindbrain boundary (MHB), are gradually distributed in anterior<posterior gradients in the tectum.

High FGF concentrations led to tectal cells producing high levels of ephrinA mRNA and low levels of EphA mRNA, whereas low concentrations of FGFs induced low levels of ephrinA and high levels of EphA (Chen et al., 2009).
This type of robustness is admittedly not infinite as it still strongly depends on a coupling of receptor and ligand expression. However, by introducing counter-gradients and relational processing of forward and reverse signalling robust topographic mapping onto a simulated tectum is achieved. This is in fact a feature simpler chemoaffinity models fail to display. This mechanism might thus substantially contribute to the robustness of topographic mapping observed *in vivo*.

Conceptual Thoughts on Adaptive Mechanisms during Topographic Guidance

Sperry's chemoaffinity theory based on the matching of gradients is now widely accepted as underlying basis for topographic brain wiring.
However, as already discussed and despite its undeniable predictive power, gradient matching imposes a degree of rigidity on the system, which is not consistent with its robust topographic precision and specificity.
Since adaptation to changing environmental conditions seems to be a recurrent theme in biological systems, one can easily envisage that adaptive mechanisms of sorts may help to overcome these limitations. Moreover, there is convincing experimental *in vivo* and *in vitro* evidence suggesting retinal growth cones might indeed be able to adapt to the guidance cues which is discussed later in this chapter (Brown et al., 2000; Rosentreter et al., 1998; von Philipsborn et al., 2006).
However, while adaptation might generally provide a means of increasing map robustness and precision, an unrestricted adaptation may potentially interfere with topography formation. That is to say, RGC growth cones that adapt perfectly to the guidance signal might loose the ability to identify their correct target position. Thus, in order to preserve topographic mapping any adaptation against the guidance signal must be adjusted precisely.

Gradient potentials provide positional as well as directional information for retinal growth cones during topographic guidance. Read-out of the directional information means that the growth cone is detecting differences of adjacent guidance cue concentrations. The positional information, in contrast, is conveyed by the absolute concentrations indicating the guiding potentials minimum or maximum. It is differentially interpreted by different growth cones due to their topographically differential endowment with chemical markers.

In this system, two conceptually different types of adaptation seem conceivable:
First, an axon might adapt against the directional information i.e. in the sense of an optimization of the growth cone's ability to sense concentration differences (Type I). Second, there might be an adaptation against the positional information, which leads to a shifting of the topographical position of the guiding potentials minimum or maximum in the target field (Type II). Of course, both types of adaptation are not mutually exclusive and might act simultaneously during topographic axon guidance.

An adaptation of a growth cone’s sensitivity to concentration differences (Type I) may help to optimize the read-out of the gradient potential dramatically. For instance, it might enable the growth cones to cope with the changing slopes in an exponential gradient. One could envisage that a growth cone continuously adjusts its sensitivity for concentration differences of guidance cues such that it is perfectly able to tell which one of the concentrations it encounters is the highest or the lowest. A possible mechanism for this could be signal amplification within the growth cone due to intracellular pattern formation (Gierer, 1981; Gierer and Meinhardt, 1972).
This type of adaptation is consistent with topographic mapping because axon differentiality is not lost during the process.
On the other hand, a Type II adaptation against the positional information might increase the robustness of topographic mapping, when for instance the gradients in retina or tectum are not matching each other. An adaptive mechanism addressing the topographic position must change the differential identity of the retinal axons e.g. by adjusting the axonal receptor and/or ligand amounts.

However, any adjustment has to be carefully regulated, because otherwise topographic differentiality will be lost. The consequence would be a drift of the axonal growth cones away from their correct target positions.
Such a continuous or also called perfect adaptation would be reminiscent of the chemotaxis mechanism in bacteria [see e.g. (Koshland, 1980; Wadhams and Armitage, 2004) and citations therein) or growth cone guidance by diffusible cues, like Netrin (Ming *et al.*, 2002). These adaptive mechanisms are solely used to steer towards or away from a source of attractant or repellent respectively instead towards a certain topographic position within a gradient.

Therefore, when the potential minimum has to be shifted, topography can only be generated if the minimum is shifted relative to some signal that remains unchanged during the adaptation process and which is in some ways correlated to target extent. This might be realised through fibre-fibre-interactions such that the growth cone targeting the most anterior or posterior target position is used as reference point.
Or it might be conveyed by an intrinsic feature of the tectal gradients, like symmetry for instance, such that the growth cone can probe the extent of the target field without actually having to survey it as a whole.
Undoubtedly, every conceivable adaptive mechanism would imply modulation of the activity of involved signal transducing molecules. This might be achieved by regulation of downstream effectors of EphA-ephrinA signalling or by post-translational modifications of the axonal receptor or ligand itself. Experiments in other systems indicate that it can also involve direct changes in membrane activity of the molecules in question by clustering, local translation, endocytosis or proteolysis (Bray *et al.*, 1998; van Horck *et al.*, 2004).

Experimental Evidence for Adaptive Mechanisms during Topographic Axon Guidance

When retinal axons were growing perpendicular to EphA3 stripes, they were able to cross the first few stripes easily (Schlupeck, 2008). This is in contrast to the axons' behaviour in usual EphA3 stripe assays in which they cannot cross the EphA3 stripes parallel in their direction of growth. Hence, there seemed to be an angle-dependence of the growth cones' response. Adaptation to EphA3 was frequently discussed to be the reason. That means, if axons due to their rigidity cannot avoid the EphA3 stripes, they have to adapt in order to cross them.
However, simulation of this experiment with the presented novel model suggests another possible explanation. That is, fibre-fibre interactions might be held accountable for the axons apparent desensitisation to the EphA3 guidance cue.
Computational simulation with the novel model presented in this work revealed that when fibre-fibre-interactions were included, axons could cross the receptor stripes whereas without fibre-fibre-interactions they could not.
The observed axons' crossing of usually avoided EphA3 stripes might be facilitated by succeeding axons pushing their forerunners over the stripes or by a covering of the stripes by axons such that their successors can easily overcome them.
Therefore, it is conceivable that the observed axon growth behaviour might be caused by fibre-fibre interactions rather than real growth cone adaptation to the guidance signal.

The ability of retinal axons to grow with ease even when placed on high homogeneous concentrations of repulsive ephrinA is another evidence often discussed as sign of a desensitisation process (Walter et al., 1987a; Walter et al., 1987b). However, simulations of such an experimental situation with the presented model point to an alternative explanation. No difference was seen when retinal explants of different origin were placed in target fields filled with various homogeneous ligand concentrations. The assumption that axons should have a hard time growing on "repulsive" ephrinAs, unless there is considerable desensitisation, might thus be based on a misunderstanding of the repulsiveness concept in general.

Repulsiveness in the context of guidance in a potential field manifests itself when concentration differences of a particular guidance cue are presented and the smaller concentration is chosen by the axons. Without any additional assumption, neither absolute concentration in this example is repulsive and cannot be interpreted by the growth cones other than as a neutral substrate, when presented homogeneously. In summary, the observed axon growth on high concentrations of ephrinAs is therefore consistent with a chemoaffinity model based on axon growth in a guidance potential without adaptation.

Although this axon growth behaviour can be explained without adaptation to the guidance signal, experimental evidence exists that there might be nonetheless an ongoing adaptive process when retinal axons are cultured on homogeneous ligand substrates.

Using micro-contact printing Anne von Philipsborn fabricated so called gap substrates, in which a high homogeneous distribution of ephrinAs is interrupted by a gap of variable width that is void of any ephrinA [(von Philipsborn, 2007) and unpublished data). Consistent with monofunctional guidance by ephrinAs, retinal growth cones do not cross sharp steps of very high ephrinA concentration. Usually, they stop in front of it.

In this experimental set-up, however, temporal retinal growth cones are placed on the homogeneous plateau of the gap substrate, growing first on homogeneous high ephrinA concentrations and subsequently, the growth cones encounter the gap filled with a neutral substrate.

Provided that the gap is short enough (<100µm), growth cones are able to overgrow the ephrinA edge on the other side of the gap with ease. If the gap is very wide though (>100µm), the growth cones stop as usual.

In summary, if temporal retinal growth cones grew for some time on high concentrations of ephrinA they seem in fact to adapt such that they loose the ability to detect a step increase in ephrinA concentration. On the other hand, when the growth cones are given the opportunity to grow some time or distance on a substrate without ephrinAs, they can become sensitive again to a step-like ephrinA distribution.

The inability to detect this step-like concentration difference might suggest an adaptation of Type I towards the concentrations differences of the gradient potential. In this scenario, the retinal axons would adapt to the high homogeneous ephrinA concentration before the gap such that they down-regulate the sensitivity of their concentrations difference detector.
This process would then be reverted depending on the distance or more likely the time the growth cones grew on the substrate in the gap which is free of any adaptation-triggering ephrinA.
An adaptation against the positional information (Type II) could be contributing as well to the outcome of this experiment. Any change of the potential minimums position in the target field would have to involve a change in differentiality of the axons. In the simplest case this might be realised by a down-regulation of the axonal receptor after growth on high homogeneous ephrinA concentrations as found before the gap. However, this mechanism might facilitate, but is not sufficient to enable axons to grow over a sharp step of ephrinAs. This is due to the monofunctional guidance effect of ephrinAs, which means that the neutral substrate found in the gap, like in an ephrinA stripe assay, is always favoured compared to any ephrinA substrate regardless of the amount of the axonal receptor.
In summary, this experiment indeed suggests an adaptation of the growth cones when they grow on substrates of homogeneous guidance cues which is not included in any current model of topography formation.

Rosentreter and colleagues reported experiments in which axons growing out from a temporal retinal explant were confronted with an increasing concentration gradient of posterior tectal membranes (Rosentreter et al., 1998).
All temporal axons grew into these gradients and subsequently showed an avoidance reaction at specific membrane concentration values. However, when the explant was placed on a “concentration pedestal” of tectal posterior membranes in front of and underlying the gradient, axons invaded the gradient and grew to correspondingly higher concentrations. This might indicate that a growth cone could adapt to levels of background guidance cues (i.e. the tectal guidance cue concentration represented by the pedestal height) without loosing the ability to detect and process the guidance signal.

The observed axon growth behaviour is in principle consistent with an adaptive mechanism of Type II against the positional signal of the guidance potential. In this scenario for instance a down-regulation of axonal receptor in response to the underlying background concentration of the tectal guidance cue seems conceivable thus changing the differential identity of the adapting growth cones. This might enable the growth cones to enter the gradient much deeper before they show an avoidance reaction.
In summary, this experiment indicates adaptation against the positional signal of the guidance potential, which is not completely desensitising the growth cones but is precisely adjusted to preserve differentiality for topographic mapping.

Results published by von Philipsborn and colleagues (von Philipsborn et al., 2006) also suggest an adaptive response of retinal growth cones *in vitro*. Because membrane preparations are poorly defined, the authors used micro-contact printing (μCP) to reproducibly fabricate substrate-bound linear ephrinA gradients.
When temporal retinal explants were placed in front of these gradients emanating growth cones showed a distinct stop reaction, which was slightly dependant on the slope of the used ephrinA gradients. It appeared that the steeper the gradient, the higher the ephrinA concentration the retinal axons were able to grow.
Further analysis revealed that the stop reaction occurred when the local ephrinA concentration was in balance with the total amount of encountered ephrinA. Thus, the authors suggested that this might be accomplished by a continuous adaptation of the growth cones to the local ephrinA concentration that is limited by a summation of already encountered ephrinA.
Although this explanation introduces path-dependence of topographic axon guidance, which is clearly not consistent with guidance in a potential field, it proves that growth cones react differently to the same concentration of guidance cues, which is not consistent with the current understanding of topography formation through chemoaffinity.

In vivo evidence for adaptation might be drawn from the work of Brown and colleagues (Brown et al., 2000). As discussed earlier, all contemporary chemoaffinity models fail to precisely reproduce the EphA3 knock-in *in vivo* data.

When analysing the mapping diagrams of the EphA3 knock-in animals more closely, it becomes apparent that the knock-in map shows a somewhat unexpected and unusual distribution (Figure III-11). In particular, even temporal knock-in RGC axons, carrying artificially high receptor concentrations, map to the SC, although no matching guidance cue concentrations are present for them in the target field.
One explanation might be that RGC growth cones are able to adapt their target position *in vivo* as well (Type II adaptation). The putative adaptation mechanism must enable the knock-in axons to enter the superior colliculus despite the guidance cues present on the target cells and at the same time maintaining their displacement ability of temporal wild-type growth cones. Of course, it is possible that adaptation is not confined to the knock-in RGC growth cones but might contribute at least in part to the seen shift of temporal wild-type map.

The above presented experiments and evidences might not be explained by one unifying adaptive mechanism. However, the data clearly show that retinal growth cones may frequently change their response to a certain guidance cue concentration, which is not easily conciliated with chemoaffinity.
Furthermore, these experiments confirm that adaptation of retinal growth cones exists and that it is intrinsically limited, which is a major prerequisite to retain topographic mapping. However, no mechanistic understanding of adaptive processes during topography formation is existent so far.

Topography & Adaptation

To demonstrate that perfect adaptation without limitation might interfere with topography, an adaptation algorithm used for a description of light adaptation and chemotaxis in bacteria (Block et al., 1983; Delbrück and Reichardt, 1956) was introduced into the counter-gradient model proposed earlier. When the axonal receptor and ligand were allowed to adapt perfectly, as expected topography was lost in the simulations and all axons grew towards the end of the target field. Therefore, it is apparent, not only from a theoretical point of view, that adaptation to the topographic signal has to be restricted in order to retain topographic mapping.

Surprisingly, when just one cue (e.g. the axonal receptor) was allowed to continuously adapt to the tectal ligand, while the other cue was kept differential and in match with its tectal counterpart, a perfect topographic map was formed.
This is caused by the underlying gradient matching. As long as one component of the axonal guidance apparatus (e.g. the ligand) is kept differential, and thus is balancing the adaptation, a guiding potential with an extreme value at the correct target position is generated.
Previous work suggested that adaptation might be switched off in a gradient (Löschinger et al., 2000) to account for the adaptation's apparent incompatibility with chemoaffinity.
However, while the mechanism proposed in this work is still relying on gradient matching, the presented circumstantial evidence indeed may suggest a potential adaptation mechanism that is acting inside the gradient, which is biologically plausible and in accordance with chemoaffinity, may be obtained.

Suggestions for Future Research

It might be a general misconception that topographic map formation in the brain is a resolved issue. This is probably an unfortunate reaction to the relative stagnation of the field indicated by the decreasing number of publications over the last few years. However, there is still no comprehensive model to explain all the data that has been gathered. Therefore, new strategies and methodological approaches are needed to truly understand how retinal axons find their topographically correct targets.

Beginning with the seminal work of Roger Sperry, the most influential experiments that laid the conceptual framework for the axon guidance field were in fact regeneration experiments [see (Goodhill and Richards, 1999) for references].
The advent of new genetic tools might facilitate ablation experiments in animals such as mice without relying on retinal axon regeneration. Genetic cell ablation methods could not only be done with higher precision than by surgical means, they might allow as well discrimination between initial mapping mechanisms and regenerative ones.

In particular, these experiments can help to rule out the possibility that the original mapping changed the target tissue during regeneration experiments.

An elegant approach recently applied for genetic ablation might be of use here (Han *et al.*, 2009): A conditional expression of Diphteria Toxin Receptor (DTR) under the control of RGC and retina region specific promotors, active e.g. in nasal, temporal or central retina, would render this RGC subset prone to Diptheria Toxin Fragment A (DTA). DTA can be injected *in utero* into the eye at time points when retinal axons are growing out to their target. DTA would then kill only the cells bearing the DTR leaving the others unharmed. Subsequently mapping defects could be visualized by focal injection of lipophilic tracers into the eye.

Of course this technique can also be used to study the influence of fibre-fibre interactions on topographic map precision *in vivo*. This could be achieved for instance by a general reduction of RGCs, resulting in reduced fibre-fibre interactions. Again using for instance DTR under the control of the previously used Isl-2 promotor (Brown et al., 2000), which is expressed in half of the RGCs evenly scattered across the retina in mice, a reduction of RGCs might be achieved after DTA injection into the eye.

Though providing the conceptual framework for topographic mapping research, the guidance cue gradients remain surprisingly poorly defined. Little is known about the gradients' distribution on mRNA and protein level apart from being visually identified as gradients. Only the EphA gradients in the retina were precisely quantified so far using *in situ* hybridization with radio-labelled probes (Reber et al., 2004).

These experiments suggested a shallow exponential distribution for the EphA receptor gradients in the retina.

Either the same strategy or maybe quantitative RT-PCR could be applied to measure all the ephrinA and EphA gradients in retina and SC/tectum to determine the existence of a potential matching of retinal and tectal gradients which is in fact a major assumption of chemoaffinity. Moreover, measurements taken from several individuals might provide insights about fluctuations in the system and hence the mechanisms for increasing robustness of the mapping.

Transgenic knock-out experiments have been a valuable tool in the past, but have been surprisingly crude as no retina or SC region-specific removal of ephrinAs or EphAs was performed. A conditional knock-out strategy, e.g. of the ephrinA gradients exclusively in the retina, seems imperative to improve the understanding of what the individual gradients contribute to topographic mapping.

While sophisticated *in vivo* studies might be useful, at the same time a need for better *in vitro* substrates that closely resemble the *in vivo* situation is evident. In the present study the foundations were laid to produce such *in vitro* substrates in a defined manner.
Since reverse signalling was shown to have an effect on retinal axon guidance, it would be important to create growth substrates that include both receptor and ligand at the same time. Moreover, neglecting reverse signalling might as well be the reason why a perfect topography is still missing *in vitro* as the present work might indicate.
A most desirable guidance substrate in this context would be continuous counter-gradients of receptor and ligand, because only under those conditions a complete topographic decision *in vitro* can be expected.

Several techniques may help achieving this goal including the use of light-patterning of caged guidance cues which was shown in this study. Functional gradients of homogeneously distributed caged guidance molecule may be produced by graded UV illumination through a neutral wedge.
Other recent techniques that might be used for generating continuous gradients are laser-assisted adsorption by photobleaching (Belisle *et al.*, 2008) or fabrication of substrate-bound protein gradients by using covalent bonding of the proteins with an epoxy-coated glass substrate (Mai *et al.*, 2009).
EphA receptors form a high-affinity complex with their ligands, the ephrinAs, raising questions about how those molecules can mediate axon guidance by contact repulsion. Several mechanisms were shown to exist that terminate this interaction.

This includes cleavage of the ephrinA ligand by the metalloprotease ADAM–10/Kuzbanian (Hattori *et al.*, 2000) or degradation of the receptor-ligand complex via endocytotic pathways (Zimmer *et al.*, 2003). Those mechanisms may not be working in tissue culture when using micro-patterned substrates of purified proteins. In fact microscopic pictures of axons, which grew over margins of the micro-patterned ephrinA substrate, show unnatural filopodia-like protrusions along the edges. They might be remnants of processes that could not be retracted. The observed stopping reaction of retinal growth cones on micro-patterned homogeneous ephrinA substrates (von Philipsborn et al., 2006) is also not consistent with the current model of topography formation and might be a sign of a receptor-ligand binding that was not properly terminated.
Furthermore, if the adhesive forces become too strong, a tearing of receptor-ligand complexes out of the membrane may occur. This might seriously influence the outcome of *in vitro* experiments due to the potential interference with axon differentiality. Therefore, it is surely worth investigating if the addition of recombinant ADAM-10 to the culture helps to improve the *in vitro* experiments.

In parallel to experimental approaches, theoretical modelling proved valuable in the past for understanding biological phenomena and may generate new experimentally verifiable hypotheses that could help to introduce new ideas and concepts into the field. Furthermore, improved modelling might help to suggest and reject possible mechanisms for the reported adaptation events during retinal axon guidance, which can then experimentally be addressed.
Thus, a major challenge remaining is the implementation of an adaptation mechanism that is consistent with topographic mapping, while at the same time explaining the underlying *in vivo* and *in vitro* experiments.

APPENDIX

Appendix 1: Abbreviations

a / p	anterior / posterior
cGMP	4',5' - cyclic guanosine monophosphate
$D(x_t,y_t)$	local guidance potential at position (x_t,y_t)
Eph	Erythropoetin producing hepatocyte
GC	Growth Cone
GPI	Glycosylphosphatidylinositol
HEPES	N - (2 - Hydroxylethyl) - piperazin - N' - 2 - ethansulfonsäure
L_a	retinal or axonal ligand
$L_{\hat{a}}$	axonal ligand seen on other axons
L_t	tectal ligand
n / t	nasal / temporal
OT	*Tectum opticum*
PBS	Phosphate buffered saline
PI - PLC	Phosphoinositide specific phospholipase C
RGC	Retinal Ganglion Cell
RTP	Retinotectal Projection
R_a	retinal or axonal receptor
$R_{\hat{a}}$	axonal receptor seen on other axons
R_t	tectal receptor
SC	*Colliculus superior*
v / v	volume per volume
w / v	weight per volume
x_a	x - axis of the retina (usually the retinal n / t-axis)
x_t	x - axis of the simulation field (usually the tectal a / p axis)
y_t	y - axis of the simulation field

Appendix 2: MATLAB – Programme Source Codes

A. Source Code of the Programme Used for Simulation of the "Text-book Model" of RTP Formation modified after Honda 1998 (v0.1, chapter III-A)

```
clear all

NoGrowthCone=1;
steps=300;
sigma=0.1;
S=1;
Qx=1;
Qy=0;
QHist=60;
RigidityX=2;                    % the higher this value the higher axon rigidity
RigidityY=2;
SizeGrowthCone=3;
offset= (SizeGrowthCone-1)/2;

FieldSizeX=100;
FieldSizeY=100;
FieldSizeXtd = FieldSizeX + 2*offset;
FieldSizeYtd = FieldSizeY + 2*offset;
LigandCirc or LigandStripe20 or LigandLinear or LigandHomog;

Lxy=zeros(FieldSizeXtd,FieldSizeYtd);
AxonReceptor=zeros(1,NoGrowthCone);

xtHistory=zeros(steps,NoGrowthCone);
ytHistory=zeros(steps,NoGrowthCone);
DxHistory=zeros(steps,NoGrowthCone);
QxHistory=zeros(steps,NoGrowthCone);
QyHistory=zeros(steps,NoGrowthCone);

%------------Calculation of the Expected Maximum Local Guidance Potential Value DxMax-----------

maxAxonRec = exp(-0.03*(0-FieldSizeX/2));
DxMax = abs(1-maxAxonRec*maxAxonRec);

%-----------------------------------------------------Initialisation Step-----------------------------------------------

for n=1:NoGrowthCone

    xt=1+offset;
    yt=50;
    %round(n*FieldSizeY/NoGrowthCone-(FieldSizeY/NoGrowthCone-1)) + offset;
    ystart(n)=yt;

    AxonReceptor(n)=1;
    %exp(-0.03*(yt-offset-FieldSizeX/2));

    random1 = rand;
    if (random1 < (1-Qx)/SizeGrowthCone)
        xtDirection = -1;
    elseif (random1 < 1/SizeGrowthCone+(1-Qx)/SizeGrowthCone)
        xtDirection = 0;
    else
        xtDirection = 1;
    end
```

```
    random2 = rand;
    if (random2 < (1-Qy)/SizeGrowthCone)
        ytDirection = -1;
    elseif (random2 < 1/SizeGrowthCone+(1-Qy)/SizeGrowthCone)
        ytDirection = 0;
    else
        ytDirection = 1;
    end

    if xt+xtDirection<1+offset
        xtDirection=0;
    elseif xt+xtDirection>FieldSizeX+offset
        xtDirection=0;
    end

    if yt+ytDirection<1+offset
        ytDirection=0;
    elseif yt+ytDirection>FieldSizeY+offset
        ytDirection=0;
    end

    Lxy=SubstrateLigand;

    Dx1=abs(S-AxonReceptor(n)*(Lxy(xt,yt)));
    Dx2=abs(S-AxonReceptor(n)*(Lxy(xt+xtDirection,yt+ytDirection)));

    DxHistory(1,n)=Dx1;

    WDx1 = wkeitpd(Dx1,sigma);
    WDx2 = wkeitpd(Dx2,sigma);

    if rand>wkeit01(WDx1,WDx2);
        xt=xt+xtDirection;
        yt=yt+ytDirection;
    end

    xtHistory(1,n) = xt;
    ytHistory(1,n) = yt;
end

%-----------------------------------------------------------------------------------------------------------------------

for i=2:steps
    for n=1:NoGrowthCone
        xt = xtHistory(i-1,n);
        yt = ytHistory(i-1,n);

        Lxy=SubstrateLigand;

        if (i-QHist-1>0)
            xAbs = xtHistory(i-1,n) - xtHistory(i-QHist-1,n);
            yAbs = ytHistory(i-1,n) - ytHistory(i-QHist-1,n);
            if (xAbs > 0)
                Qx = (DxHistory(i-1,n)/DxMax)^(1/RigidityX);
            elseif (xAbs < 0)
                Qx = (-1)*(DxHistory(i-1,n)/DxMax)^(1/RigidityX);
            else
                Qx = 0;
            end
```

```
            if (yAbs > 0)
                Qy = (DxHistory(i-1,n)/DxMax)^(1/RigidityY);
            elseif (yAbs < 0)
                Qy = (-1)*(DxHistory(i-1,n)/DxMax)^(1/RigidityY);
            else
                Qy = 0;
            end
        end

        QxHistory(i,n) = Qx;
        QyHistory(i,n) = Qy;

        random1 = rand;
        if (random1 < (1-Qx)/SizeGrowthCone)
            xtDirection = -1;
        elseif (random1 < 1/SizeGrowthCone+(1-Qx)/SizeGrowthCone)
            xtDirection = 0;
        else
            xtDirection = 1;
        end

        random2 = rand;
        if (random2 < (1-Qy)/SizeGrowthCone)
            ytDirection = -1;
        elseif (random2 < 1/SizeGrowthCone+(1-Qy)/SizeGrowthCone)
            ytDirection = 0;
        else
            ytDirection = 1;
        end

        if xt+xtDirection<1+offset
            xtDirection=0;
        elseif xt+xtDirection>FieldSizeX+offset
            xtDirection=0;
        end
        if yt+ytDirection<1+offset
            ytDirection=0;
        elseif yt+ytDirection>FieldSizeY+offset
            ytDirection=0;
        end

        Dx1 = abs(S-AxonReceptor(n)*(Lxy(xt,yt)));
        Dx2 = abs(S-AxonReceptor(n)*(Lxy(xt+xtDirection,yt+ytDirection)));

        DxHistory(i,n) = Dx1;

        WDx1 = wkeitpd(Dx1,sigma);
        WDx2 = wkeitpd(Dx2,sigma);

        if rand>=wkeit01(WDx1,WDx2);
            xt = xt+xtDirection;
            yt = yt+ytDirection;
        end

        xtHistory(i,n) = xt;
        ytHistory(i,n) = yt;

    end
end

plot(xtHistory-offset, ytHistory-offset);
```

B. Source code of the Programme Used for Simulation the Novel Model of Topography Formation (v0.2)

```
clear all

NoGrowthCone = 60;
SizeGrowthCone = 3;
offset = (SizeGrowthCone-1)/2;
steps = 900;
Qx = 0.1;
Qy = 0;
sigma = 0.05;

FieldSizeX = 100;
FieldSizeXtd = FieldSizeX + 2*offset;
FieldSizeY = 100;
FieldSizeYtd = FieldSizeY + 2*offset;
SubstrateStripe20 or SubstrateExpon or SubstrateStripe20ortho;

AxonalLigandMatrix = zeros(FieldSizeXtd,FieldSizeYtd);
GrowthConeLigandMatrix = zeros(FieldSizeXtd,FieldSizeYtd);
SurCorGL = zeros(FieldSizeXtd,FieldSizeYtd);
Lxy2 = zeros(FieldSizeXtd,FieldSizeYtd);
Lxy3 = zeros(FieldSizeXtd,FieldSizeYtd);

AxonalReceptorMatrix = zeros(FieldSizeXtd,FieldSizeYtd);
GrowthConeReceptorMatrix = zeros(FieldSizeXtd,FieldSizeYtd);
SurCorGR = zeros(FieldSizeXtd,FieldSizeYtd);
Rxy2 = zeros(FieldSizeXtd,FieldSizeYtd);
Rxy3 = zeros(FieldSizeXtd,FieldSizeYtd);

AxonReceptor = zeros(1,NoGrowthCone);
AxonLigand = zeros(1,NoGrowthCone);

xtHistory = zeros(steps,NoGrowthCone);
ytHistory = zeros(steps,NoGrowthCone);

xPos = zeros(1,NoGrowthCone);
yPos = zeros(1,NoGrowthCone);
Qos = zeros(1,NoGrowthCone);

%----------------------------------------------------Initialisation Step---------------------------------------------

for n=1:NoGrowthCone
    xt=1+offset;
    yt=round(n*FieldSizeY/NoGrowthCone-(FieldSizeY/NoGrowthCone-1)) + offset;

    AxonReceptor(n)=exp(0.01*(yt-offset-FieldSizeX/2));
    AxonLigand(n)=exp(-0.01*(yt-offset-FieldSizeX/2));

    xrandom=rand;
    if xrandom<((1+Qx)/2)
        xtDirection=1;
    else
        xtDirection=-1;
    end
```

```
    yrandom=rand;
    if yrandom<((1+Qy)/2)
        ytDirection=1;
    else
        ytDirection=-1;
    end
    if (xt-offset)<=-xtDirection
        xtDirection=0;
    elseif (xt+offset + xtDirection)>=FieldSizeXtd
        xtDirection=0;
    end
    if (yt-offset)<=-ytDirection
        ytDirection=0;
    elseif (yt+offset + ytDirection)>=FieldSizeYtd
        ytDirection=0;
    end

    Lxy3=SubstrateLigand;
    Rxy3=SubstrateReceptor;

    Dx1=abs(log(((AxonReceptor(n)*(Lxy3(xt,yt)+AxonLigand(n)))/(AxonLigand(n)*(Rxy3(xt,yt)...
    +AxonReceptor(n))))));
    Dx2=abs(log(((AxonReceptor(n)*(Lxy3(xt+xtDirection,yt+ytDirection)+AxonLigand(n)))...
    /(AxonLigand(n)*(Rxy3(xt+xtDirection,yt+ytDirection)+AxonReceptor(n))))));

    WDx1=wkeitpd(Dx1,sigma);
    WDx2=wkeitpd(Dx2,sigma);

    xrandom=rand;
    if xrandom>=wkeit01(WDx1,WDx2);
        xt=xt+xtDirection;
    end

    yrandom=rand;
    if yrandom>=wkeit01(WDx1,WDx2);
        yt=yt+ytDirection;
    end

    xtHistory(1,n)=xt;
    ytHistory(1,n)=yt;
end

%-------------------------------------------------------------------------------------------------------------------------------

for i=2:steps
    n=1:NoGrowthCone;
    xPos = xtHistory(i-1,n);
    yPos = ytHistory(i-1,n);
    Qos = (ytHistory(i-1,n)-1)*(FieldSizeYtd) + xPos;

    for n=1:NoGrowthCone
        xt=xtHistory(i-1,n);
        yt=ytHistory(i-1,n);

        AxonalLigandMatrix(Qos)=AxonLigand-SubstrateLigand(Qos);
        AxonalReceptorMatrix(Qos)=AxonReceptor-SubstrateReceptor(Qos);

        Lxy2=SubstrateLigand+AxonalLigandMatrix;
        Rxy2=SubstrateReceptor+AxonalReceptorMatrix;

        GrowthConeLigandMatrix=zeros(FieldSizeXtd,FieldSizeYtd);
        SurCorGL=zeros(FieldSizeXtd,FieldSizeYtd);
```

```
GrowthConeReceptorMatrix=zeros(FieldSizeXtd,FieldSizeYtd);
SurCorGR=zeros(FieldSizeXtd,FieldSizeYtd);

for nG=1:NoGrowthCone
    n1=xPos(nG)-1;
    n2=xPos(nG)+1;
    m1=yPos(nG)-1;
    m2=yPos(nG)+1;

    if nG~=n
        Lxy2(n1:n2,m1:m2)=0;
        Rxy2(n1:n2,m1:m2)=0;
        GrowthConeLigandMatrix(n1:n2,m1:m2)=AxonLigand(nG);
        GrowthConeReceptorMatrix(n1:n2,m1:m2)=AxonReceptor(nG);
    end

end

%----------------------Surround Correction of Superimposed Guidance Cues-------------

xa=xtHistory(i-1,n);
ya=ytHistory(i-1,n);

b1=1;
while ((i-b1>=1)&& (b1<11))
    if ((xa-1)==xtHistory(i-b1,n) && (ya-1)==ytHistory(i-b1,n)) && ...
    (GrowthConeLigandMatrix(xa-1,ya-1)==0 || ...
    Lxy3(xa-1,ya-1)==SubstrateLigand(xa-1,ya-1))
        SurCorGL(xa-1,ya-1)=-AxonLigand(n)+SubstrateLigand(xa-1,ya-1);
        SurCorGR(xa-1,ya-1)=-AxonReceptor(n)+SubstrateReceptor(xa-1,ya-1);
        break
    end
    b1=b1+1;
end

b2=1;
while ((i-b2>=1)&& (b2<11))
    if ((xa-1)==xtHistory(i-b2,n) && (ya)==ytHistory(i-b2,n)) && ...
    (GrowthConeLigandMatrix(xa-1,ya)==0 || ...
    Lxy3(xa-1,ya)==SubstrateLigand(xa-1,ya))
        SurCorGL(xa-1,ya)=-AxonLigand(n)+SubstrateLigand(xa-1,ya);
        SurCorGR(xa-1,ya)=-AxonReceptor(n)+SubstrateReceptor(xa-1,ya);
        break
    end
    b2=b2+1;
end

b3=1;
while ((i-b3>=1)&& (b3<11))
    if ((xa-1)==xtHistory(i-b3,n) && (ya+1)==ytHistory(i-b3,n)) && ...
    (GrowthConeLigandMatrix(xa-1,ya+1)==0 || ...
    Lxy3(xa-1,ya+1)==SubstrateLigand(xa-1,ya+1))
        SurCorGL(xa-1,ya+1)=-AxonLigand(n)+SubstrateLigand(xa-1,ya+1);
        SurCorGR(xa-1,ya+1)=-AxonReceptor(n)+SubstrateReceptor(xa-1,ya+1);
        break
    end
    b3=b3+1;
end
```

```
b4=1;
while ((i-b4>=1)&& (b4<11))
    if ((xa)==xtHistory(i-b4,n) && (ya-1)==ytHistory(i-b4,n)) && ...
    (GrowthConeLigandMatrix(xa,ya-1)==0 || ...
    Lxy3(xa,ya-1)==SubstrateLigand(xa,ya-1))
        SurCorGL(xa,ya-1)=-AxonLigand(n)+SubstrateLigand(xa,ya-1);
        SurCorGR(xa,ya-1)=-AxonReceptor(n)+SubstrateReceptor(xa,ya-1);
        break
    end
    b4=b4+1;
end

b5=1;
while ((i-b5>=1)&& (b5<11))
    if ((xa)==xtHistory(i-b5,n) && (ya+1)==ytHistory(i-b5,n)) && ...
    (GrowthConeLigandMatrix(xa,ya+1)==0 || ...
    Lxy3(xa,ya+1)==SubstrateLigand(xa,ya+1))
        SurCorGL(xa,ya+1)=-AxonLigand(n)+SubstrateLigand(xa,ya+1);
        SurCorGR(xa,ya+1)=-AxonReceptor(n)+SubstrateReceptor(xa,ya+1);
        break
    end
    b5=b5+1;
end

b6=1;
while ((i-b6>=1)&& (b6<11))
    if ((xa+1)==xtHistory(i-b6,n) && (ya-1)==ytHistory(i-b6,n)) && ...
    (GrowthConeLigandMatrix(xa+1,ya-1)==0 || ...
    Lxy3(xa+1,ya-1)==SubstrateLigand(xa+1,ya-1))
        SurCorGL(xa+1,ya-1)=-AxonLigand(n)+SubstrateLigand(xa+1,ya-1);
        SurCorGR(xa+1,ya-1)=-AxonReceptor(n)+SubstrateReceptor(xa+1,ya-1);
       break
    end
    b6=b6+1;
end

b7=1;
while ((i-b7>=1)&& (b7<11))
    if ((xa+1)==xtHistory(i-b7,n) && (ya)==ytHistory(i-b7,n)) && ...
    (GrowthConeLigandMatrix(xa+1,ya)==0 || ...
    Lxy3(xa+1,ya+1)==SubstrateLigand(xa+1,ya+1))
        SurCorGL(xa+1,ya)=-AxonLigand(n)+SubstrateLigand(xa+1,ya);
        SurCorGR(xa+1,ya)=-AxonReceptor(n)+SubstrateReceptor(xa+1,ya);
        break
    end
    b7=b7+1;
end

b8=1;
while ((i-b8>=1)&& (b8<11))
    if ((xa+1)==xtHistory(i-b8,n) && (ya+1)==ytHistory(i-b8,n)) && ...
    (GrowthConeLigandMatrix(xa+1,ya+1)==0 || ...
    Lxy3(xa+1,ya+1)==SubstrateLigand(xa+1,ya+1))
        SurCorGL(xa+1,ya+1)=-AxonLigand(n)+SubstrateLigand(xa+1,ya+1);
        SurCorGR(xa+1,ya+1)=-AxonReceptor(n)+SubstrateReceptor(xa+1,ya+1);
        break
    end
    b8=b8+1;
end
```

```
        b9=1;
        while ((i-b9>=1)&& (b9<11))
            if (xa==xtHistory(i-b9,n) && ya==ytHistory(i-b9,n)) && ...
            (GrowthConeLigandMatrix(xa,ya)==0 || Lxy3(xa,ya)==SubstrateLigand(xa,ya))
                SurCorGL(xa,ya)=-AxonLigand(n)+SubstrateLigand(xa,ya);
                SurCorGR(xa,ya)=-AxonReceptor(n)+SubstrateReceptor(xa,ya);
                break
            end
            b9=b9+1;
        end

        %----------------End of Surround Correction of Superimposed Guidance Cues ------------------

        xrandom=rand;
        if xrandom<((1+Qx)/2)
            xtDirection=1;
        else
            xtDirection=-1;
        end
        yrandom=rand;
        if yrandom<((1+Qy)/2)
            ytDirection=1;
        else
            ytDirection=-1;
        end
        if (xt-offset)<=-xtDirection
            xtDirection=0;
        elseif (xt+offset + xtDirection)>=FieldSizeXtd
            xtDirection=0;
        end
        if (yt-offset)<=-ytDirection
            ytDirection=0;
        elseif (yt+offset + ytDirection)>=FieldSizeYtd
            ytDirection=0;
        end

        Lxy3=Lxy2+GrowthConeLigandMatrix+SurCorGL;
        Rxy3=Rxy2+GrowthConeReceptorMatrix+SurCorGR;

        Dx1=abs(log(((AxonReceptor(n)*(Lxy3(xt,yt)+AxonLigand(n)))/...
        (AxonLigand(n)*(Rxy3(xt,yt)+AxonReceptor(n))))));
        Dx2=abs(log(((AxonReceptor(n)*(Lxy3(xt+xtDirection,yt+ytDirection)+…
        AxonLigand(n)))/(AxonLigand(n)*(Rxy3(xt+xtDirection,yt+ytDirection)…
        +AxonReceptor(n))))));

        WDx1=wkeitpd(Dx1,sigma);
        WDx2=wkeitpd(Dx2,sigma);

        xrandom=rand;
        if xrandom>=wkeit01(WDx1,WDx2);
            xt=xt+xtDirection;
        end
        yrandom=rand;
        if yrandom>=wkeit01(WDx1,WDx2);
            yt=yt+ytDirection;
        end
        xtHistory(i,n)=xt;
        ytHistory(i,n)=yt;
    end
end

h1=plot(xtHistory-offset,ytHistory-offset);
```

C. Source code of the Programme Used for Simulating Experimental Evidence Suggesting Fibre-Fibre-Interactions (Brown et al. 2000, Figure III-12, v0.25)

```
clear all

NoGrowthCone=2000;
SizeGrowthCone = 3;
offset = (SizeGrowthCone-1)/2;
steps = 20000;
Qx = 0.1;
Qy = 0;
sigma = 0.1;
knockIn = 3;

FieldSizeX = 100;
FieldSizeXtd = FieldSizeX + 2*offset;
FieldSizeY = 100;
FieldSizeYtd = FieldSizeY + 2*offset;
LigandExpon;

YDrang = [(1-Qy)/3 1/3+(1-Qy)/3 1];
GrowthConeLigandMatrix = zeros(FieldSizeXtd,FieldSizeYtd);
Lxy2 = zeros(FieldSizeXtd,FieldSizeYtd);
Lxy3 = zeros(FieldSizeXtd,FieldSizeYtd);
GrowthConeReceptorMatrix = zeros(FieldSizeXtd,FieldSizeYtd);
Rxy2 = zeros(FieldSizeXtd,FieldSizeYtd);
Rxy3 = zeros(FieldSizeXtd,FieldSizeYtd);

AxonReceptor = zeros(1,NoGrowthCone);
AxonLigand = zeros(1,NoGrowthCone);

xtHistory = zeros(steps,NoGrowthCone);
ytHistory = zeros(steps,NoGrowthCone);

DxHistory = zeros(steps,NoGrowthCone);
AbsDxHistory = zeros(steps,NoGrowthCone);
QxHistory = zeros(steps,NoGrowthCone);

YStartPos = (FieldSizeY-1)*rand(1,NoGrowthCone) + 1 + offset;

%----------------------------------------------------Initialisation Step-----------------------------------------

for n=1:NoGrowthCone
    xt = 1+offset;
    yt = round(((FieldSizeY-1)/(NoGrowthCone-1))*n+((NoGrowthCone-FieldSizeY)...
    /(NoGrowthCone-1))) + offset;

    rcptr = exp(-0.03*(YStartPos(n)-offset-FieldSizeX/2));
    lgnd = 1/rcptr;

    for f=1:floor(NoGrowthCone/2)
        if n==2*f                                          %knock-in GCs
            AxonReceptor(n) = rcptr+knockIn;
            AxonLigand(n) = 1/AxonReceptor(n);
            break
        else                                               %wild-type GCs
            AxonReceptor(n) = rcptr;
            AxonLigand(n) = 1/AxonReceptor(n);
        end
    end
```

```
xrandom = rand;
if (xrandom < (1-Qx)/SizeGrowthCone)
    xtDirection = -1;
elseif (xrandom < 1/SizeGrowthCone+(1-Qx)/SizeGrowthCone)
    xtDirection = 0;
else
    xtDirection = 1;
end

yrandom = rand;
if (yrandom < YDrang(1))
    ytDirection = -1;
elseif (yrandom < YDrang(2))
    ytDirection = 0;
else
    ytDirection = 1;
end

if xt+xtDirection<1+offset
    xtDirection=0;
elseif xt+xtDirection>FieldSizeX+offset
    xtDirection=0;
end
if yt+ytDirection<1+offset
    ytDirection=0;
elseif yt+ytDirection>FieldSizeY+offset
    ytDirection=0;
end

Lxy3 = SubstrateLigand;
Rxy3 = SubstrateReceptor;

bereichLigandAktuell = sum(sum(Lxy3((xt-offset):(xt+offset),(yt-offset):(yt+offset))))/...
nnz(Lxy3((xt-offset):(xt+offset),(yt-offset):(yt+offset)));

bereichRezeptorAktuell = sum(sum(Rxy3((xt-offset):(xt+offset),(yt-offset):(yt+offset))))/...
nnz(Lxy3((xt-offset):(xt+offset),(yt-offset):(yt+offset)));

bereichLigandZiel = sum(sum(Lxy3((xt+xtDirection-offset):(xt+xtDirection+offset),...
(yt+ytDirection-offset):(yt+ytDirection+offset))))/ nnz(Lxy3((xt+...
xtDirection-offset):(xt+xtDirection+offset),(yt+ytDirection-offset):(yt+ytDirection+offset)));

bereichRezeptorZiel = sum(sum(Rxy3((xt+xtDirection-offset):(xt+xtDirection+offset),...
(yt+ytDirection-offset):(yt+ytDirection+offset)))) / nnz(Lxy3((xt+...
xtDirection-offset):(xt+xtDirection+offset),(yt+ytDirection-offset):(yt+ytDirection+offset)));

Dx1 = abs(log((AxonLigand(n)*(bereichRezeptorAktuell+AxonReceptor(n)))/...
(AxonReceptor(n)*(bereichLigandAktuell+AxonLigand(n)))));

Dx2 = abs(log((AxonLigand(n)*(bereichRezeptorZiel+AxonReceptor(n)))/...
(AxonReceptor(n)*(bereichLigandZiel+AxonLigand(n)))));

absDx1 = (log((AxonLigand(n)*(bereichRezeptorAktuell+AxonReceptor(n)))/...
(AxonReceptor(n)*(bereichLigandAktuell+AxonLigand(n)))));

DxHistory(1,n) = Dx1;
AbsDxHistory(1,n) = absDx1;

WDx1 = wkeitpd(Dx1,sigma);
WDx2 = wkeitpd(Dx2,sigma);
```

```
    if rand>wkeit01(WDx1,WDx2);
        xt = xt+xtDirection;
        yt = yt+ytDirection;
    end

    xtHistory(1,n) = xt;
    ytHistory(1,n) = yt;
end

%---------Calculation of the Expected Maximum Local Guidance Potential Value DxMax-------

minRec = min(AxonReceptor);
maxRecAll = max([max(AxonReceptor)
max(SubstrateReceptor(1+offset,1+offset:FieldSizeX+offset))]);
minLigAll = min([min(AxonLigand) min(SubstrateLigand(1+offset,1+offset:FieldSizeX+offset))]);
DxMax = abs(log(((minRec*minLigAll+1)/(1/minRec*maxRecAll+1))));

%-----------------------------------------------------------------------------------------------------------------

for i=2:steps
    for n=1:NoGrowthCone
        linIndex = (ytHistory(i-1,1:NoGrowthCone)-1)*(FieldSizeYtd) +…
        xtHistory(i-1,1:NoGrowthCone);
        xt = xtHistory(i-1,n);
        yt = ytHistory(i-1,n);

        Lxy2 = SubstrateLigand;
        Rxy2 = SubstrateReceptor;

        GrowthConeLigandMatrix = zeros(FieldSizeXtd,FieldSizeYtd);
        GrowthConeReceptorMatrix = zeros(FieldSizeXtd,FieldSizeYtd);

        for nG=1:NoGrowthCone
            n1 = xtHistory(i-1,nG)-1;
            n2 = xtHistory(i-1,nG)+1;
            m1 = ytHistory(i-1,nG)-1;
            m2 = ytHistory(i-1,nG)+1;

            if nG~=n
                Lxy2(n1:n2,m1:m2) = 0;
                Rxy2(n1:n2,m1:m2) = 0;
                GrowthConeLigandMatrix(n1:n2,m1:m2) = AxonLigand(nG);
                GrowthConeReceptorMatrix(n1:n2,m1:m2) = AxonReceptor(nG);
            end
        end

        Qx = AbsDxHistory(i-1,n)/DxMax;
        QxHistory(i,n) = Qx;

        xrandom = rand;
        if (xrandom < (1-Qx)/SizeGrowthCone)
            xtDirection = -1;
        elseif (xrandom < 1/SizeGrowthCone+(1-Qx)/SizeGrowthCone)
            xtDirection = 0;
        else
            xtDirection = 1;
        end
```

```
yrandom = rand;
if (yrandom < YDrang(1))
    ytDirection = -1;
elseif (yrandom < YDrang(2))
    ytDirection = 0;
else
    ytDirection = 1;
end

if xt+xtDirection<1+offset
    xtDirection=0;
elseif xt+xtDirection>FieldSizeX+offset
    xtDirection=0;
end
if yt+ytDirection<1+offset
    ytDirection=0;
elseif yt+ytDirection>FieldSizeY+offset
    ytDirection=0;
end

Lxy3 = Lxy2+GrowthConeLigandMatrix;
Rxy3 = Rxy2+GrowthConeReceptorMatrix;

for d=1:offset
    Lxy3(offset,:)=0;Lxy3(:,offset)=0;Lxy3(FieldSizeXtd,:)=0;Lxy3(:,FieldSizeYtd)=0;
    Rxy3(offset,:)=0;Rxy3(:,offset)=0;Rxy3(FieldSizeXtd,:)=0;Rxy3(:,FieldSizeYtd)=0;
end

bereichLigandAktuell = sum(sum(Lxy3((xt-offset):(xt+offset),…
(yt-offset):(yt+offset))))/ nnz(Lxy3((xt-offset):(xt+offset),(yt-offset):(yt+offset)));

bereichRezeptorAktuell = sum(sum(Rxy3((xt-offset):(xt+offset),…
(yt-offset):(yt+offset))))/ nnz(Lxy3((xt-offset):(xt+offset),(yt-offset):(yt+offset)));

bereichLigandZiel = sum(sum(Lxy3((xt+xtDirection-offset):(xt+xtDirection+offset),...
(yt+ytDirection-offset):(yt+ytDirection+offset)))) / nnz(Lxy3((xt+xtDirection-offset):...
(xt+xtDirection+offset),(yt+ytDirection-offset):(yt+ytDirection+offset)));

bereichRezeptorZiel = sum(sum(Rxy3((xt+…
xtDirection-offset):(xt+xtDirection+offset),…
(yt+ytDirection-offset):(yt+ytDirection+offset)))) / nnz(Lxy3((xt+xtDirection-offset):...
(xt+xtDirection+offset),(yt+ytDirection-offset):(yt+ytDirection+offset)));

Dx1 = abs(log((AxonLigand(n)*(bereichRezeptorAktuell+AxonReceptor(n)))/...
(AxonReceptor(n)*(bereichLigandAktuell+AxonLigand(n)))));
Dx2 = abs(log((AxonLigand(n)*(bereichRezeptorZiel+AxonReceptor(n)))/...
(AxonReceptor(n)*(bereichLigandZiel+AxonLigand(n)))));

absDx1 = (log((AxonLigand(n)*(bereichRezeptorAktuell+AxonReceptor(n)))/...
(AxonReceptor(n)*(bereichLigandAktuell+AxonLigand(n)))));

DxHistory(i,n) = Dx1;
AbsDxHistory(i,n) = absDx1;

wDx1 = wkeitpd(Dx1,sigma);
wDx2 = wkeitpd(Dx2,sigma);

if rand>=wkeit01(wDx1,wDx2);
    xt = xt+xtDirection;
    yt = yt+ytDirection;
end
```

```
        xtHistory(i,n) = xt;
        ytHistory(i,n) = yt;

        % ----------------------Change of Previous Positions in Case Two Growth Cones Try to
        % Occupy the Same Prospective Position-----------------------------------------------------------

        for m=n+1:NoGrowthCone
            if (xtHistory(i,n) == xtHistory(i-1,m)) && (ytHistory(i,n) == ytHistory(i-1,m))
                xtHistory(i-1,m) = xtHistory(i-1,n);
                ytHistory(i-1,m) = ytHistory(i-1,n);
            end
        end
        if n>1
            for m=1:n-1
                if (xtHistory(i,n) == xtHistory(i,m)) && (ytHistory(i,n) == ytHistory(i,m))
                    xtHistory(i,m) = xtHistory(i-1,n);
                    ytHistory(i,m) = ytHistory(i-1,n);
                end
            end
        end

        %-------------------------------------------------------------------------------------------------------------

    end
end

%------------------Routine for Obtaining the Wild-Type and Knock-in Mapping Functions---------

if NoGrowthCone>1
    for i=1:round(NoGrowthCone/2)
        xEndWildeType(i,1) = xtHistory(steps, 2*i-1)-offset;
        ystartWT(i,1)=FieldSizeXtd-YStartPos(2*i-1)-offset;
    end
    for i=1:floor(NoGrowthCone/2)
        xEndKnockIn(i,1) = xtHistory(steps, 2*i)-offset;
        ystartKI(i,1)=FieldSizeYtd-YStartPos(2*i)-offset;
    end
end
```

D. Source code of the Programme Used for Simulating Adaptation during Topographic Mapping (Figure III-23, v0.3)

```
clear all

NoGrowthCone = 30;
SizeGrowthCone = 3;
offset = (SizeGrowthCone-1)/2;
steps = 10000;
Qx = 0.2;
Qy = 0;
sigma = 0.1;
tau = 4;

FieldSizeX = 100;
FieldSizeXtd = FieldSizeX + 2*offset;
FieldSizeY = 100;
FieldSizeYtd = FieldSizeY + 2*offset;
LigandExpon;

YDrang = [(1-Qy)/3 1/3+(1-Qy)/3 1];

GrowthConeLigandMatrix = zeros(FieldSizeXtd,FieldSizeYtd);
Lxy2 = zeros(FieldSizeXtd,FieldSizeYtd);
Lxy3 = zeros(FieldSizeXtd,FieldSizeYtd);

GrowthConeReceptorMatrix = zeros(FieldSizeXtd,FieldSizeYtd);
Rxy2 = zeros(FieldSizeXtd,FieldSizeYtd);
Rxy3 = zeros(FieldSizeXtd,FieldSizeYtd);

AxonReceptor = zeros(1,NoGrowthCone);
AxonLigand = zeros(1,NoGrowthCone);

xtHistory = zeros(steps,NoGrowthCone);
ytHistory = zeros(steps,NoGrowthCone);
DxHistory = zeros(steps,NoGrowthCone);

YStartPos = round(((FieldSizeY-1)/(NoGrowthCone-1))*(1:NoGrowthCone)+...
((NoGrowthCone-FieldSizeY)/(NoGrowthCone-1))) + offset;

AdaptationCoeffizientRec = zeros(steps,NoGrowthCone);

%----------------------------------------------------------Initialisation Step-----------------------------------------------

for n=1:NoGrowthCone
    xt = 1+offset;
    yt = YStartPos(n);

    AxonReceptor(n)=exp(0.03*(yt-offset-FieldSizeX/2));
    AxonLigand(n)=exp(-0.03*(yt-offset-FieldSizeX/2));

    xrandom = rand;
    if (xrandom < (1-Qx)/SizeGrowthCone)
        xtDirection = -1;
    elseif (xrandom < 1/SizeGrowthCone+(1-Qx)/SizeGrowthCone)
        xtDirection = 0;
    else
        xtDirection = 1;
    end
```

```
    yrandom = rand;
    if (yrandom < YDrang(1))
        ytDirection = -1;
    elseif (yrandom < YDrang(2))
        ytDirection = 0;
    else
        ytDirection = 1;
    end

    if xt+xtDirection<1+offset
        xtDirection=0;
    elseif xt+xtDirection>FieldSizeX+offset
        xtDirection=0;
    end
    if yt+ytDirection<1+offset
        ytDirection=0;
    elseif yt+ytDirection>FieldSizeY+offset
        ytDirection=0;
    end

    Lxy3 = SubstrateLigand;
    Rxy3 = SubstrateReceptor;

    Dx1=abs(log(((AxonReceptor(n)*(Lxy3(xt,yt)+AxonLigand(n)))/(AxonLigand(n)*(Rxy3(xt,yt)+...
    AxonReceptor(n))))));
    Dx2=abs(log(((AxonReceptor(n)*(Lxy3(xt+xtDirection,yt+ytDirection)+AxonLigand(n)))...
    /(AxonLigand(n)*(Rxy3(xt+xtDirection,yt+ytDirection)+AxonReceptor(n))))));

    DxHistory(1,n) = Dx1;

    WDx1 = wkeitpd(Dx1,sigma);
    WDx2 = wkeitpd(Dx2,sigma);

    if rand>wkeit01(WDx1,WDx2);
        xt = xt+xtDirection;
        yt = yt+ytDirection;
    end

    xtHistory(1,n) = xt;
    ytHistory(1,n) = yt;
end


%----------Calculation of the Expected Maximum Local Guidance Potential Value DxMax---------

minRec = min(AxonReceptor);
maxRecAll= max([max(AxonReceptor)
max(SubstrateReceptor(1+offset,1+offset:FieldSizeX+offset))]);
minLigAll = min([min(AxonLigand) min(SubstrateLigand(1+offset,1+offset:FieldSizeX+offset))]);
dXMax = abs(log(((minRec*minLigAll+1)/(1/minRec*maxRecAll+1))));

%-----------------------------------------------------------------------------------------------------------------------

for i=2:steps
    for n=1:NoGrowthCone
        linIndex = (ytHistory(i-1,1:NoGrowthCone)-1)*(FieldSizeYtd) + xtHistory(i-
1,1:NoGrowthCone);
        xt = xtHistory(i-1,n);
        yt = ytHistory(i-1,n);

        Lxy2 = SubstrateLigand;
        Rxy2 = SubstrateReceptor;
```

```
GrowthConeLigandMatrix = zeros(FieldSizeXtd,FieldSizeYtd);
GrowthConeReceptorMatrix = zeros(FieldSizeXtd,FieldSizeYtd);

for nG=1:NoGrowthCone
    n1 = xtHistory(i-1,nG)-1;
    n2 = xtHistory(i-1,nG)+1;
    m1 = ytHistory(i-1,nG)-1;
    m2 = ytHistory(i-1,nG)+1;

    if nG~=n
        Lxy2(n1:n2,m1:m2) = 0;
        Rxy2(n1:n2,m1:m2) = 0;
        GrowthConeLigandMatrix(n1:n2,m1:m2) = AxonLigand(nG);
        GrowthConeReceptorMatrix(n1:n2,m1:m2) = AxonReceptor(nG);
    end
end

Qx = DxHistory(i-1,n)/dXMax;
QxHistory(i,n)=Qx;

xrandom = rand;
if (xrandom < (1-Qx)/SizeGrowthCone)
    xtDirection = -1;
elseif (xrandom < 1/SizeGrowthCone+(1-Qx)/SizeGrowthCone)
    xtDirection = 0;
else
    xtDirection = 1;
end

yrandom = rand;
if (yrandom < YDrang(1))
    ytDirection = -1;
elseif (yrandom < YDrang(2))
    ytDirection = 0;
else
    ytDirection = 1;
end

if xt+xtDirection<1+offset
    xtDirection=0;
elseif xt+xtDirection>FieldSizeX+offset
    xtDirection=0;
end
if yt+ytDirection<1+offset
    ytDirection=0;
elseif yt+ytDirection>FieldSizeY+offset
    ytDirection=0;
end

%------------------Adaptation Routine according to Delbrück and Reichardt 1956-----------

AdaptationCoeffizientRec(i,n) = (AdaptationCoeffizientRec(i-1,n)*exp(-1/tau) + ...
SubstrateLigand(xt,yt));
if (AdaptationCoeffizientRec(i,n)~=0)
    AxonReceptor(n) = tau/(AdaptationCoeffizientRec(i,n));
    %AxonLigand(n) = 1/AxonReceptor(n);    Simultaneous Ligand Adapatation
end

AdaptR(i,n) = AxonReceptor(n);
AdaptL(i,n) = AxonLigand(n);

%-----------------------------------------------------------------------------------------------------------
```

```
        Lxy3 = Lxy2+GrowthConeLigandMatrix;
        Rxy3 = Rxy2+GrowthConeReceptorMatrix;

        Dx1 =abs(log(((AxonReceptor(n)*(Lxy3(xt,yt)+AxonLigand(n)))/(AxonLigand(n)*…
        (Rxy3(xt,yt)+AxonReceptor(n))))));
        Dx2=abs(log(((AxonReceptor(n)*(Lxy3(xt+xtDirection,yt+ytDirection)+AxonLigand(n)))/...
        (AxonLigand(n)*(Rxy3(xt+xtDirection,yt+ytDirection)+AxonReceptor(n))))));

        DxtHistory(i,n) = Dx1;

        WDx1 = wkeitpd(Dx1,sigma);
        WDx2 = wkeitpd(Dx2,sigma);

        if rand>=wkeit01(WDx1,WDx2);
            xt = xt+xtDirection;
            yt = yt+ytDirection;
        end

        xtHistory(i,n) = xt;
        ytHistory(i,n) = yt;

    end
end
```

References

Belisle, J.M., Correia, J.P., Wiseman, P.W., Kennedy, T.E., and Costantino, S. (2008). Patterning protein concentration using laser-assisted adsorption by photobleaching, LAPAP. Lab Chip *8*, 2164-2167.

Block, S.M., Segall, J.E., and Berg, H.C. (1983). Adaptation kinetics in bacterial chemotaxis. J Bacteriol *154*, 312-323.

Bonhoeffer, F., and Huf, J. (1980). Recognition of cell types by axonal growth cones in vitro. Nature *288*, 162-164.

Bonhoeffer, F., and Huf, J. (1982). In vitro experiments on axon guidance demonstrating an anterior-posterior gradient on the tectum. Embo J *1*, 427-431.

Bonhoeffer, F., and Huf, J. (1985). Position-dependent properties of retinal axons and their growth cones. Nature *315*, 409-410.

Bray, D., Levin, M.D., and Morton-Firth, C.J. (1998). Receptor clustering as a cellular mechanism to control sensitivity. Nature *393*, 85-88.

Brown, A., Yates, P.A., Burrola, P., Ortuno, D., Vaidya, A., Jessell, T.M., Pfaff, S.L., O'Leary, D.D., and Lemke, G. (2000). Topographic mapping from the retina to the midbrain is controlled by relative but not absolute levels of EphA receptor signaling. Cell *102*, 77-88.

Cambridge, S.B., Davis, R.L., and Minden, J.S. (1997). Drosophila mitotic domain boundaries as cell fate boundaries. Science *277*, 825-828.

Cang, J., Wang, L., Stryker, M.P., and Feldheim, D.A. (2008). Roles of ephrin-as and structured activity in the development of functional maps in the superior colliculus. J Neurosci *28*, 11015-11023.

Carvalho, R.F., Beutler, M., Marler, K.J., Knoll, B., Becker-Barroso, E., Heintzmann, R., Ng, T., and Drescher, U. (2006). Silencing of EphA3 through a cis interaction with ephrinA5. Nat Neurosci *9*, 322-330.

Chen, Y., Mohammadi, M., and Flanagan, J.G. (2009). Graded levels of FGF protein span the midbrain and can instruct graded induction and repression of neural mapping labels. Neuron *62*, 773-780.

Cheng, H.J., Nakamoto, M., Bergemann, A.D., and Flanagan, J.G. (1995). Complementary gradients in expression and binding of ELF-1 and Mek4 in development of the topographic retinotectal projection map. Cell *82*, 371-381.

Connor, R.J., Menzel, P., and Pasquale, E.B. (1998). Expression and tyrosine phosphorylation of Eph receptors suggest multiple mechanisms in patterning of the visual system. Dev Biol *193*, 21-35.

Davis, S., Gale, N.W., Aldrich, T.H., Maisonpierre, P.C., Lhotak, V., Pawson, T., Goldfarb, M., and Yancopoulos, G.D. (1994). Ligands for EPH-related receptor tyrosine kinases that require membrane attachment or clustering for activity. Science *266*, 816-819.

Davy, A., Gale, N.W., Murray, E.W., Klinghoffer, R.A., Soriano, P., Feuerstein, C., and Robbins, S.M. (1999). Compartmentalized signaling by GPI-anchored ephrin-A5 requires the Fyn tyrosine kinase to regulate cellular adhesion. Genes Dev *13*, 3125-3135.

Delbrück, M., and Reichardt, W. (1956). System analysis for the light growth reactions of Phycomyces. In Cellular mechanisms in differentiation and growth, D. Rudnick, ed. (Princeton, N.J.: Princeton University Press), pp. 3-44.

Dickson, B.J. (2002). Molecular mechanisms of axon guidance. Science *298*, 1959-1964.

DiMilla, P.A., Barbee, K., and Lauffenburger, D.A. (1991). Mathematical model for the effects of adhesion and mechanics on cell migration speed. Biophys J *60*, 15-37.

Drescher, U. (2004). Aber Lenken Sie Auch? (But do they also guide?). J Neurobiol *59*, 3-7.

Drescher, U., Kremoser, C., Handwerker, C., Löschinger, J., Noda, M., and Bonhoeffer, F. (1995). In vitro guidance of retinal ganglion cell axons by RAGS, a 25 kDa tectal protein related to ligands for Eph receptor tyrosine kinases. Cell *82*, 359-370.

Egea, J., Nissen, U.V., Dufour, A., Sahin, M., Greer, P., Kullander, K., Mrsic-Flogel, T.D., Greenberg, M.E., Kiehn, O., Vanderhaeghen, P., and Klein, R. (2005). Regulation of EphA 4 kinase activity is required for a subset of axon guidance decisions suggesting a key role for receptor clustering in Eph function. Neuron *47*, 515-528.

Fan, J., and Raper, J.A. (1995). Localized collapsing cues can steer growth cones without inducing their full collapse. Neuron *14*, 263-274.

Feldheim, D.A., Kim, Y.I., Bergemann, A.D., Frisen, J., Barbacid, M., and Flanagan, J.G. (2000). Genetic analysis of ephrin-A2 and ephrin-A5 shows their requirement in multiple aspects of retinocollicular mapping. Neuron *25*, 563-574.

Fraser, S.E. (1980). Differential adhesion approach to the patterning of nerve connections. Dev Biol *79*, 453-464.

Fraser, S.E., and Hunt, R.K. (1980). Retinotectal specificity: models and experiments in search of a mapping function. Annu Rev Neurosci *3*, 319-352.

Fraser, S.E., and Perkel, D.H. (1990). Competitive and positional cues in the patterning of nerve connections. J Neurobiol *21*, 51-72.

Frisén, J., Yates, P.A., McLaughlin, T., Friedman, G.C., O'Leary, D.D., and Barbacid, M. (1998). Ephrin-A5 (AL-1/RAGS) is essential for proper retinal axon guidance and topographic mapping in the mammalian visual system. Neuron *20*, 235-243.

Fujisawa, H. (1981). Retinotopic analysis of fiber pathways in the regenerating retinotectal system of the adult newt cynops Pyrrhogaster. Brain Res *206*, 27-37.

Fujisawa, H., Watanabe, K., Tani, N., and Ibata, Y. (1981a). Retinotopic analysis of fiber pathways in amphibians. I. The adult newt Cynops pyrrhogaster. Brain Res *206*, 9-20.

Fujisawa, H., Watanabe, K., Tani, N., and Ibata, Y. (1981b). Retinotopic analysis of fiber pathways in amphibians. II. The frog Rana nigromaculata. Brain Res *206*, 21-26.

Gebhardt, C. (2005). Theoretische und experimentelle Untersuchungen zur Entstehung topographisch organisierter neuronaler Karten am Beispiel der retinotektalen Projektion. (Diploma Thesis, Friedrich-Schiller Universität Jena).

Gierer, A. (1981). Development of projections between areas of the nervous system. Biol Cybern *42*, 69-78.

Gierer, A. (1983). Model for the retino-tectal projection. Proc R Soc Lond B Biol Sci *218*, 77-93.

Gierer, A. (1987). Directional cues for growing axons forming the retinotectal projection. Development *101*, 479-489.

Gierer, A., and Meinhardt, H. (1972). A theory of biological pattern formation. Kybernetik *12*, 30-39.

Goodhill, G.J., and Richards, L.J. (1999). Retinotectal maps: molecules, models and misplaced data. Trends Neurosci *22*, 529-534.

Goodhill, G.J., and Xu, J. (2005). The development of retinotectal maps: a review of models based on molecular gradients. Network *16*, 5-34.

Gosse, N.J., Nevin, L.M., and Baier, H. (2008). Retinotopic order in the absence of axon competition. Nature *452*, 892-895.

Han, J.H., Kushner, S.A., Yiu, A.P., Hsiang, H.L., Buch, T., Waisman, A., Bontempi, B., Neve, R.L., Frankland, P.W., and Josselyn, S.A. (2009). Selective erasure of a fear memory. Science *323*, 1492-1496.

Hansen, M.J., Dallal, G.E., and Flanagan, J.G. (2004). Retinal axon response to ephrin-as shows a graded, concentration-dependent transition from growth promotion to inhibition. Neuron *42*, 717-730.

Hattori, M., Osterfield, M., and Flanagan, J.G. (2000). Regulated cleavage of a contact-mediated axon repellent. Science *289*, 1360-1365.

Honda, H. (1998). Topographic mapping in the retinotectal projection by means of complementary ligand and receptor gradients: a computer simulation study. J Theor Biol *192*, 235-246.

Honda, H. (2003). Competition between retinal ganglion axons for targets under the servomechanism model explains abnormal retinocollicular projection of Eph receptor-overexpressing or ephrin-lacking mice. J Neurosci *23*, 10368-10377.

Hopker, V.H., Shewan, D., Tessier-Lavigne, M., Poo, M., and Holt, C. (1999). Growth-cone attraction to netrin-1 is converted to repulsion by laminin-1. Nature *401*, 69-73.

Hornberger, M.R., Dutting, D., Ciossek, T., Yamada, T., Handwerker, C., Lang, S., Weth, F., Huf, J., Wessel, R., Logan, C., Tanaka, H., and Drescher, U. (1999). Modulation of EphA receptor function by coexpressed ephrinA ligands on retinal ganglion cell axons. Neuron *22*, 731-742.

Huai, J., and Drescher, U. (2001). An ephrin-A-dependent signaling pathway controls integrin function and is linked to the tyrosine phosphorylation of a 120-kDa protein. J Biol Chem *276*, 6689-6694.

Huber, A.B., Kolodkin, A.L., Ginty, D.D., and Cloutier, J.F. (2003). Signaling at the growth cone: ligand-receptor complexes and the control of axon growth and guidance. Annu Rev Neurosci *26*, 509-563.

Kapfhammer, J.P., and Raper, J.A. (1987). Collapse of growth cone structure on contact with specific neurites in culture. J Neurosci *7*, 201-212.

Kolpak, A.L., Jiang, J., Guo, D., Standley, C., Bellve, K., Fogarty, K., and Bao, Z.Z. (2009). Negative guidance factor-induced macropinocytosis in the growth cone plays a critical role in repulsive axon turning. J Neurosci *29*, 10488-10498.

Konstantinova, I., Nikolova, G., Ohara-Imaizumi, M., Meda, P., Kucera, T., Zarbalis, K., Wurst, W., Nagamatsu, S., and Lammert, E. (2007). EphA-Ephrin-A-mediated beta cell communication regulates insulin secretion from pancreatic islets. Cell *129*, 359-370.

Koshland, D.E., Jr. (1980). Bacterial chemotaxis in relation to neurobiology. Annu Rev Neurosci *3*, 43-75.

Kossel, A.H., Cambridge, S.B., Wagner, U., and Bonhoeffer, T. (2001). A caged Ab reveals an immediate/instructive effect of BDNF during hippocampal synaptic potentiation. Proc Natl Acad Sci U S A *98*, 14702-14707.

Koulakov, A.A., and Tsigankov, D.N. (2004). A stochastic model for retinocollicular map development. BMC Neurosci *5*, 30.

Lim, Y.S., McLaughlin, T., Sung, T.C., Santiago, A., Lee, K.F., and O'Leary, D.D. (2008). p75(NTR) mediates ephrin-A reverse signaling required for axon repulsion and mapping. Neuron *59*, 746-758.

Löschinger, J., Weth, F., and Bonhoeffer, F. (2000). Reading of concentration gradients by axonal growth cones. Philos Trans R Soc Lond B Biol Sci *355*, 971-982.

Mai, J., Fok, L., Gao, H., Zhang, X., and Poo, M.M. (2009). Axon initiation and growth cone turning on bound protein gradients. J Neurosci *29*, 7450-7458.

Marcus, R.C., Gale, N.W., Morrison, M.E., Mason, C.A., and Yancopoulos, G.D. (1996). Eph family receptors and their ligands distribute in opposing gradients in the developing mouse retina. Dev Biol *180*, 786-789.

Marler, K.J., Becker-Barroso, E., Martinez, A., Llovera, M., Wentzel, C., Poopalasundaram, S., Hindges, R., Soriano, E., Comella, J., and Drescher, U. (2008). A TrkB/EphrinA interaction controls retinal axon branching and synaptogenesis. J Neurosci *28*, 12700-12712.

Marquardt, T., Shirasaki, R., Ghosh, S., Andrews, S.E., Carter, N., Hunter, T., and Pfaff, S.L. (2005). Coexpressed EphA receptors and ephrin-A ligands mediate opposing actions on growth cone navigation from distinct membrane domains. Cell *121*, 127-139.

Marriott, G. (1994). Caged protein conjugates and light-directed generation of protein activity: preparation, photoactivation, and spectroscopic characterization of caged G-actin conjugates. Biochemistry *33*, 9092-9097.

McLaughlin, T., Hindges, R., and O'Leary, D.D. (2003a). Regulation of axial patterning of the retina and its topographic mapping in the brain. Curr Opin Neurobiol *13*, 57-69.

McLaughlin, T., Torborg, C.L., Feller, M.B., and O'Leary, D.D. (2003b). Retinotopic map refinement requires spontaneous retinal waves during a brief critical period of development. Neuron *40*, 1147-1160.

Mey, J., and Thanos, S. (2000). Development of the visual system of the chick. I. Cell differentiation and histogenesis. Brain Res Brain Res Rev *32*, 343-379.

Ming, G.L., Wong, S.T., Henley, J., Yuan, X.B., Song, H.J., Spitzer, N.C., and Poo, M.M. (2002). Adaptation in the chemotactic guidance of nerve growth cones. Nature *417*, 411-418.

Monschau, B., Kremoser, C., Ohta, K., Tanaka, H., Kaneko, T., Yamada, T., Handwerker, C., Hornberger, M.R., Löschinger, J., Pasquale, E.B., Siever, D.A., Verderame, M.F., Muller, B.K., Bonhoeffer, F., and Drescher, U. (1997). Shared and distinct functions of RAGS and ELF-1 in guiding retinal axons. Embo J *16*, 1258-1267.

Mueller, B.K. (1999). Growth cone guidance: first steps towards a deeper understanding. Annu Rev Neurosci *22*, 351-388.

Nakamoto, M., Cheng, H.J., Friedman, G.C., McLaughlin, T., Hansen, M.J., Yoon, C.H., O'Leary, D.D., and Flanagan, J.G. (1996). Topographically specific effects of ELF-1 on retinal axon guidance in vitro and retinal axon mapping in vivo. Cell *86*, 755-766.

Nakamura, H., and O'Leary, D.D. (1989). Inaccuracies in initial growth and arborization of chick retinotectal axons followed by course corrections and axon remodeling to develop topographic order. J Neurosci *9*, 3776-3795.

Nguyen-Ba-Charvet, K.T., Brose, K., Marillat, V., Sotelo, C., Tessier-Lavigne, M., and Chedotal, A. (2001). Sensory axon response to substrate-bound Slit2 is modulated by laminin and cyclic GMP. Mol Cell Neurosci *17*, 1048-1058.

Nishiyama, M., Hoshino, A., Tsai, L., Henley, J.R., Goshima, Y., Tessier-Lavigne, M., Poo, M.M., and Hong, K. (2003). Cyclic AMP/GMP-dependent modulation of Ca2+ channels sets the polarity of nerve growth-cone turning. Nature *423*, 990-995.

Prestige, M.C., and Willshaw, D.J. (1975). On a role for competition in the formation of patterned neural connexions. Proc R Soc Lond B Biol Sci *190*, 77-98.

Rashid, T., Upton, A.L., Blentic, A., Ciossek, T., Knoll, B., Thompson, I.D., and Drescher, U. (2005). Opposing gradients of ephrin-As and EphA7 in the superior colliculus are essential for topographic mapping in the mammalian visual system. Neuron *47*, 57-69.

Reber, M., Burrola, P., and Lemke, G. (2004). A relative signalling model for the formation of a topographic neural map. Nature *431*, 847-853.

Rosentreter, S.M., Davenport, R.W., Löschinger, J., Huf, J., Jung, J., and Bonhoeffer, F. (1998). Response of retinal ganglion cell axons to striped linear gradients of repellent guidance molecules. J Neurobiol *37*, 541-562.

Ruthazer, E.S., and Cline, H.T. (2004). Insights into activity-dependent map formation from the retinotectal system: a middle-of-the-brain perspective. J Neurobiol *59*, 134-146.

Schlupeck, B. (2008). In vitro- Versuche zur Ausbildung interstitieller Seitenäste im retinotektalen System des Hühnchens. (Diplomarbeit, Friedrich-Schiller-Universität Jena).

Simon, D.K., and O'Leary, D.D. (1990). Limited topographic specificity in the targeting and branching of mammalian retinal axons. Dev Biol *137*, 125-134.

Simon, D.K., and O'Leary, D.D. (1992a). Development of topographic order in the mammalian retinocollicular projection. J Neurosci *12*, 1212-1232.

Simon, D.K., and O'Leary, D.D. (1992b). Responses of retinal axons in vivo and in vitro to position-encoding molecules in the embryonic superior colliculus. Neuron *9*, 977-989.

Song, H.J., Ming, G.L., and Poo, M.M. (1997). cAMP-induced switching in turning direction of nerve growth cones. Nature *388*, 275-279.

Sperry, R.W. (1943). Effect of 180 degree rotation of the retinal field on visuomotor coordination. Journal of Experimental Zoology *92*, 263-279.

Sperry, R.W. (1963). Chemoaffinity in the Orderly Growth of Nerve Fiber Patterns and Connections. Proc Natl Acad Sci U S A *50*, 703-710.

Thanos, S., and Bonhoeffer, F. (1987). Axonal arborization in the developing chick retinotectal system. J Comp Neurol *261*, 155-164.

Thanos, S., and Dütting, D. (1987). Outgrowth and directional specificity of fibers from embryonic retinal transplants in the chick optic tectum. Brain Res *429*, 161-179.

Thanos, S., and Mey, J. (2001). Development of the visual system of the chick. II. Mechanisms of axonal guidance. Brain Res Brain Res Rev *35*, 205-245.

Torborg, C.L., and Feller, M.B. (2005). Spontaneous patterned retinal activity and the refinement of retinal projections. Prog Neurobiol *76*, 213-235.

van Horck, F.P., Weinl, C., and Holt, C.E. (2004). Retinal axon guidance: novel mechanisms for steering. Curr Opin Neurobiol *14*, 61-66.

Vielmetter, J., Stolze, B., Bonhoeffer, F., and Stuermer, C.A. (1990). In vitro assay to test differential substrate affinities of growing axons and migratory cells. Exp Brain Res *81*, 283-287.

von Boxberg, Y., Deiss, S., and Schwarz, U. (1993). Guidance and topographic stabilization of nasal chick retinal axons on target-derived components in vitro. Neuron *10*, 345-357.

von der Malsburg, C., and Willshaw, D.J. (1977). How to label nerve cells so that they can interconnect in an ordered fashion. Proc Natl Acad Sci U S A *74*, 5176-5178.

von Philipsborn, A.C. (2007). Axon guidance in substrate-bound protein gradients. In Cell- and Neurobiology (Universität Karlsruhe (TH)).

von Philipsborn, A.C., Lang, S., Loeschinger, J., Bernard, A., David, C., Lehnert, D., Bonhoeffer, F., and Bastmeyer, M. (2006). Growth cone navigation in substrate-bound ephrin gradients. Development *133*, 2487-2495.

Wadhams, G.H., and Armitage, J.P. (2004). Making sense of it all: bacterial chemotaxis. Nat Rev Mol Cell Biol *5*, 1024-1037.

Walter, J., Henke-Fahle, S., and Bonhoeffer, F. (1987a). Avoidance of posterior tectal membranes by temporal retinal axons. Development *101*, 909-913.

Walter, J., Kern-Veits, B., Huf, J., Stolze, B., and Bonhoeffer, F. (1987b). Recognition of position-specific properties of tectal cell membranes by retinal axons in vitro. Development *101*, 685-696.

Walter, J., Muller, B., and Bonhoeffer, F. (1990). Axonal guidance by an avoidance mechanism. J Physiol (Paris) *84*, 104-110.

Waterston, R.H., Lindblad-Toh, K., Birney, E., Rogers, J., Abril, J.F., Agarwal, P., Agarwala, R., Ainscough, R., Alexandersson, M., An, P.*, et al.* (2002). Initial sequencing and comparative analysis of the mouse genome. Nature *420*, 520-562.

Weinl, C., Drescher, U., Lang, S., Bonhoeffer, F., and Loschinger, J. (2003). On the turning of Xenopus retinal axons induced by ephrin-A5. Development *130*, 1635-1643.

Willshaw, D. (2006). Analysis of mouse EphA knockins and knockouts suggests that retinal axons programme target cells to form ordered retinotopic maps. Development *133*, 2705-2717.

Willshaw, D.J., and von der Malsburg, C. (1979). A marker induction mechanism for the establishment of ordered neural mappings: its application to the retinotectal problem. Philos Trans R Soc Lond B Biol Sci *287*, 203-243.

Yates, P.A., Holub, A.D., McLaughlin, T., Sejnowski, T.J., and O'Leary, D.D. (2004). Computational modeling of retinotopic map development to define contributions of EphA-ephrinA gradients, axon-axon interactions, and patterned activity. J Neurobiol *59*, 95-113.

Yates, P.A., Roskies, A.L., McLaughlin, T., and O'Leary, D.D. (2001). Topographic-specific axon branching controlled by ephrin-As is the critical event in retinotectal map development. J Neurosci *21*, 8548-8563.

Zimmer, M., Palmer, A., Kohler, J., and Klein, R. (2003). EphB-ephrinB bi-directional endocytosis terminates adhesion allowing contact mediated repulsion. Nat Cell Biol *5*, 869-878.

Abstract

Topographic projections are a preeminent feature of embryonic brain wiring. The retinotectal projection, i.e. the connection of retinal ganglion cells in the eye and the *Tectum opticum* in the midbrain, is the best studied model system for this type of connectivity in the brain. This projection is characterised by neighbouring neurons in the retina sending their axons to neighbouring neurons in the tectum. Therefore, the representation of an object in the retina is functionally recast in the optic tectum.

Roger Sperry postulated the existence of chemical markers on retinal and tectal cells which would enable the retinal axons to find the appropriate target positions (chemoaffinity). The discovery of graded guidance cues on tectal cells (ephrinAs) and correspondingly graded axon guidance receptors on RGC growth cones (EphAs) essentially corroborated a “text-book model” of topography formation.

However, this “text-book model” is oversimplified and, as shown in this work, some of its predictions are not fully consistent with important axon guidance experiments, like the stripe assay or the gradient assay.

Additional counter-gradients of ephrinA in the retina and of EphA gradients in the tectum have been reported. And since it is established that the ephrin/Eph system is capable of transducing a reverse signal, in contrast to the “text-book model”, guidance of retinal growth cones by two antagonistic gradients (tectal receptor + ligand) can be envisaged. Furthermore, it was demonstrated that fibre-fibre- and axonal ephrinA/EphA interactions in *cis* play a major role. Neither of those interactions, however, is included so far in the “text-book model”. Adaptation against the topographic guidance signal occurs as well, although, from a theoretical point of view, this process seems difficult to reconcile with topographic map formation.

In order to understand the complex system behaviour, a computational model based on cellular automata was developed, which incorporates all major guidance cues and potentially arising molecular interactions.

The novel model reproduced experimental evidence suggesting a contribution of forward and reverse signalling and *cis*- and fibre-fibre-interactions to topographic axon guidance. Furthermore, it is shown experimentally in this work that reverse and forward signalling are guiding primary RGC growth cones of the chick. The presented model achieved robust topographic mapping when varying the gradients in the tectum, which is a feature rigid chemoaffinity models are not able to provide.

Most importantly, however, the novel model predicted topographically differential decision behaviour of retinal axons in a stripe assay with alternating stripes of EphA receptor and ephrinA ligand. Consistent with this prediction, after performing this experiment *in vitro,* a topographically differential behaviour of RGC axons was seen for the first time under defined conditions. That is to say, retinal axons differentially grew on the stripes that corresponded to their *in vivo* target (temporal axons on EphA receptor and nasal axons on ephrinA ligand).

Moreover, an adaptation mechanism was proposed that is consistent with the formation of topographic maps.

Zusammenfassung

Die Entstehung axonaler Verbindungen zwischen Netzhaut und Mittelhirn gilt als das am besten verstandene Modell für die Ausbildung von topographischen Karten im Nervensystem von Wirbeltieren. Diese Art der Verschaltung ist dadurch gekennzeichnet, dass die Nachbarschaftsbeziehungen zwischen den Nervenzellen der Netzhaut hinsichtlich ihrer axonalen Verknüpfungen mit dem Zielgebiet erhalten bleiben. Auf diesem Weg werden Bilder vom Auge in einer zweidimensional intakten Form ins Gehirn transferiert.

Roger Sperry formulierte erstmals die Idee, dass die dafür notwendige Lenkung der Axone in ihr Zielgebiet durch die Erkennung spezifischer chemischer Marker gewährleistet werden kann (Chemoaffinitätstheorie). Die Entdeckung gradiert verteilter Lenkungssignale im Zielgebiet (ephrinAs) und gradierter Axonlenkungsrezeptoren (EphAs) auf den Wachstumskegeln der projizierenden Neuronen bildeten in der Folge die Grundlage für ein „Lehrbuchmodell“ der Entstehung topographischer Projektionen.

Allerdings, ist dieses Model zu stark vereinfacht und macht, wie in der vorliegenden Arbeit dargestellt, Vorhersagen, die mit dem Ausgang wichtiger Axonlenkungsexperimente, wie zum Beispiel dem Streifenassay und dem Gradientenassay, nicht übereinstimmen.

Weiterhin wurde bereits gezeigt, dass das gradierte Lenkungssignals auch auf den retinalen Axonen und der gradierte Lenkungsrezeptor im Tektum exprimiert ist. Da für diese Moleküle auch eine reversen Signaltransduktion nachgewiesen wurde, wäre es entgegen dem Lehrbuchmodell auch möglich, dass die Lenkung der Wachstumskegel ins Zielgebiet über zwei funktionell antagonistische Gradienten (tektalen Rezeptor und Liganden) gewährleistet wird. Außerdem ist bekannt, dass Faser-Faser- sowie eine axonale ephrin / EphA-Wechselwirkung in *cis* eine zentrale Rolle spielen. All diese Wechselwirkungen werden jedoch bisher vom „Lehrbuchmodell“ der Entstehung topographischer Projektionen nicht berücksichtigt. Schließlich findet auch Adaptation gegen das topographische Signal statt, obwohl diese von einem theoretischen Standpunkt aus nur schwer mit einer Topographie zu vereinbaren scheint.

Um diese Komplexität zu erfassen, wurde in dieser Arbeit ein Computermodell entwickelt, das die wichtigen Axonlenkungsmoleküle enthält sowie alle potentiell auftretenden molekularen Interaktionen integriert.

Das neu entwickelte Model reproduziert, den Einfluss von *forward* und *reverse signalling*, sowie von *cis*- und Faser-Faser-Wechselwirkungen auf die topographische Axonlenkung. Die Lenkungsfunktion von *forward* und *reverse signalling* auf primäre Wachstumskegel von RGC-Axonen des Huhns wurde hier experimentell bestätigt. Das Model zeigte außerdem einen erhöhten Grad an Robustheit gegenüber Veränderungen der Gradienten im Zielgebiet, etwas, das andere aktuelle Chemoaffinitätsmodelle derzeit nicht in der Lage sind zu leisten.

Insbesondere aber prognostizierte das Modell ein topographisch differenzielles Entscheidungsverhalten der Axone in einem Streifenassay mit alternierenden Streifen von Rezeptor und Ligand. Nach Durchführung dieses Experiments konnte zum ersten Mal eine topographisch differenzielle Axonentscheidung unter definierten *in vitro* Bedingungen beobachtet werden. Das heißt die Axone entschieden sich entsprechend ihrer Herkunft in diesem Assay für den Streifen (Rezeptor oder Ligand), der auch ihrem Zielgebiet *in vivo* entspricht.

Ein Adaptationsmechanismus wurde ebenso vorgeschlagen, der, wie sich zeigte, konsistent mit der Entstehung topographischer Projektionen ist.

Curriculum Vitae

Name: Christoph Gebhardt

Geburtsdatum und Geburtsort: 14.01.1980 in Altenburg

Ausbildung:

1986 – 1998	Allgemeine polytechnische Oberschule und Gymnasium
1998 – 1999	Wehrdienst
1999 – 2003	FSU Jena: Studium des Diplomfaches Biologie
2004 - 2005	Diplom Universitätsklinikum der FSU Jena, Nachwuchsgruppe Neurogenetik: Betreuer: Dr. Franco Weth
April 2005	Promotionsstudium Nachwuchsgruppe Neurogenetik, Friedrich-Schiller-Universität Jena Betreuer: Dr. Franco Weth
Februar 2007	Weiterführung der Promotion Universität Karlsruhe (TH) Zoologisches Institut I: Lehrstuhl für Zell- und Neurobiologie Betreuer: Prof. Dr. Martin Bastmeyer

Stipendien:

2000 - 2004	Stipendiat der Studienstiftung des Deutschen Volkes
2005 - 2007	Landesgraduiertenstipendium Thüringen
2007 - 2009	Doktorandenstipendium der Karlsruhe School of Optics and Photonics (KSOP)